CHEMICAL ENGINEERING

January 2019

ESSENTIALS FOR THE CPI PROFESSIONAL

www.chemengonline.com

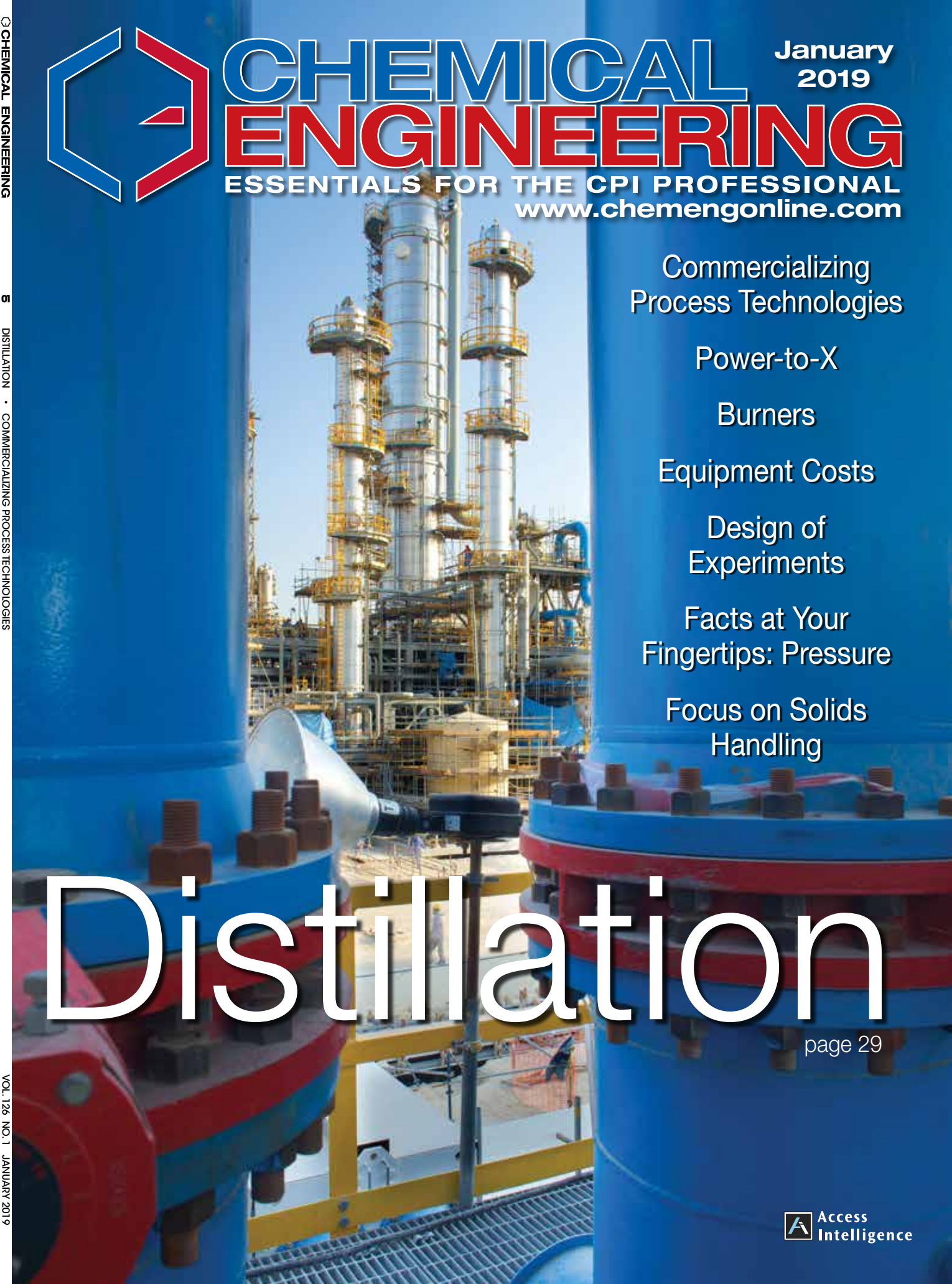

Commercializing Process Technologies

Power-to-X

Burners

Equipment Costs

Design of Experiments

Facts at Your Fingertips: Pressure

Focus on Solids Handling

Distillation

page 29

Access Intelligence

CHEMICAL ENGINEERING
ESSENTIALS FOR THE CPI PROFESSIONAL
www.chemengonline.com

January 2019 Volume 126 | no. 1

Cover Story

29 **An Investigation of Premature Flooding in a Distillation Column** Surprising observations regarding flooding in the upper fractionation trays of an atmospheric crude-petroleum distillation column are investigated

In the News

7 **Chementator**
Recovering rare-earth elements from coal byproducts; A catalyst that mimics enzymes; A more efficient way to convert CO_2 into chemicals via MER; Making jet fuel from wood; A methane fuel cell that operates at lower temperatures; Nanoengineered cellulose prevents scaling; and more

12 **Business News**
Ingevity starts up activated-carbon extrusion plant in Changshu; Borealis announces European PP expansion plans; Evonik to increase sodium methylate production in Mobile, Ala.; Sulzer, TechnipFMC and Futerro form bioplastics initiative; and more

14 **Newsfront** **Power-to-X: Batteries Not Required**
As renewable energy becomes increasingly available (and less expensive), Europeans are looking to Power-to-X as a way to couple the energy, CPI and transportation sectors

18 **Newsfront** **The Balanced Burner**
Modern combustion technologies help processors safely meet emissions standards, while optimizing the process

Technical and Practical

27 **Facts at your Fingertips** **Pressure Measurement for Real Gases** This one-page reference provides information on equations of state that have been used to improve the accuracy for the Van der Waals modification of the ideal gas law for real (non-ideal) gases

28 **Technology Profile** **HDPE Production via a Slurry-Loop Process** This column outlines the production of high-density polyethylene (HDPE) using a slurry-loop process

40 **Feature Report** **Commercializing Process Technologies** New processes can provide competitive advantages compared to established processes, but significant effort is required to transition a promising concept into a commercial reality

51 **Engineering Practice** **Cost Engineering: Equipment Purchase Costs** A methodology and examples for estimating equipment costs are presented

23

25

54 **Engineering Practice** **Accelerating Six-Sigma Research with the Definitive Screening Design (DSD) Technique** DSD is a new design-of-experiments (DoE) technique that is expected to bring huge benefits when using a Six Sigma optimization strategy

Equipment and Services

23 **Focus on Handling Powders and Bulk Solids**
Vibrator-mounting solution requires no welding or boiling; This level detector is suitable for use in dusty environments; These dust collectors are designed for easy maintenance; Small-footprint cyclone competes with larger units; This small centrifuge allows for continuous processing; and more

25 **New Products**
This AODD pump has multiple mounting orientations; Slash the total cost of ownership with this new aseptic valve; A new generation of valve positioners; A new control system for smart control of separators; Fast, simple and accurate on-the-go steam-trap testing; and more

Departments

5 **Editor's Page** **Honoring Process Commercialization**
Nominations are now being accepted for the 2019 Kirkpatrick Chemical Engineering Achievement Award

64 **Economic Indicators**

Advertisers

59 **Hot Products**

61 **Classified**

62 **Subscription and Sales Representative Information**

63 **Ad Index**

Chemical Connections

Follow @ChemEngMag on Twitter

Join the *Chemical Engineering* Magazine LinkedIn Group

Visit us on www.chemengonline.com for more articles, Latest News, Webinars, Test your Knowledge Quizzes, Bookshelf and more

Coming in February

Look for: **Feature Reports** on Steam; and Drones; A **Focus** on Filtration; A **Facts at your Fingertips** on Pumps; **News Articles** on Safety and Industrial Housekeeping; and Artificial Intelligence Technology; **New Products**; and much more

Cover design: Rob Hudgins
Cover photo: Courtesy of Fluor Corp.

CHEMICAL ENGINEERING
ESSENTIALS FOR THE CPI PROFESSIONAL

HEADQUARTERS

40 Wall Street, 50th floor, New York, NY 10005, U.S.
Tel: 212-621-4900
Fax: 212-621-4694

EUROPEAN EDITORIAL OFFICES

Zeilweg 44, D-60439 Frankfurt am Main, Germany
Tel: 49-69-9573-8296
Fax: 49-69-5700-2484

CIRCULATION REQUESTS:

Tel: 847-559-7314
Fax: 847-564-9453
Fulfillment Manager; P.O. Box 3588,
Northbrook, IL 60065-3588
email: chemeng@omeda.com

ADVERTISING REQUESTS: SEE P. 62

ACCESS INTELLIGENCE, LLC

DON PAZOUR
Chief Executive Officer

HEATHER FARLEY
Chief Operating Officer

JAMES OGLE
Executive Vice President
& Chief Financial Officer

MACY L. FECTO
Chief People Officer

JENNIFER SCHWARTZ
Senior Vice President & Group Publisher
Aerospace, Energy, Healthcare

ROB PACIOREK
Senior Vice President,
Chief Information Officer

JONATHAN RAY
Vice President, Digital

MICHAEL KRAUS
Vice President,
Production, Digital Media & Design

GERALD STASKO
Vice President/Corporate Controller

Access Intelligence
9211 Corporate Blvd., 4th Floor
Rockville, MD 20850-3240
www.accessintel.com

BPA

Editor's Page

The 2019 Kirkpatrick Award: Nominations are now open

As chemical engineers, many of us work on developing new processes or improving current ones, often with goals of better efficiency, new or improved products and more sustainability. Taking concepts and laboratory work to a commercial scale requires significant effort, and often significant time. Our feature report this month, Commercializing Process Technologies (pp. 40–50) offers a glimpse into the types and amounts of effort that go into process commercialization.

In recognition of the achievements associated with commercialization, every other year *Chemical Engineering* honors the most-noteworthy chemical engineering technology that was commercialized anywhere in the world during the previous two years with the Kirkpatrick Chemical Engineering Achievement Award. We are now accepting nominations for the 2019 award.

Chemical Engineering has bestowed the Kirkpatrick Award continuously since 1933. The most recent winner in 2017 was CB&I (The Woodlands, Texas; www.cbi.com) and Albemarle Corp. (Charlotte, N.C.; www.albemarle.com), for the AlkyClean process — the world's first solid-catalyst alkylation process. Details of the winning achievement can be found in our January 2018 issue (Process Commercialization: The 2017 Kirkpatrick Chemical Engineering Achievement Award, pp. 22–28). The full list of past winners can be found at www.chemengoline.com/kirkpatrick.

How to nominate

Any person or company may submit a nomination. The procedure is simple and consists of sending a nominating brief of up to 500 words to awards@chemengonline.com by March 15.

In order to be considered for the 2019 award, each nomination should include the following three items: 1) a summary of the achievement and novelty of the technology; 2) a description of the difficult chemical-engineering problems solved; and 3) a description of how, where and when the development first became commercial in 2017 or 2018.

If you are aware of a qualifying achievement, but do not have information to write a brief, contact the company involved, either to get the information or to propose that the firm itself submit a nomination. Companies are welcome to nominate achievements of their own.

The selection procedure

After nominations are reviewed for validity, they will be sent to department heads at accredited university chemical-engineering departments, who will vote, independently of each other, for a maximum of five best achievements.

The entries that receive the most votes will become the finalists in the competition. Each finalist will then be asked to submit additional information describing the technology, performance and examples of teamwork that generated the achievement. This detailed information will be sent to a Board of Judges, which will have been chosen from the university department heads. The Board will judge the entries to select the most noteworthy, and thus the winner. The winner will be announced in the fall. ■

Dorothy Lozowski, Editorial Director

Recovering rare-earth elements from coal byproducts

Edited by:
Gerald Ondrey

University of Kentucky

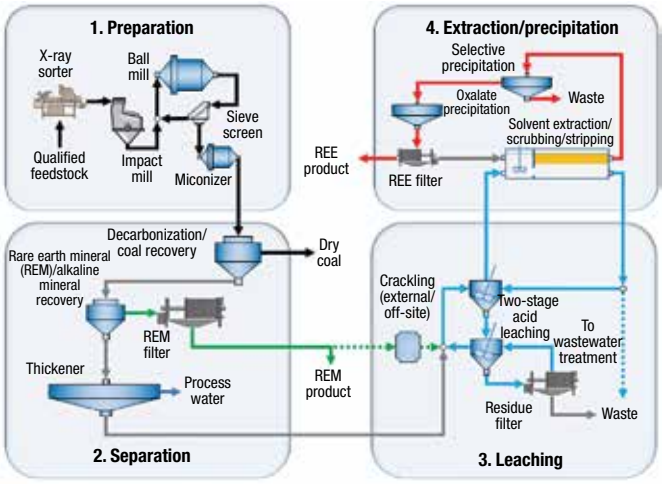

A team from the University of Kentucky (Lexington, Ky.; www.uky.edu) and Virginia Polytechnic Institute (Blacksburg, Va.; www.vt.edu) has set up a novel pilot plant to recover rare-earth elements (REEs) from coal-based sources, aiming to produce high-grade REE concentrates from coal-based leachate. Byproducts of coal mining are a promising source for highly in-demand REEs, says Rick Honaker, professor of mining engineering at the University of Kentucky. "All of the REEs, including scandium and yttrium, are present in coal, whereas most other sources contain only a select number of REEs," he explains.

Leaching conditions from coal sources require milder sulfuric-acid concentrations than leaching from other mineral sources, but the low REE composition in the leachate (<100 parts per million; ppm), along with the high concentration of contaminant ions, including iron, magnesium, aluminum, calcium and others, requires a rigorous solvent-extraction and scrubbing circuit designed by the team specifically for handling coal-based resources. Prior to solvent extraction, the leachate is chemically reduced to convert Fe^{3+} to Fe^{2+} ions using ascorbic acid, which enables effective rejection of iron ions in the solvent-extraction circuit.

The pilot plant utilizes a sorting technology based on dual X-ray transmission to effectively extract higher-grade REE content. "The material extracted by the sorter is more leachable than other portions of the material," explains Honaker. The pilot plant has produced concentrates containing greater than 99% total REEs from coarse coal refuse material, coal-based mine acid water and precipitate waste material generated from the treatment of mine acid water.

The 0.25-ton/h pilot plant is currently the world's largest unit focused on REE recovery and concentration from coal sources, and with funding from the U.S. Department of Energy (DOE), the team is currently designing a 20-ton/h commercial plant utilizing this technology. According to Honaker, this commercial plant would likely produce three different REE concentrations: 99% scandium; a mixture of neodymium, praseodymium and dysprosium (Nd-Pr-Dy); and an yttrium product.

RENEWABLE JET FUEL

At the end of last October, euglena Co. (Tokyo, Japan; www.euglena.jp) completed the construction of Japan's first demonstration plant for the production of renewable jet and diesel fuel in Yokohama. The $58-million pilot plant, located at the company's Yokohama site, has a production capacity of 5 barrels per day (bbl/d; about 125,000 L/yr) of renewable liquid fuels, using the Biofuels Isoconversion Process (BIC). Euglena expects to supply a next-generation renewable diesel fuel this summer, and to achieve revenue-generating flights with renewable jet fuel in 2020. On this project, euglena is collaborating with the City of Yokohama, Chiyoda Corp., Itochu Enex Co., Isuzu Motors Ltd., ANA Holdings Inc., and Hiroshima Council for the Promotion of Collaboration between Government, Academia and the Automobile Industry.

The demonstration plant will begin full-scale operation in spring 2019 and begin producing renewable jet and diesel fuel using *Euglena*,

(Continues on p. 8)

A catalyst that mimics enzymes

A research team from the University of New South Wales (Sydney, Australia; www.unsw.edu.au) and Ruhr-Universität Bochum (Bochum, Germany; www.ruhr-universität-bochum.de) has succeeded in transferring structural characteristics of natural enzymes to metallic nanoparticles, achieving high catalytic activity.

In the case of enzymes, the reacting substances must pass through a channel from the surrounding solution to the active enzyme center, where the structure provides favorable reaction conditions. To mimic enzyme structures, the team proposed nanoparticles with etched substrate channels. The team first produced nanoparticles (10-nm dia.) of nickel and platinum. The nickel is then removed by chemical etching to form channels. An oleylamine (a long-chain unsaturated fatty amine) is used as a capping layer that blocks the external surface of the nanoparticles participating in the catalytic reaction. Finally, the active centers on the particle surface are deactivated to ensure that only the active centers within the channels participate in the reactions.

Using the oxygen-reduction reaction as a model reaction (an important step in fuel-cell operation), the catalytic activity of these channeled particles were compared to those of conventional particles having active centers only on the surface. It was observed that the oxygen reaction occurs mainly within the etched channels, which provide a nanoconfined reaction volume different from the bulk electrolyte conditions. Active centers in the channels catalyze the reactions three times more efficiently than active centers on the particle surfaces, showing the potential of nanozymes.

The team plans to extend the concept to other reactions, such as electrocatalytic CO_2 reduction. The researchers believe the concept will make energy conversion processes more efficient using electricity generated from renewable sources.

microalgae and waste cooking oil as raw material.

Hg REMOVAL

Researchers from Chalmers University of Technology (Göteborg, Sweden; www.chalmers.se) have developed a patent-pending method for removing mercury from wastewater. The technique, known as electrochemical alloying, is described in a recent issue of *Nature Communications*.

In the process, a platinum electrode is used to draw the mercury ions out of solution to form a stable alloy. Because each Pt atom can "bond" with four Hg atoms, the electrode has a high capacity, and it can be regenerated when loaded in a controlled way. The method is selective for removing only Hg from water, and has been shown to reduce Hg concentrations in a liquid by more than 99%. A company, Atium AB (Göteborg, Sweden; www.atium.se), has been established to commercialize the discovery. Currently, a prototype device is being developed for performing field tests.

P-RECOVERY

A 10-gal/min pilot system for a phosphorus-recovery technology was operated at the Madison (Wisconsin) Metropolitan Sewerage District dur-

(Continues on p. 10)

A more efficient way to convert CO_2 into chemicals via MER

Microbial electrochemical reduction (MER) of CO_2 into value-added chemicals is a potential way to curb greenhouse gas (GHG) emissions. MER uses chemolithoautotrophs, which are microbes found in the deep sea, in caves and in hydrothermal vents. These bacteria get their energy by oxidizing inorganic compounds and reducing CO_2 into organic compounds. Typically, MER reactors use planar cathodes with microbes growing as a biofilm on the surface of the cathode, and supply CO_2 by bubbling the gas into the solution. However, such systems have poor efficiencies due to the low solubility of CO_2 in water and the small surface area of the cathode.

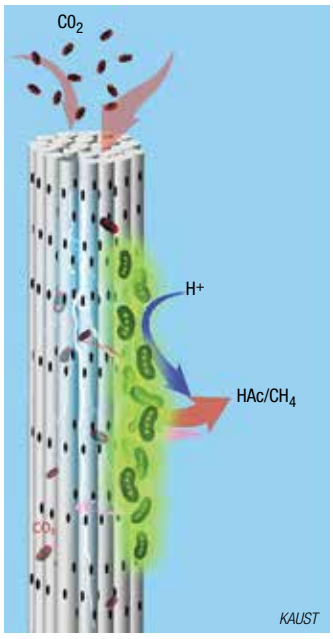

Now, an alternative design is being developed by the research group of professor Pascal Saikaly, associate professor of Environmental Science and Engineering at King Abdullah University of Science and Technology (KAUST; Thuwai, Saudia Arabia; https://kaust.edu.sa). In this new design, the cathode is made of porous nickel hollow-fibers (Ni-PHFs). In a microbial electrosynthesis (MES) reactor (diagram), the CO_2 is pumped through the pores of Ni-PHFs and delivered directly to the biofilm chemolithotrophs growing on the surface of Ni-PHFs. Initial studies showed a 77% conversion efficiency for CO_2 to methane by methanogens when CO_2 is delivered through the pores of Ni-PHFs, compared to 3% when bubbling CO_2 into the solution, according to the study published in a recent issue of *Advanced Functional Materials*. In a follow-up study, published in the *Journal of Materials Chemistry A*, the group showed that by modifying the Ni-PHFs with carbon nanotubes (CNTs), an 11-fold increase in CO_2 adsorption capability was achieved, along with a 76% reduction of cathode electron-transfer resistance, which nearly doubled the production of acetate (HAc) from CO_2 using *Sporomusa ovata*.

So far, "we have demonstrated the new design at lab-scale, since this was a proof-of-concept," says Saikaly. "We are currently working on developing easier approaches to make conductive and porous cylindrical electrodes for large-scale applications. Also, at the same time we are exploring alternative anode materials (photoanodes) to reduce the cost of operation," explains Saikaly. "These systems are currently being operated using a power source. Ultimately, we can couple this process with renewable energy sources, such as sun or wind," he says.

Making jet fuel from wood

Last month, construction began on a demonstration facility that integrates high-performance entrained-flow gasification technology and Fischer-Tropsch (F-T) synthesis for making jet fuel from woody biomass. The demonstration project is being carried out by a Japanese consortium, led by Mitsubishi Hitachi Power Systems, Ltd. (MHPS; Yokohama City, Japan; www.mhps.com), with partners CEPCO, Toyo Engineering Corp. and the Japan Aerospace Exploration Agency (JAXA), and support from the New Energy and Industrial Technology Development Organization (NEDO; Kawasaki City; www.nedo.go.jp). The demonstration facility is located at CEPCO's Shin-Nagoya power station in Nagoya, Japan. The demonstration facility will have the capacity to process 0.7 ton/d of woody biomass, producing about 20 L/d of "neat" biojet fuel. The consortium plans to start trial operation of the facility this year, and to verify operations — including combustion and jet-engine testing at JAXA — in 2020–2021.

On the fuel-production process, MHPS is responsible for the entrained-bed gasification technology, Toyo for micro-channel F-T synthesis technology and the reforming of the synthesized oil, CEPCO for equipment operation and fuel procurement, and JAXA for evaluation of combustion characteristics. MHPS has been developing coal-gasification technology since the 1980s, and has established high-performance gasification furnace technology. The gasification technology realizes uniform and highly efficient gasification due to the following features; oxygen is blown at high velocity into the bottom of the special cylindrical gasifier, and among solid biomass, larger particles are circulated in suspension to be pyrolytically gasified in the lower part of gasifier where upward gas-flow velocity is high, and smaller particles are gasified in the upper part of gasifier where gas-flow velocity is low. The F-T synthesis system adopted for this project is compact, highly efficient and suitable for small- to medium-scale plants, and the reactor is easily scaled up for commercial-scale systems, says Toyo.

ing October and November 2018. The technology, known as CalPrex, incorporates a thickened sludge fermentation tank to increase the amount of soluble and reactive species of phosphorus, thereby increasing the recovery potential of that phosphorus, and produces a P-containing mineral for use as agricultural fertilizer (see *Chem. Eng.*, June 2017, p. 9). The pilot project is being run by the Water Research Foundation (WRF), and the technology was developed at the University of Wisconsin at Madison. Results of the project will help water-resource recovery facilities evaluate and benchmark state-of-the-art alternatives for removing phosphorus from sludge going to digesters. An expert review of the project findings will be conducted, and the results will be disseminated to industry professionals in May 2019.

PENNYCRESS OIL

Researchers from the University of North Texas (Denton, Tex.; www.unt.edu) are working on a project to boost the production of seed oil produced by the pennycress plant. This research, supported by the U.S. Dept. of Energy's Office of Biological and Environmental Research, aims to optimize the amount of seed

(Continues on p. 11)

A methane fuel cell that operates at lower temperatures

Georgia Tech

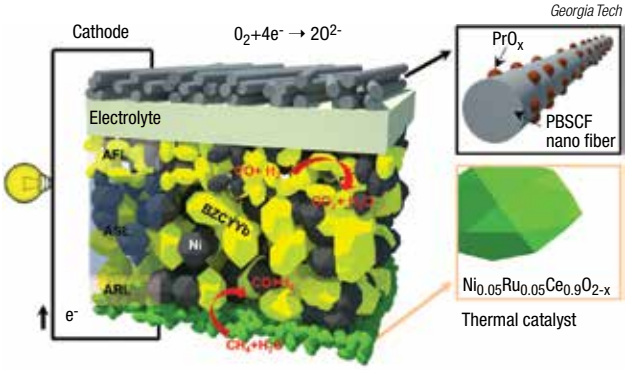

Existing methane fuel cells typically require high (750–800°C) temperatures to activate methane in a separate methane reformer that creates hydrogen gas. Now researchers at the Georgia Institute of Technology (Georgia Tech; Atlanta; www.gatech.edu) have developed a solid oxide fuel cell (SOFC) design that eliminates the need for a methane reformer and requires temperatures of only 500°C. The cost savings enabled by the lower-temperature operation could make this type of fuel cell, which uses no platinum, commercially viable for several applications, including distributed power generation and automobile engines.

"In our fuel cell, we integrated thermal catalysis and electrocatalysis at 500°C," explains Meilin Liu, Georgia Tech professor and lead researcher. "Methane is first reformed to CO and H_2 within the fuel cell, and then the H_2 and CO are electrochemically oxidized to H_2O and CO_2 on the electrode."

The lower-temperature fuel cell would allow ordinary stainless steel, rather than exotic materials, to be used for the interconnectors that link the cells into a stack. "Above 750°C, no metal can withstand the temperature without oxidation," Liu says, so the materials needed are "expensive and fragile, and would contaminate the active components of the cell."

To eliminate the need for steam reforming, the fuel cell features a new catalyst developed for this project by University of Kansas (Lawrence; www.ku.edu) researchers. The catalyst contains nickel and ruthenium active sites anchored on cerium oxide, and aids the chemical cleavage of methane and water, the products of which recombine as H_2 and CO. The catalyst material is applied as a coating on the anode of the fuel cell (diagram).

As electrical current flows, the CO and H_2 are oxidized to CO_2 (in amounts lower than in a combustion engine) and water, which is cycled back into the fuel cell to combine with the methane.

Liu and colleagues have also developed a specialized cathode that accelerates the reduction of oxygen and its movement through the system by using nanofiber cathodes — work which the group previously published. The nanofiber cathode has high surface area, high porosity and lower tortuousity, Liu says, providing more efficient paths for mass and electron transfer.

The researchers are working on stacking the fuel cell into a prototype power device.

Utilizing plastic waste into useful aerogels

Plastic-bottle waste is toxic and non-biodegradable, and has become a major environmental issue. It often ends up in the oceans, affecting marine life, or in landfills, contaminating groundwater and affecting land use. Now a team led by professors Nhan Phan-Thien and Hai Minh Duong, from the National University of Singapore (Singapore; www.nus.edu.sg), has developed recycled polyethylene tetraphthalate (rPET) silica aerogels using rPET fibers obtained from plastic bottle waste via sol-gel and ambient-pressure drying methods.

The team prepared the rPET aerogels through a direct gelation of silica onto PET. rPET fibers are treated with dichloromethane to partially dissolve the fibers. The fibers were then dipped and allowed to swell in a mixture of tetraethoxysilane (TEOS) and ethanol, with the pH controlled to 2.5 using HCl to promote hydrolysis. After acid hydrolysis, the pH was controlled to 7 with an ammonium hydroxide solution to promote condensation.

The PET aerogels thus produced have properties such as lightness, softness and flexibility, making them suitable for many industrial applications, such as in thermal insulation, filtering and sound insulation. They can undergo various surface treatments to customize them for different applications.

For example, when incorporated with methyl groups, PET aerogels can absorb large amounts of oil very quickly, making them very suitable for oil-spill cleaning. When coated with fire retardants, the aerogels show superior thermal resistance and stability, and can withstand temperatures up to 620°C.

When coated with an amine group, the PET aerogel can quickly absorb CO_2. To demonstrate this application, the team embedded a thin layer of PET aerogel into a fine particle that can effectively absorb both dust particles and CO_2.

The developed rPET silica aerogels exhibit super-hydrophobicity with an average water-contact angle of 149.9 deg.

The team has filed a patent for its PET aerogel technology, and is seeking a business partner to commercialize the technology.

Simpler, more selective scandium recovery

Rare-earth elements (REEs), such as scandium, are in high demand, but it is often difficult to economically recover and extract them. Now, II-VI Inc. (Saxonburg, Pa.; www.ii-vi.com) has developed a patent-pending process utilizing selective ion recovery (SIR) that enables highly selective extraction of scandium and other targeted REEs from streams with concentrations as low as 6 ppm. The process is also more economical than other REE extraction methods, since it eliminates the solvent-extraction and ion-exchange steps, as well as the processing and disposal costs associated with handling large volumes of solvents and reagents, says Shailesh Patkar, senior corporate development manager at II-VI. "Conventional extraction methods also face practical issues with rheology, phase separations and interference from competing ions, which can result in low yields," adds Patkar, comparing SIR to a chemical "magnet" that separates desired REEs from other metals, even in the presence of undesirable elements, such as iron.

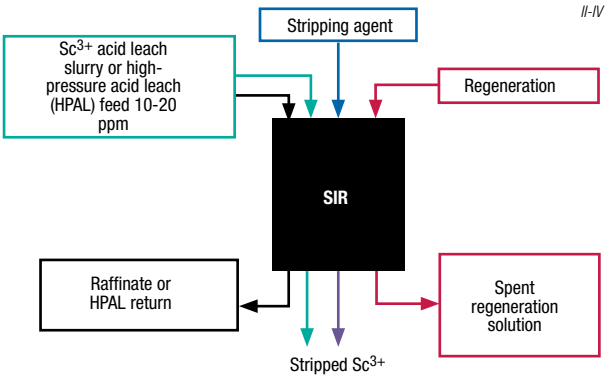

In the SIR method, an acidic slurry containing scandium, typically generated in the production of titanium, aluminum, nickel, tungsten or other metals, is passed through a series of columns containing II-VI's selective extraction material, which is a chemically modified polymeric resin designed to capture the targeted element. After the resin is saturated with the desired metal, the columns are flushed with a proprietary stripping agent to retrieve the metal. Both the resin and the stripping agent are recyclable and can be used for multiple cycles, reducing the cost of the process, explains Patkar.

II-VI has demonstrated the technology at rates of 10 L/h, and plans are underway for a 250-L/h pilot plant, which will be installed in Greece during 2019. The process is designed for integration into larger chemical-processing facilities, and considers the widely varied feedstream concentrations encountered in commercial operations. "The process is designed to accommodate this variation and cause minimal disruption in the main process," says Patkar.

Nano-engineered cellulose prevents scaling


McGill University

Efforts to find more environmentally friendly anti-scalant approaches have yielded a new form of functionalized nanocellulose that can prevent the nucleation and growth of calcium carbonate, the most common component of industrial scale. Based on the biopolymer cellulose, the anti-scaling agents do not contain phosphorus, which can cause environmental damage in water runoff.

To engineer the anti-scaling agents, researchers at McGill University (Montreal, Que.; www.mcgill.ca) worked with a form of nanocellulose, known as hairy nanocellulose, that had been previously discovered at McGill. This form of cellulose is so named because it results from cellulose nanofibrils (the building blocks of plant cell walls) that are cut at precise locations to produce nanoparticles with amorphous regions on either end of crystalline regions. The amorphous "hairs" can be chemically functionalized to a much greater degree than other forms of nanocellulose.

Onto the strands of nanocellulose, the researchers added negatively charged dicarboxyl groups, which interact with positively charged calcium ions and interferes with the formation of $CaCO_3$.

Lead author Amir Sheikhi, now a postdoctoral researcher at the University of California at Los Angeles (www.ucla.edu), says complete scale inhibition is observed when 10 parts per million (ppm) of the hairy nanocellulose is added to an already scaled surface under a supersaturated condition.

The researchers are studying planar silica surfaces coated with hairy nanocelluloses as scale-resistant interfaces. ■

oil produced per plant. "This can be done using traditional cross-breeding methods or bioengineering (or both)," says Ana Alonso, associate professor in the BioDiscovery Institute and the Dept. of Biological Sciences. Alonso is planning to increase the seed-oil yield because, when properly processed, the common pennycress can produce 100 gal/acre of oil, which can then be processed into aviation fuel. "The main variety of pennycress found in the U.S. produces around 30 wt.% seed oil. But, we have found some varieties that can produce upwards of 42 wt.%," she says.

HYBRID CO_2 CAPTURE

Cement manufacture accounts for as much as 7% of global greenhouse gas (GHG) emissions. A new hybrid technology being developed at Sintef (Tronheim, Norway; www.sintef.no) promises to make it easier and less expensive to capture and purify CO_2 from the fluegas of cement plants. The technology, which combines membrane separation and "forced liquification" of CO_2, can be retrofitted to an existing plant.

Sintef researchers anticipate that the method can be utilized by cement factories and in other industrial processes in coastal areas and along European rivers, because liquefied CO_2 can be transported by ship.

Normally, the fluegas emitted from a cement factory contains about 20 vol.% CO_2. In order to transport or store the CO_2 from these gases, the CO_2 has to be captured and concentrated to a minimum of 95% purity. However, conventional scrubbing technology requires large amounts of heat for regenerating solvents.

In Sintef's hybrid approach, membrane separation is first used to generate 70% purity CO_2. Then, an in-house-developed system is used to liquefy the CO_2 by cooling it under pressure. In a laboratory test rig, the system has achieved a CO_2 purity of up to 99.8%. The process uses electricity to cool and compress the gas, instead of steam to regenerate solvents, which is important for facilities lacking a steam generator. ❑

LINEUP

ÅF
ASHLAND
BOREALIS
CORBION
DOW
EASTMAN
EVONIK
HANWHA
HEXCEL
INGEVITY
KEMIRA
NESTE
OUTOTEC
OXITENO
PERSTORP
PÖYRY
SULZER
TECHNIPFMC
TOTAL

Look for more latest news on chemengonline.com

Plant Watch

Neste moves forward with expansion of renewable products in Singapore

December 12, 2018 — Neste Corp. (Espoo, Finland; www.neste.com) plans to add production capacity for renewable products at its existing facilities in Singapore. The approximately €1.4-billion investment will extend Neste's renewable product capacity in Singapore by up to 1.3 million metric tons per year (m.t./yr), bringing the total renewable product capacity to nearly 4.5 million m.t./yr. The company's target is to start up the new production line during the first half of 2022.

Ingevity starts up activated-carbon extrusion plant in Changshu

December 7, 2018 — Ingevity Corp. (North Charleston, S.C.; www.ingevity.com) has begun production at its new activated-carbon extrusion plant in Changshu, China. The new $20-million facility currently houses one new extrusion line. The company has also relocated the extrusion line from its Wujiang, China, facility to Changshu, and that line is expected to begin production by the second quarter of 2019.

Borealis announces European PP expansion plans

December 7, 2018 — Borealis AG (Vienna, Austria; www.borealisgroup.com) will expand the capacity of its polypropylene (PP) plant in Kallo, Belgium, by 80,000 m.t./yr. The added capacity is expected to come onstream in mid-2020. Borealis also approved the start of the front-end engineering and design (FEED) phase for the expansion of its PP plant in Beringen, Belgium. This expansion is in the range of 250,000–300,000 m.t./yr, and is expected to start up in mid-2022.

Outotec to deliver technologies for battery-chemicals plant in Finland

December 6, 2018 — Outotec Oyj (Espoo, Finland; www.outotec.com) will deliver pressure-leaching and solvent-extraction technologies for a battery chemicals plant to be built in Sotkamo, Finland. The battery chemicals plant, expected to be ready for commissioning in 2020, will have the capacity to produce around 170,000 m.t./yr of nickel sulfate and around 7,400 m.t./yr of cobalt sulfate to be used for electric-vehicle batteries. As a byproduct, the plant will also produce around 115,000 m.t./yr of ammonium sulfate to be used as a fertilizer.

Evonik to increase sodium methylate production in Alabama

December 4, 2018 — Evonik Industries AG (Essen, Germany; www.evonik.com) will undertake a significant capacity expansion at its sodium methylate facility located in Mobile, Ala. Upon completion, the Mobile plant will be capable of producing up to 90,000 m.t./yr of sodium methylate. Besides Mobile, Evonik also produces sodium methylate in Germany and Argentina.

Ashland completes expansion of hydroxyethylcellulose plant in Nanjing

December 4, 2018 — Ashland Inc. (Columbus, Ohio; www.ashland.com) completed a capacity expansion for hydroxyethylcellulose (HEC) in Nanjing, China. This expansion increased the manufacturing capacity of the site by nearly 30%. Key markets for HEC include coatings, personal care, oil-and-gas, construction and pharmaceuticals.

Total and Corbion start up joint bioplastics plant in Thailand

December 3, 2018 — Total Corbion PLA, a 50/50 joint venture (JV) between Total S.A. (Paris, France; www.total.com) and Corbion (Amsterdam, the Netherlands; www.corbion.com), started up a 75,000-m.t./yr polylactic acid (PLA) bioplastics plant in Rayong, Thailand. The new facility will produce a broad range of PLA resins from renewable sugarcane, sourced locally in Thailand. With this new facility, the global production of PLA bioplastics will increase by almost 50%.

Hanwha Total Petrochemical invests in a new PP plant

December 3, 2018 — Hanwha Total Petrochemical (www.hanwha-total.com), a 50/50 JV between Total and Hanwha Group (Seoul, South Korea; www.hanwha.com), will invest nearly $500 million to further expand its Daesan integrated petrochemical complex in South Korea. The planned investment will increase PP capacity by 60%, to 1.1 million m.t./yr, by the end of 2020. The ethylene capacity will simultaneously increase by 10%, to 1.5 million m.t./yr.

Eastman completes construction of new isobutyric acid manufacturing facility

November 28, 2018 — Eastman Chemical Co. (Kingsport, Tenn.; www.eastman.com) has completed a new isobutyric acid manufacturing facility at its Kingsport site. The new facility, when added to Eastman's Longview, Texas isobutyric acid plant, doubles Eastman's production capacity. Isobutyric acid is used in a number of end-markets, including agriculture, food, fragrance and protective coatings.

New Thailand plant expands Dow's polyol capacity

November 28, 2018 — The Dow Chemical Co. (Midland, Mich.; www.dow.com) opened a new

polyol plant for rigid polyurethane foam in Rayong, Thailand. The new polyol plant has a designed annual capacity of 79,000 m.t., and is located at the Asia Industrial Estate (AIE) site, which is home to six Dow manufacturing plants.

Oxiteno marks opening of new alkoxylation plant in Texas

November 19, 2018 —Oxiteno (São Paulo, Brazil; www.oxiteno.com) officially opened its first alkoxylation plant in Pasadena, Tex. This unit, planned to support mainly U.S. customers, has alkoxylation capacity of around 170,000 m.t./yr.

Mergers & Acquisitions

Pöyry to merge with Swedish engineering company ÅF AB

December 12, 2018 — ÅF AB (Stockholm, Sweden; www.afconsult.com) and Pöyry PLC (Helsinki, Finland; www.poyry.com) have signed an agreement to combine the two companies to form a leading engineering and consulting company. The offer price values Pöyry at €611 million. The combined company, to be headquartered in Stockholm, will operate under the united brand ÅF-Pöyry.

Perstorp to sell its caprolactone business to Ingevity

December 10, 2018 — Perstorp AB (Malmö, Sweden; www.perstorp.com) has agreed to sell Capa, its caprolactone business, including the production site in Warrington, U.K., to Ingevity for approximately €590 million. The business has annual revenues of approximately €150 million. Perstorp expects to close the transaction in the first quarter of 2019.

Sulzer, TechnipFMC and Futerro form bioplastics initiative

December 6, 2018 — Sulzer Ltd. (Winterthur, Switzerland; www.sulzer.com), TechnipFMC (Houston; www.technipfmc.com) and Futerro (Escanaffles, Belgium; www.futerro.com) have formed the PLAnet initiative, in equal partnership, to promote the production of sustainable plastics made from PLA. The strategic collaboration will support manufacturers interested in entering the bioplastics market by delivering integrated PLA technology packages.

Hexel acquires manufacturer of microwave-absorbing composites

December 3, 2018 — Hexcel Corp. (Stamford, Conn.; www.hexcel.com) has agreed to acquire Massachusetts-based ARC Technologies, Inc., a supplier of microwave-absorbing composite materials for military, aerospace and industrial applications, for $160 million. The transaction is expected to close in early 2019.

Kemira forms AKD wax joint venture in China

December 3, 2018 — Kemira Oyj (Helsinki, Finland; www.kemira.com) has formed a JV with Shandong Tiancheng Wanfeng Chemical Technology, a producer of alkyl ketene dimer (AKD) wax in China. The JV, named Kemira TC Wanfeng Chemicals Yanzhou, will mainly produce AKD wax and its key raw material, fatty acid chloride (FACl). ■

Mary Page Bailey

Power-to-X: Batteries Not Required

As renewable energy becomes increasingly available (and less expensive), Europeans are looking to Power-to-X as a way to couple the energy, CPI and transportation sectors

thyssenkrupp

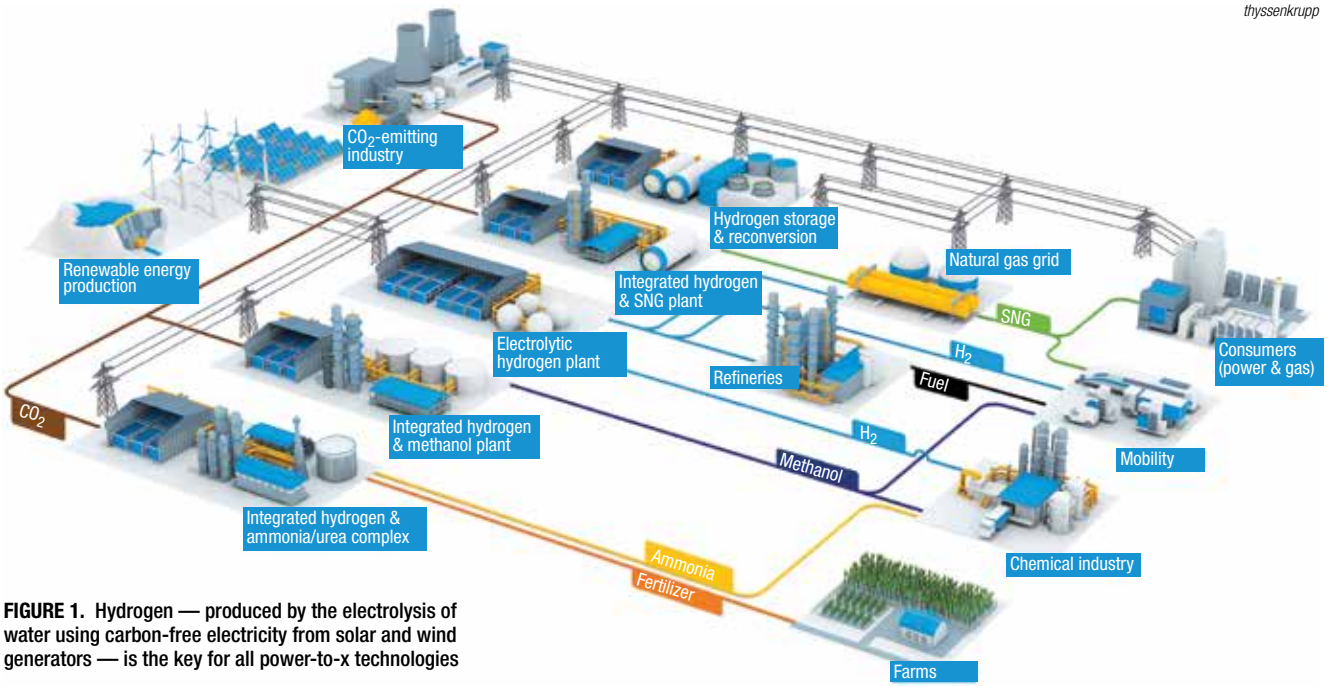

FIGURE 1. Hydrogen — produced by the electrolysis of water using carbon-free electricity from solar and wind generators — is the key for all power-to-x technologies

Germany's energy transition (*Energiewende*) from fossil-based fuels to renewables, such as solar and wind, is sparking a revolution that may change the way companies in the chemical process industries (CPI) operate in the not-to-distant future. With more than 33% of its power already supplied by renewables, and a goal to be virtually greenhouse-gas (GHG) neutral by 2050 (as outlined in the Climate Action Plan 2050, adopted November 2016), Germany is leading the charge, with many European countries joining the effort to meet the E.U.'s GHG targets set out in the Paris Agreement.

With the increased emphasis on carbon-free electricity from solar and wind power generation, many different technologies are being investigated to make this fluctuating electricity source more reliable, which is essential for industrial processes. Some of the options being actively investigated are power-to-x (PTX) technologies, which are ways to store and utilize excess renewable electricity in the form of a gas or liquid (X) that can be easily transported for use in transportation and heating, and as feedstock for producing bulk chemicals (Figure 1).

In 2016, the Federal Ministry of Education and Research (BMBF; Bonn, Germany; www.bmbf.de) introduced four "Kopernikus Projects for the Energy Transition." One of the projects selected was PTX, which is coordinated by RWTH Aachen University, Forschungszentrum Jülich, and Dechema e.V. (Frankfurt am Main; www.dechema.de). The major project focuses on the storage of excess power into other energy carriers, with €30 million in funding from the BMBF for the first of three development phases.

Today, there are about 35 PTX projects in Germany, according to the German Energy Agency (dena; Berlin; www.dena.de), which maintains a database of the projects as part of its Power-to-Gas (PTG) Strategy Platform (www.powertogas.info). Dena established the PTG Strategy Platform in 2011 in order for partners from industry, associations and science to pool their diverse expertise and experience. The core objective is to establish PTG as a reliable, cost-efficient and large-scale multi-purpose option at least by the beginning of the years 2020–2025, with at least 1,000 MW of electrolysis power installed in Germany.

Power-to-gas: hydrogen is key

Splitting water into hydrogen and oxygen is a key step in almost all PTX schemes. Although the technology has been around for decades, water electrolysis only accounts for about 5% of the world's H_2 production, with the remaining bulk supplied from fossil feedstock, according to Manfred Baldauf, head of research group Electrochemistry, Siemens AG (Erlan-

gen, Germany; www.siemens.com). Speaking at Dechema's *PraxisForum* "Electrolysis in Industry" (22–23 November; Dechema Haus, Frankfurt), Baldauf presented the advances being made by Siemens to develop new, industrial-scale electrolyzers in order to decarbonize the production of H_2 by taking advantage of the falling prices and increasing availability of renewable electricity — especially that produced from wind and solar energy. Siemens has focused on proton-exchange membrane (PEM) electrolysis — in principle, a fuel cell operating in reverse — for H_2 production. Compared to acid or alkaline electrolysis, PEM offers good dynamic operation, which is especially important for fluctuating electricity, explained Baldauf, as well as producing higher purity (>99.9%) H_2, and no chemicals are added. "We believe electrolysis is the chief technology for sector coupling," said Baldauf, referring to the coupling of the power, process and transportation sectors.

Siemens first introduced its PEM technology in 2011, with the Silyzer 100, followed by the Silyzer 200 in 2015 — a 1.25-MW system with a 65% efficiency. Since 2015, three Silyzer 200 PEM systems have been operating at the Energiepark Mainz, converting wind energy into H_2, which is then stored and fed into the local gas grid or delivered to surrounding industry and H_2-filling stations via tank trailers. This facility, a joint project of Stadtwerke Mainz AG, the Linde Group and Siemens, was, at the time, the world's largest PEM electrolyzer facility.

In 2016, the Silyzer 200 was used in Germany's first PTG plant at Windgas Haßfurt GmbH & Co. KG, which is owned by partners Greenpeace Energy eG and Städttische Betrieb Haßfurt GmbH. The 1.25-MW unit is used to stabilize the total power network by drawing excess electricity from wind and solar plants.

Last year, Siemens launched the Silyzer 300, consisting of up to 24 PEM modules for a total capacity of 20 MW, and an efficiency of 75% (without H_2 compression). The first commercial application of the Silyzer 300 — a 6-MW pilot unit with only 12 modules — was commissioned at the end of 2018 in Linz, Austria, where it is featured in the E.U.-funded (€18-million) flagship project H2Future. The plant is scheduled to be fully operational this spring, producing 1,200 m^3/h of H_2 that will be used for steelmaking processes at voestalpine AG (Linz, Austria; www.voestalpine.com), using hydroelectric power supplied by Verbund — Austria's largest electricity company, which operates 128 hydropower plants.

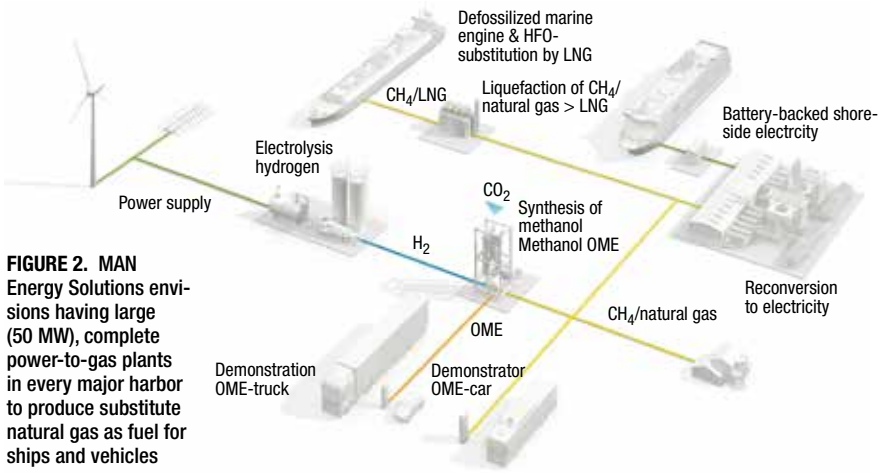

FIGURE 2. MAN Energy Solutions envisions having large (50 MW), complete power-to-gas plants in every major harbor to produce substitute natural gas as fuel for ships and vehicles

Also scaling up to industrial scale is thyssenkrupp AG (Essen, Germany; wwww.thyssenkrupp.com), which commercially launched its advanced water electrolysis technology last year (*Chem. Eng.*, August 2018, p. 6). To make deployment of large H_2 projects as easy as possible, the thyssenkrupp technology is available in prefabricated, skid-mounted standard modules (5, 10 and 20 MW each). The pre-mounted skid modules allow easy transport and quick installation with minimum effort. By simply adding them up, desired project sizes can easily be realized, up into the range of several hundred megawatts, explained Gergor Polcyn, head of Product Management & Technology Dept, Energy Storge & Hydrogen at thyssenkrupp Uhde Chlorine Engineers GmbH (Dortmund, Germany). More than 200,000 elements have already been manufactured, said Polcyn at the Dechema forum. The first demonstration unit — a 2-MW electrolyzer producing 440 Nm^3/h H_2 with 99.95% purity, started up last summer in Duisburg, Germany as part of the Carbon2Chem project (www.thyssenkrupp.com/en/carbon2chem). That project aims to develop technology for converting the emissions from steel mills — composed of about 44% N_2, 23% CO_2, 21% CO 10% H_2 and 2% CH_4 — to make chemicals, such as ammonia and methanol.

Power-to-gas: methane

Although there is a large market for H_2, its use as a fuel is still limited, due to a lack of infrastructure, says Marc Grünewald, head of Business Development and New Energies, Power Unit, MAN Energy Solutions SE (MAN ES; Augsburg, Germany; www.man-es.com). Therefore, MAN ES aims to build large-scale PTG plants as a way to utilize surplus electricity to make methane, or synthetic natural gas (SNG). SNG has the advantage over H_2 in that it can be directly injected into existing infrastructure, where it can be pipelined for use for power generation, heating in households and as a transportation fuel, including for ships (Figure 2). "This is not simply energy storage, but rather the production of green fuels," Grünewald says. About 50% of energy used for industry today is consumed by transportation vessels — "vessels do not want batteries, but green fuels," he says. To reduce CO_2 emissions and achieve more stringent emission targets, ships can shift from oil or diesel fuel to liquefied natural gas (LNG) or SNG, Grünewald explains. "We envision having a 50-MW power-to-gas plant in all the major harbors to supply ships."

Since 2012, MAN ES has been operating a pilot methanation plant at an Audi site in Werlte, Germany for the production of SNG directly from CO_2 and H_2. The process takes place in a

microbEnergy

FIGURE 3. This biomethanation unit in Allendorf, Germany, uses microbes to convert hydrogen and CO_2 into methane

tubular fixed-bed reactor operating at about 260°C and 6–8 bars pressure. CO_2 and H_2 (mole ratio of 1-to-4) are fed into the reactor and react over a nickel catalyst to form CH_4 and H_2O. The water can easily be removed.

"The 6-MW power-to-gas plant in Werlte is still the world's largest PTG plant today, and continues to run quite well," says Grünewald. "Since it started up in 2012, we have made a number of improvements," he explains: "The methane content has been improved from 92% to 95% today, the footprint has been reduced by 30%, and the costs have fallen by 20–30%. We can say that the methanation technology is now industrially ready," he says. With MAN ES's new corporate strategy, the company is targeting to have 50% renewable-energy business by 2030, with a billion or more in sales in *new* business, Grünewald says.

Meanwhile, others are also working to develop more efficient PTG technology. In Switzerland, for example, the Institute for Energy Technology (IET) at the HSR Hochschule für Technik (Rapperswil, Switzerland; www.iet.hsr.ch) is working on two E.U. PTG projects, says Sandra Moebus, manager, Power-to-Gas. Implemented in the E.U. project Pentagon of the framework program Horizon 2020, the project High Efficiency Power-to-Methane Pilot (HEPP) aims to boost the PTG efficiency from 55% to 70% for an industrial scale of megawatts. To achieve this efficiency boost, the researchers are using a high-temperature electrolyzer (around 600°C) to make H_2, which will then be used in a methanation reactor to produce CH_4. Improvements in efficiency will be achieved by tight heat integration — using the heat from the exothermic methanation reaction to heat up water for the steam electrolyzer, Moebus says. Also, a new methanation catalyst is being tested that absorbs water, a product of the equilibrium reaction, to boost the product yield. A membrane-separation process is also being used for gas purification. The 10-kW pilot plant, located in Rapperswil, was inagurated last October, and the first production of methane is expected this month, with operation to run through 2019.

In a second E.U.-funded project, dubbed STORE&GO, three different PTG technologies will be investigated, with pilot units located in Germany, Italy and Switzerland. The first two units started last year, and the third will start up this month in Switzerland, says Moebus. These units use conventional electrolyzers, and the goal is to compare the performance and economics of the different technologies, she says.

Meanwhile, last February, 75% efficiency was first achieved in a PTG project coordinated by the Karlsruhe Institute of Technology (KIT; Germany; www.kit.edu). The four-year, €3.8-million Helmeth project, funded under the E.U.'s 7th Framework Program, achieved this milestone by optimal use of process heat from the methanation for heating the water used in the high-temperature (about 800°C) solid-oxide cell (SOC) electrolyzer of Sunfire GmbH (Dresden, Germany: www.sunfire.com). The goal of the project is to achieve 80% efficiency on the industrial scale.

Taking a completely different PTG approach is Viessmann Werke GmbH & Co, KG (Allendorf, Germany; www.viessmann.com). Its subsidiary MicrobEnergy GmbH (Schwandorf, Germany; www.microbenergy.com) has been developing and implementing various PTG projects involving its biological methanation process known as BION, in which archaea microorganisms produce CH_4 from H_2 and CO_2. Since 2015, the first PTG plant with biological methanation, located in Allendorf (Figure 3), has been producing methane that is directly fed into the gas grid for storage and distribution, says marketing manager Eva Sonnleitnerworking. The company is currently involved in a number of PTX projects all over Europe. "The storage of renewable electricity, the production green gases and the upgrading of CO_2-rich sources are our main scopes," says Sonnleitnerworking. "In these projects, we expect a planning and realization period, from initial contact until commissioning, of two to three years. These are plants in the megawatt range. For individual projects, we are close to the official announcement now," she says.

Power-to-liquids

"Many recent studies predict an ongoing dependency on carbon-based fuels," says Tim Böltken, managing director, Ineretec GmbH (Karlsruhe, Germany; https://ineratec.de). "In this context, we are absolutely convinced that power-to-fuels, such as gaseous energy carriers (PTG, especially power-to-methane), as well as liquid energy carriers, such as gasoline, kerosene and diesel (power-to-liquids via Fischer-Tropsch (F-T) synthesis) will be one of the foundations for the coupling of the sectors transport, energy and industry," says Böltken.

Ineratec — a spinoff company from KIT — has developed chemical microstructured reactors that are suit-

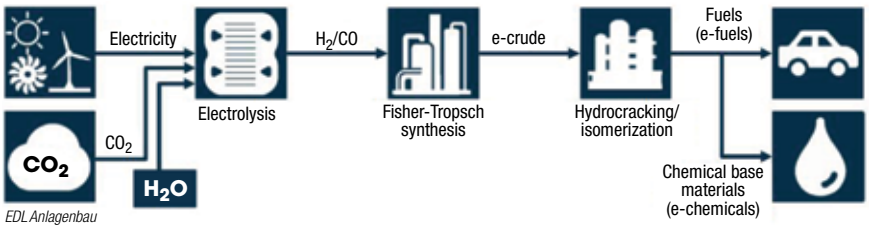

FIGURE 4. Scheduled to start up in 2020, the power-to-liquids plant in Norway will use hydroelectric power to make H_2 from water, the water-shift reaction to make CO from CO_2, and F-T synthesis to make liquid fuels and waxes

able for integration into containerized plants. Because they are modular, the plants can be integrated into various energy related sectors. The core of the synthesis reactors is microstructured, which provides a large surface area for heat and mass transfer. Reactors are available for methanation, F-T synthesis and methanol synthesis.

The company is participating in numerous public and industrial PTX projects with various foci, both on the national and international level, Bölton continues. "Objectives of these projects are, for example, the scaleup of the technology in the megawatt class and the industrial production of liquid fuels for transportation and aviation. In the future we will standardize our modules in order to accelerate the realization of the PTX plants and focus on the energy-efficient integration of our synthesis technology in industrial sites."

"We have successfully delivered a PTX plant with a 250-kW electrolyzer capacity," Böltken continues. "Now we are building the first plant in megawatt class and we are currently taking the step from manufacturing to serial production. The interest of the industry, especially the energy and the gas industry, is very high: we just received [last November] the innovation award of the German gas industry."

Ineratec is already commercializing its technology, having installed plants in Spain and Switzerland. A large megawatt facility will be realized in 2019, with even larger capacities to come soon. By 2021, it is very likely the company will have sold more than 50 plants worldwide, says Böltken.

Meanwhile, EDL Anlagenbau GmbH (Leipzig, Germany; www.edl.poerner.de) is involved in several PTX projects, mainly for the production of fuels and chemicals, with capacities ranging from 65 to 8,000 tons. These PTX projects use the CO_2 direct air-capture technology from Climeworks (Hinwill/Zurich, Switzerland; www.climeworks.com) for the CO_2 source. One key technology driver for PTX, on the production side of synthesis gas (syngas) from CO_2 and H_2O, is the combination of the steam electrolysis with the CO_2 conversion to CO in a single electrolysis cell. Sunfire's solid-oxide electrolysis cell (SOEC) technology will be used in EDL's upcoming projects for the first time for syngas production. The syngas is converted to paraffinic hydrocarbons (e-crude) using a F-T process. For smaller capacities, EDL will rely on the F-T technology from Ineratec. The e-crude is converted to finished products, such as fuels or waxes, by a combination of catalytic process steps.

One PTX project for which EDL has recently completed the conceptual design phase, together with its strategic partners Climeworks and Sunfire, is the Norwegian Nordic Blue Crude (NBC) PTL project to be implemented in Norway, in the industrial park of Heroya, located 140 km southeast of Oslo. The PTL plant will produce 8,000 ton/yr of raw e-fuels and e-waxes from renewable hydropower (Figure 4). It is planned to start up in 2022.

Three other PTX projects cover the production of e-Jet A1 aviation fuel in modular plants, with capacities of 65, 130 and 260 ton/yr. These plants are installed in close vicinity to local airports. The engineering for all three projects will start in 2019, says EDL. ■

Gerald Ondrey

The Balanced Burner

Modern combustion technologies help processors safely meet emissions standards, while optimizing the process

IN BRIEF

A BALANCING ACT
BETTER BURNERS
CONTROLS FOR SAFETY & OPTIMIZATION

Combustion is integral to many chemical processes; however, it is not without challenges. Safety is, of course, always paramount when it comes to fired equipment and constantly changing and tightening permissible emission levels are becoming more arduous to meet. If these concerns aren't enough, higher efficiencies, more flexibility and greater reliability from combustion equipment are also required. As a result, combustion often becomes a difficult balancing act.

To help meet these needs, burners that offer the lowest possible emissions are being made available and are usually combined with a burner management system that offers top-notch safety. More recently, controls, monitoring systems and instrumentation are being employed to provide greater efficiency and reliability. Together, this equipment helps optimize today's combustion processes.

A balancing act

"Safety, environmental performance and reliability are the primary challenges when it comes to designing and implementing any combustion system, and a lot of these requirements revolve around prescribed standards or internal guidelines," explains John Becker, national sales manager — business development, with Profire Energy (Lindon, Utah; www.profireenergy.com). "All these factors dovetail each other. Safety is critical and necessary and will never be sacrificed to gain efficiency. While safety is the common denominator for combustion systems, processors are often faced with balancing the efficiency, flexibility and reliability of the fired device with its environmental impact."

Further adding to the challenge is the fact that there are many combustion processes in a chemical plant, each with a different purpose and goal. "There is a large variety of combustion applications in a chemical plant, which leads to different challenges that depend upon the purpose of the process," says Paolo Schmidt-Holzmann, department manager, Proposals Combustion Systems, with Steinmüller Engineering GmbH (Gummersbach, Germany; www.steinmueller.com).

John Zink Hamworthy Combustion

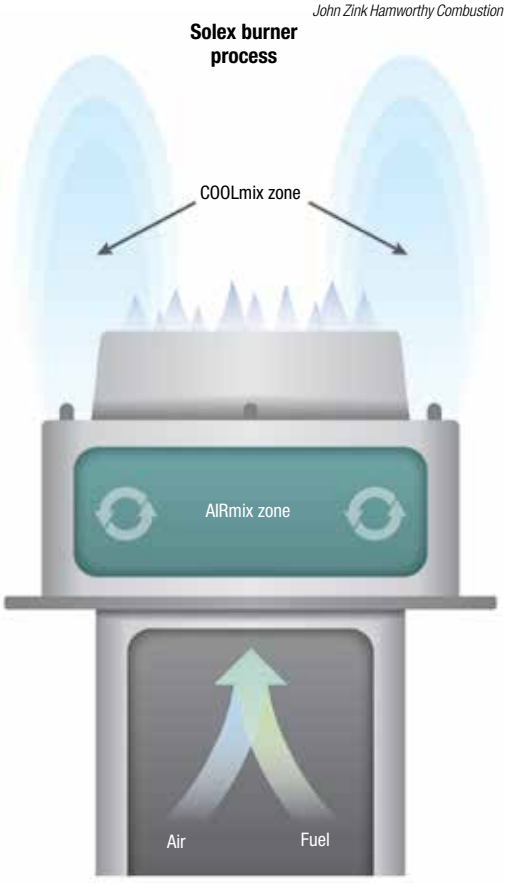

FIGURE 1. The Solex burner can achieve 5 ppm NOx emissions across a range of fuel compositions and furnace temperatures. The burner is designed with two significant combustion zones to achieve these emissions levels from start-up to full-capacity with minimal CO emissions

"But the overriding factors that govern all combustion projects include safety, reliability and flexibility. Whether it is a change implemented on existing components or the installation of new components, operation of the plant under safe conditions must be certain."

Schmidt-Holzmann continues to say that efficiency, reliability, low emissions and flexibility are also important goals and these can change, depending on the requirements of the project. "Following safety, other priorities depend upon the task you would like to fulfill. For example, in a residue combustion project, the reliability and availability might be of higher value than fuel conversion efficiency. But in cases where very specific gas streams are produced with very specific characteristics,

the fuel efficiency and reliability might be the focus."

So finding the proper balance for each combustion process becomes dependent upon designing and installing the appropriate technologies. "It's not an easy task," says Profire Energy's Becker. "Safety is at the top of the list of concerns, so there are governing bodies and internally developed guidelines that provide direction and standards to follow. Then, you must add in the aspects of the [U.S.] Environmental Protection Agency (EPA: Washington, D.C.; www.epa.gov), plant owners and third-party agencies that have requirements about what is allowed out of the stack and that has led to the design of better burners that reduce NOx and CO production."

He continues: "So when you look at the environmental aspects, you look at the burner. When you look at safety, efficiency and optimization, that's where automation and controls come in to fine tune the process based on temperatures or other factors tied to the fired devices."

Siemens

FIGURE 2. Siemens SIS Compact is a stand-alone, safety PLC certified solution for process safety that was designed specifically for use in safety-critical applications such as burner management systems

Better burners

Burners are evolving every year to include new techniques and designs with different orifices, features and fuel-ratio measurement technologies to help achieve better, more environmentally friendly combustion, which is a necessity in the ever-changing environmental landscape.

"One of the biggest challenges is that the emission rates around the world for NOx and CO are getting lower and they vary by regions around the world, as well as locations within those regions," says Rex Isaacs, chief technical officer with Zeeco (Broken Arrow, Okla.; www.zeeco.com). "As a result, burner technology is getting better from all manufacturers. Often this involves looking at ways to pull in more flue-gas for circulation, which lowers NOx emissions. Some manufacturers look

John Zink Hamworthy Combustion

FIGURE 3. The ZoloSCAN employs wavelength – multiplexed tunable diode laser absorption spectroscopy, which combines lasers and fiber optics to measure and profile the combustion zone across multiple paths. The information provided by these in-situ measurements allows operators to balance, optimize and automate combustion for higher efficiency along with lower NOx, CO and CO_2 emissions

at lean premixing to achieve lower NOx emissions. Burners are modified for more fluegas, which also helps lower emissions during start up and lower CO emissions."

Zeeco's Free Jet Power Burner is one such example. The burner uses technology that adds fuel staging to the Venturi design and free jet mixing theory, which reduces emissions in some applications to as low as single-digit numbers. The clean, fuel-conservative system operates on refinery gas, natural gas or dual fuels and offers 9 parts per million (ppm) NOx, sub-50 ppm CO with minimal external fluegas recirculation (EFGR) or 30 ppm NOx potential without EFGR, as well as a 20:1 fuel turndown potential. When coupled with the company's burner management system, it ensures the process remains in compliance while maximizing efficiency and eliminating downtime due to aging controls.

Often industry emissions regulations force users to adopt fluegas treatment solutions, such as selective catalytic reduction (SCR) systems; however, the new Solex burner from John Zink Hamworthy Combustion (Tulsa, Okla.; www.johnzinkhamworthy.com), can achieve 5 ppm NOx emissions across a range of fuel compositions and furnace temperatures (Figure 1). The burner is designed with two significant combustion zones to achieve these emissions levels from startup to full-capacity with minimal CO emissions. In addition, it produces compact flame lengths, which solve many issues ultra-low NOx burner technologies face.

"This is the next step-change in burner technology that can be applied to reduce emissions in process heaters," says Eric Gebhard, senior sales engineer, with John Zink Hamworthy Combustion. "And, it has been strategically developed to eliminate the need to apply an SCR. The burner is designed with two combustion zones that are dynamically operated to achieve these emissions through the entire operating range."

Controls for safety & optimization

More and more, automation and controls are being employed to improve safety and optimize the combustion process. For example, burner management systems are employed on combustion processes to facilitate safety, while combustion control systems are used to meter fuel and airflows to increase efficiency.

"Burner management systems take care of safety issues, such as sequencing the lighting of the burners, going through a safe startup process, monitoring to make sure everything is within limits and automating emergency shutdown, if necessary," says Jack Valentine, general manager, with Pacific Combustion Engineering, a strategic division of Nationwide Boiler (Washougal, Wash.; www.nationwideboiler.com). "Combustion control systems control the fuel-to-air ratio of the burner, which provides better control, more efficiency and a more economical operating system. They are separate systems but they have to work in conjunction with each other."

Because burner management systems provide safety, it is important to protect them against different types of failures, says Charles Fialkowski, director of process safety with Siemens (Harleysville, Pa.; www.siemens.com), including everything from memory failure to corruption to lost I/O signals and communications to the application program being compromised. "In the past, designers used to apply generic equipment with costly external solutions to protect against these known failure modes, but today, modern, safety-certified equipment is able to handle and protect against these events. Safety-certified equipment has these safeguards built in, tested and certified for the program you're running," he says.

Siemens offers its Simatic SIS Compact as a stand-alone, safety PLC (programmable logic controller) certified solution for process safety that was designed specifically for use in safety-critical applications, such as burner management systems (Figure 2). The system leverages field-proven and certified Simatic hardware and software components, which automatically provide dedicated Safety Instrumented Systems (SIS) functionality. The SIS monitors critical processes and performs immediate and automatic responses to the process when a problem occurs without the complexity of an integrated distributed control system (DCS) solution.

Profire has developed its 3100 platform to provide an alternative to traditional burner management systems with a PLC, modular-based design that allows quick configuration, intuitive alarm and a packaged burner management system, says Becker. A module is made up of an enclosure and one or more cards. Each module is certified with the appropriate regulatory bodies to ensure that installation is as quick as possible. The entire system is made up of modules and is intended to expand to accommodate future needs and applications. It can be used to control multiple burners and manage a single appliance or to control multiple pilots and manage a single appliance via one user interface. Up to 32 modules can be combined to control a variety of natural draft appliances from a single user interface. Profire's integrated I/O technology can also be used to take control of specific forced-air applications.

In addition to these safety systems, adds Zeeco's Isaacs, more chemi-

Yokogawa

FIGURE 4. TDLS analyzers deliver direct and realtime measurements using long-path average measurement across the furnace. This can be used to control the air-to-fuel ratio and to control CO to ensure safety

cal processors are adding additional layers of safety to their burners and burner management systems. "Ten years ago it was not common to see flame scanners on process burners in chemical plants, but now we are starting to see scanners on each burner," he says. "Flame monitoring is linked to the control room so that they can see that each individual burner is firing to ensure safety. In addition, electronic ignition can be used with flame scanners so they can light the burners from the control room and ensure that the flame is on via the flame scanners before operators go out to the furnace. This isn't the norm yet, but it is a trend processors are starting to explore more readily."

John Zink Hamworthy Combustion's Gebhard agrees: "We are seeing customers going to more automated systems and it is mostly safety driven. However, we are also seeing processors adding more control and sensors to help better optimize the overall performance of their units."

As such, the company recently launched a "Smart Combustion" initiative, which includes a variety of digital solutions that can be used to further optimize combustion systems. One such technology is the ZoloSCAN combustion monitoring and diagnostic system, which is used for combustion optimization (Figure 3). The technology employs wavelength–multiplexed, tunable-diode-laser absorption spectroscopy (WM-TDLAS), which combines lasers and fiber optics to measure and profile the combustion zone across multiple paths. The information provided by these in-situ measurements allows operators to balance, optimize and automate combustion for higher efficiency, along with lower NOx, CO and CO_2 emissions. "This results in improved efficiency and higher process yield while increasing equipment life," says Gebhard.

Masanari Yokogawa, manager of the Analytical Product Sales Division in the IA Products and Service Business Headquarters at Yokogawa (Tokyo, Japan; www.yokogawa.com), adds that this type of optimization is important. "Combustion systems use large quantities of costly fuel, so operation managers responsible for large furnaces are faced with the triple challenge of minimizing costs while maximizing output and ensuring safety at all times," he says. "Currently, air-to-fuel ratio control is only used on a few systems, and fewer still compensate for changing fuel composition. Conventional technology typically only provides automated control of the fuel supply and not the air supply, so excess air is often used in the combustion process. This increases costs, reduces efficiency and creates an unsafe situation."

The ability to continually measure methane, O_2 and CO levels is critical to maximizing efficiency and safety. Conventional analyzer technologies only provide spot measurement, so they can't capture the combustion

condition throughout the furnace. Instead, he says, the recommended method is to use a tunable-diode-laser-spectroscopy (TDLS) analyzer in the tail of the radiant section of a combustion furnace to measure O_2 (Figure 4). "TDLS analyzers deliver direct and realtime measurements using long-path average measurement across the furnace. This can be used to control the air-to-fuel ratio and to control CO to ensure safety," he says.

While most fired heaters use natural draft rather than a forced air supply, continuous measurement enables proactive airflow control, he says. To control combustion in a fired heater, the fuel flow and arch draft can be managed through the existing plant DCS or other logic solver, while combustion airflow can be controlled directly by a CO override function. "TDLS technology provides the data required for real-time control of the combustion process," says Yokogawa. "This safely minimizes excess O_2 concentration, resulting in higher heat-transfer efficiency and longer maintenance cycles for the furnace."

And, for specific combustion issues where very accurate temperature measurements across a wide dynamic range are required in order to optimize a combustion process, thermal imaging may be a useful tool, says Christopher Leonard, director development and product management with Ametek Land (Dronfield, England; www.ametek-land.com). The company's NIR-B 3XR near infrared borescope can be used to help optimize thermally driven processes. For example in the oil-and-gas industry within steam reformer applications, says Leonard, the temperature range between the furnace walls and reaction tubes containing the catalyst and reactants can be over a large temperature range. The reaction tubes in this application are typically made from an expensive nickel alloy, which, if the process is run just 10% below the design temperature, can reduce production capacity, yet running just 59°F too high can reduce the life of the reaction tubes by 50%. This makes it critical to use accurate temperature measurement to maximize productivity and maintain the integrity of the asset, which over the range of 1,112 to 3,272°F can be a major challenge.

In addition, he states, another example is in the glass industry, where the instrument gives operators and system builders further insight into the dynamics of glass melt tanks. The high-quality thermal images provided by the instrument enable the identification of burner imbalance, which can be used to optimize combustion and control NOx emissions, helping to reduce fuel bills and maintain compliance with environmental targets.

At the end of the day, all processors are looking to safely run combustion processes while also maintaining environmental compliance and improving their bottom line via efficiency, reliability and flexibility. Today's combustion solutions may be key to doing just that. ■

Chemical Engineering Staff

Focus on Handling Powders and Bulk Solids

Vibrator-mounting system requires no welding or bolting

This versatile mounting solution (photo) allows operators to quickly and easily attach the company's compact, pneumatic, piston-type Bantam Series vibrators directly to process vessels, such as bins, hoppers and chutes, with no need for welding, drilling or tapping. Designed to soundly adhere to circumferences of less than 24 in. (610 mm), the Stick-and-Shake Mounting System provides all the necessary components, including a stainless-steel faceplate, mounting studs, lock washers and hex nuts, two-component adhesive cartridge, mixing nozzle, double-sided adhesive strips and an easy-to-use applicator gun. The glue adheres to nearly every common industrial structural material, including painted metals, polycarbonate, acrylics and acrylonitrile butadiene styrene (ABS) plastics, says the company. The system is useful for small hoppers, specialized vessels or cramped spaces where traditional vibration brackets won't fit, to keep powders and pellets free-flowing. — *Martin Vibration Systems & Solutions, Marine City, Mich.*
www.shake-it.com

This level detector is suitable for use in dusty environments

The Dynatrol CL10DJ Level Detection System (photo) handles products ranging from low-density flakes and powders to heavy granules and pellets. It is available in abrasion-resistant 400 Series stainless steel and with Hastelloy C-276 construction for corrosive chemical service. The device functions reliably in dusty environments, says the company, and specialized units can be used for applications with temperatures in excess of 500°F. All detectors are factory calibrated and thus do not require any field calibration before installation. The related control unit can be used to actuate alarms, indicator lights or process control equipment. — *Automation Products, Dynatrol Div., Houston*
www.dynatrolusa.com

These dust collectors are designed for easy maintenance

This company offers an array of dust, fume and mist collectors for a variety of chemical process industries (CPI) applications. The latest connected solution (photo) monitors dust and fume-collection equipment promptt owners to manage preventive maintenance actions cost-effectively. Using cloud connectivity, the system gathers realtime data via sensors installed on an operating collection system, and using the company's proprietary analytics, the system relays actionable insights back to the owner via a Web-based dashboard and text or email alerts, says the company. This new enabling technology can be installed on existing or new industrial dust and fume equipment. — *Donaldson Filtration Solutions, Bloomington, Minn.*
www.donaldson.com

Customize your pneumatic conveying system

A properly designed and custom-engineered Dynamic Air pneumatic conveying system (photo) can help process operators to move dry, granular materials gently and reliably with minimal product degradation or system wear. This company has developed 16 different pneumatic conveying concepts, using both pressure and vacuum, for the appropriate, cost-effective handing of a diverse array of dry bulk solids. Such flexibility allows for system designs that fit process-specific needs, under a wide array of operating conditions (which can greatly impact the successful handling of powders and bulk solids). — *Dynamic Air Conveying Systems, St. Paul, Minn.*
www.dynamicair.com

Martin Vibration Systems & Solutions

Automation Products

Donaldson Filtration Solutions

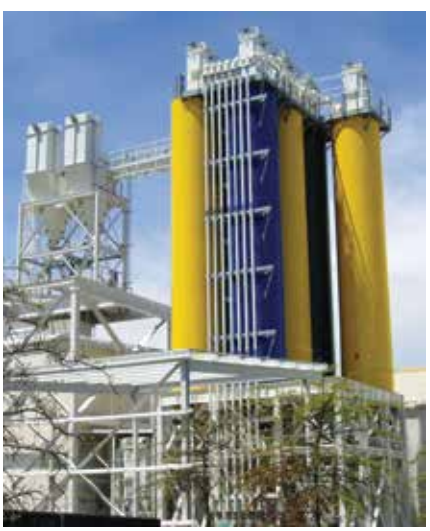

Dynamic Air

Note: For more information, circle the 3-digit number on p. 62, or use the website designation.

Lödige Process Technology

This particle-size monitoring portfolio continues to grow

This company recently acquired Malvern's Panalytical's Mastersizer 3000 particle-sizing instrument. This laser-diffraction analyzer delivers rapid, accurate particle-size distributions with minimal effort, says the company. This small-footprint device provides accurate measurements of particles with sizes in the nanometer-to-millimeter range. — *Particle Testing Authority, Div. of Micromeritics Instrument Corp., Norcross, Ga.*
www.particletesting.com

The Witte Co.

This device blends hard-to-handle, abrasive solids

This company offers an array of mixing systems for the hard-to-handle bulk solids (including powdery, finely crystalline and fibrous components) that are typically used in braking systems. These mixing systems combine specifically designed mixing tools and choppers to ensure the required mix homogeneity and proper dispersion of fibers in the final blend. The Ploughshare Mixer (photo) is designed to both mix these components in a homogeneous manner, and disperse the fibrous components (typically aramid fibers introduced to the mixer as pulp) properly. — *Lödige Process Technology, Paderborn, Germany*
www.loedige.de

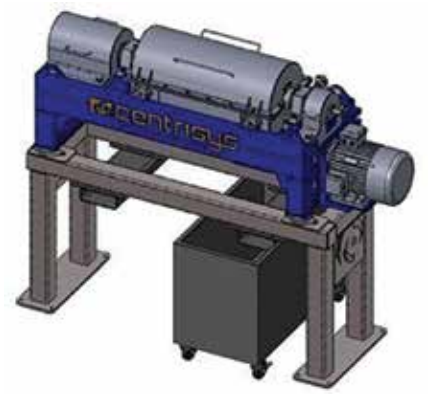

Centrisys

Integral baghouse helps this dryer to contain fine particles

This vibrating fluidized-bed dryer (photo) has an integral baghouse for dust collection that is positioned directly above the fluidized-bed drying zone. This configuration allows 100% of the fine particles (below 250 µm) entrained in the airstream to be contained in the drying system as product, rather than being collected and removed as waste, says the manufacturer. The space-saving system is designed for closed-cycle drying applications that require a nitrogen purge or solvent recovery. — *The Witte Co., Washington, N.J.*
www.witte.com

Munson Machinery

This small centrifuge enables continuous processing

The CS6-4 dewatering centrifuge (photo) is the company's smallest centrifuge to date. The CS6-4 bridges the gap between benchtop studies and full-scale systems. The scaleable CS6-4 continuously treats flows from 4 to 10 gal/min, making this centrifuge a better alternative to conventional laboratory centrifuges that typically process samples in batches. — *Centrisys Corp., Kenosha, Wis.*
www.centrisys.com

Custom-engineered systems can optimize bulk-bag filling

The full line of bulk bag handling equipment includes the company's Bulk Bag Unloading Systems and Bulk Bag Filling Stations. The filling systems include scales, variable-speed filling devices, multiple filling lines, bag vibration and more, depending on the needs of the application. These custom-designed systems can incorporate many features, such as a bag lift hoist (electric or pneumatic), bag paddle massagers, material lump breaker, material weighing and dosing equipment, dust-containment options, fixed or portable, floor or through-floor mounting, and can be operated as a standalone system or integrated into a material-batching system. Several process control and automation options are available. — *Sterling Systems & Controls Inc., Sterling, Ill.*
www.sterlingcontrols.com

High-capacity classifying cutter has a 6-ft-dia. inlet

The Magnum 72-AR Screen Classifying Cutter system (photo) has an inlet throat that measures 72 in. x 22.5 in., and a rotor with an 18-in. overall dia. It reduces the size of hard-to-handle abrasive materials, such as gypsum, metal scrap and fiberglass, at high rates. The ultra-heavy-duty unit features a progressively stacked array of interconnected, abrasion-resistant cutter tip holders to continuously shear oversize materials against the cutting knives. Operating at speeds from 30 to 3,600 rpm, with a 40+ hp (30+ kW) motor, the cutter can process up to 720 ft^3/h, depending on the application, with little or no fines, and virtually no heat generation, says the company. Discharge is via gravity, pneumatic collection or independently powered belt or screw conveyor. — *Munson Machinery Corp., Utica, N.Y.*
www.munsonmachinery.com ■

Suzanne Shelley

New Products

This AODD pump has multiple mounting orientations

This company has extended its line of specialty air-operated double-diaphragm (AODD) pumps with the addition of the new V150 13-mm Velocity Series pump (photo). Featuring a unique detachable mounting foot, Velocity Series pumps can easily be reoriented into a vertical or horizontal position with multiple inlet and discharge port options. With this design, the pump can be installed in multiple orientations, a critical consideration for systems and skids. The Velocity Series is available in 13- and 6-mm sizes, and features a bore-seal design, which eliminates leaks that can result from torque decay. It also delivers improved dry-suction lift up to 4.3 m in the 6-mm size and 5.1 m in the 13-mm size. The Velocity Series pumps also incorporate a proven and simple air distribution system (ADS) with only two moving parts that reduces the risk of downtime for long-term reliability. — *Wilden Pump and Engineering, part of PSG, a Dover company, Grand Terrace, Calif.*
www.wildenpump.com

A new generation of valve positioners

At Valve World Expo (Düsseldorf, Germany; November 27–29), this company introduced two new positioners from the Series 3730: Trovis 3730-1 and Trovis 3730-3. The new positioners (photo) for 4–20-mA applications combine the latest technological developments with the proven device base known from the Type 3730-1 and Type 3730-3 predecessor models. Both positioners are particularly rugged thanks to their no-wear, non-contact travel-sensing system. Two inductive-limit contacts are available to reliably indicate both valve end positions. At the same time, the positioners' air consumption has been reduced considerably by upgrading the pneumatics block. The 3730-3 communicates over the HART 7 protocol and comes with the proven EXPERT-plus valve diagnostics with optimized features. To facilitate operation, the positioners are fitted with a plain-text display that indicates the condensed state according to Namur, measured values, start-up settings, as well as messages in English or German. The 3730-3 is additionally ready for interconnection with Sam Chemicals, the cloud-based business application for the process industry. — *Samson AG, Frankfurt am Main, Germany*
www.samson.de

Slash the total cost of ownership with this new aseptic valve

Reducing the total cost of ownership is paramount for manufacturers of dairy, food and beverage products. Using the new Aseptic Mixproof Valve (photo) instead of alternatives can deliver a total cost saving of up to 45% for manufacturers using aseptic processing. Estimated savings are based on a comparison of capital expenses and maintenance costs of an aseptic 2.5-in. valve over a five-year period if service is done onsite. If maintenance is done offsite by a third-party provider, competing technologies become even more expensive. Instead of steel bellows, this new aseptic double-seat valve uses a well-proven diaphragm with a PTFE face and reinforced EPDM backing. This drastically reduces the total cost of ownership of a double-seat valve, yet still ensures the hermetic seal required for sterile processing. The optimized design of the Aseptic Mixproof Valve makes cleaning and sterilization easier, proven by computational fluid dynamics (CFD) simulations. — *Alfa Laval Kolding A/S, Kolding, Denmark*
www.alfalaval.com

A new control system for smart control of separators

The new Metris addIQ (photo) is a state-of-the-art digital control system for separation applications. Metris addIQ provides added value by enhancing availability and minimizing production costs through increased equipment efficiency and fewer operating errors. Metris addIQ control systems enable users to analyze and optimize separation processes. Features like predictive analysis allow operators to optimize availability and take preventive action to avoid downtime. Capacity and quality are easy to control and enhance with customizable systems. The Metris addIQ con-

Wilden Pump and Engineering

Samson

Alfa Laval Kolding

Andritz Group

trol system is based on the latest PLC (programmable logic control) and HMI (human-machine interface) technologies and has an integrated fail-safe system. The company offers various Metris addIQ packages, thus allowing every business involved in solid/liquid separation to optimize its performance — whether a huge municipal wastewater operation or a niche family brewery. — *Andritz Group, Graz, Austria*
www.andritz.com

This new digital float switch uses transistors instead of reeds

Said to be the first instrument of its kind, this company has launched a float switch with a PNP/NPN output signal. The model GLS-1000 (photo) detects the level of liquids with an accuracy of ≤ 1 mm. The digitized float-measuring principle of the new level switch is implemented using semiconductor sensors. These enable an unlimited number of switching cycles. Users can define up to four switch points with a minimum distance of only 2.5 mm. Thus, the instrument reacts to even the smallest changes in level. At the same time, the GLS-1000 can monitor the temperature of the medium via a temperature output with a Pt100/Pt1000 resistance thermometer. With the GLS-1000, traditional PNP/NPN limit level switches can now also be replaced by a float switch. — *WIKA Alexander Wiegand SE & Co. KG, Klingenberg/Germany*
www.wika.de


Andritz Group

Fast, simple and accurate on-the-go steam-trap testing

The SAGE UMT (photo) is a wireless, hand-held steam-trap-testing solution that enables accurate, on-the-go testing of steam-trap performance. SAGE UMT leverages radio-frequency identification (RFID) technology to quickly locate and identify steam traps. Its piezoelectric acoustic and non-contact infrared (IR) temperature sensor delivers accurate and precise detection to identify steam traps that are performing in good, cold, blow-through and leaking conditions. SAGE UMT integrates with the company's SAGE Smart Thermal Utility System Management platform and syncs wirelessly via Bluetooth to the SAGE Mobile app to deliver realtime diagnostics and eliminate manual data entry associated with offline steam-trap survey data collection. Data can be instantly uploaded to the cloud by SAGE for secure storage and ongoing steam-trap analysis to support system-wide utility management. — *Armstrong International, Three Rivers, Mich.*
www.armstronginternational.com ■


Armstrong International

Gerald Ondrey

Pressure Measurement for Real Gases

Department Editor: Scott Jenkins

The ideal gas law ($PV = nRT$), relating molar volume of a gas to pressure and temperature, is predicated on two assumptions: 1) that the volume occupied by the gas molecules is negligible compared to the volume of the vessel; and 2) that no intermolecular attractive forces are present. In reality, these assumptions limit the applicability of the ideal gas law, especially at higher pressures and densities, and low temperatures. For accurate calculations of *PVT* behavior of real gases in industrial settings, engineers have developed many equations of state (EoS) for various conditions. This reference provides information on several key cubic equations of state that attempt to accurately predict real gas behavior.

Van der Waals equation

In 1873, Dutch physicist Johannes D. Van der Waals noted the non-ideality of gases and proposed modifications to the ideal gas law that addressed the size of gas molecules and accounted for the strength of the mutual attraction among them. He introduced the two constants (*a* and *b*) to the ideal gas law to correct for intermolecular attractive forces (*a*) and for finite molecular size (*b*) (Equation (1)). The coefficients *a* and *b* are characteristic of each individual gas and were determined experimentally from the critical temperature and pressure.

$$\left[P + a\left(\frac{n}{V}\right)^2\right](V - nb) = nRT \qquad (1)$$

The Van der Waals (VdW) EoS is not sufficiently accurate for most industrial applications, but has provided a platform for many important refinements that better model fluids at different *P* and *T* conditions.

The VdW equation, along with its subsequent modifications, are referred to as cubic EoS, because they can be written as cubic (as opposed to linear or quadratic) functions of molar volume. Cubic EoS have the advantages of simplicity and tunability, but also have disadvantages, so other types of EoS, such as molecular-based and virial (not discussed here) have also been developed.

No single equation of state can correctly predict pressure, volume and temperature behavior for all types of gases, including mixtures, under all possible conditions.

Nomenclature

P pressure, bar
V volume, cm^3/mol
T temperature, K
R universal gas constant, 83.14 cm^3 ·bar/mol· K
$a(T)$, b substance-specific constants, dependent on T
ω acentric factor for given species
V_m molar volume
T_c critical temperature, K
P_c critical pressure, bars

Redlich-Kwong equation

In 1949, Otto Redlich and J. Kwong developed what would become a widely used modification to the VdW equation (Equation (2)), using the coefficients for *a* and *b* found in VdW.

$$P = \frac{RT}{V_m - b} - \frac{a}{\sqrt{T}\,V_m(V_m + b)} \qquad (2)$$

The Redlich-Kwong (RK) equation can be expressed in terms of the compressibility factor (*Z*), a dimensionless ratio of the product of pressure and specific volume to the product of gas constant and temperature (Equation (3)).

$$Z = (PV)\,/\,(RT) \quad \text{or} \quad Z = v_{actual}\,/\,v_{ideal} \qquad (3)$$

The compressibility factor is a measure of deviation from the ideal-gas behavior. For ideal gases, *Z* is equal to one, and can be either greater or less than one for real gases. The further the value of *Z* lies away from one, the greater the degree of deviation from ideal-gas behavior.

The RK equation has itself been modified by many subsequent researchers, as they sought to widen its applicability or improve its accuracy at specific conditions. A highly used modification of the RK equation was developed by G. Soave in 1972. Soave's contribution was to express the attractive term from the VdW equation not only as a function of temperature, but also as a function of the sphericity of the molecule. This is accomplished by including a term α that includes an acentric factor for the species of gas (SRK equation; Equation (4)). The acentric factor α is a measure of non-sphericity and is specific to each gas species.

$$P = \frac{RT}{V_m - b} - \frac{a\,\alpha}{V_m(V_m + b)} \qquad (4)$$

$\alpha = (1 + (0.48508 + 1.55171\omega - 0.15613\omega^2)$
$T_r = T/T_c$
$(1 - T_r^{0.5}))^2$
$T_r = T/T_c$

Peng-Robinson

The SRK equation was further modified by other researchers, and one of the most useful modifications was developed in 1976 at the University of Alberta by Ding-yu Peng and Donald Robinson. The Peng-Robinson (PR) equation recalculated the α function and modified the volume dependency of the attractive term.

$$P = \frac{RT}{V_m - b} - \frac{a\alpha}{V_m^2 + 2bV_m - b^2}$$

$$a \approx 0.45724\frac{R^2T_c^2}{P_c}$$

$$b \approx 0.07780\frac{RT_C}{P_c}$$

$$\alpha = \left(1 + \kappa\left(1 - T_r^{\frac{1}{2}}\right)\right)^2$$

$$\kappa = 0.37464 + 1.54226\omega - 0.26992\omega^2$$

$$T_r = \frac{T}{T_c}$$

References

1. Valderrama, J.O., The state of the cubic equations of state, *Ind. Eng. Chem. Res.*, 42, pp. 1,603-1,618, 2003.
2. Aleksandrov, A.A., PVT Relationships, Thermopedia: A-Z guide to thermodynamics, February 2011, accessed at http://www.thermopedia.com/content/1067/
3. Huang, M. and Gramoll, K., Ideal Gas Equation of State, University of Oklahoma, Thermodynamics ebook, chapter 2, www.ecourses.ou.edu/

HDPE Production via Slurry-Loop Process

By Intratec Solutions

High-density polyethylene (HDPE) is one of the three main types of polyethylene, and is among the most commonly used polymers worldwide. HDPE applications include blow-molding, injection molding, blown and cast film, pipes and tubing, wire and cable coating and more.

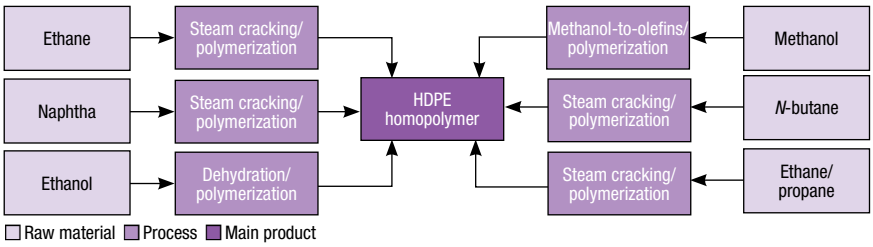

FIGURE 2. Production pathways for HDPE are available for a number of different starting materials

The process

The following paragraphs describe a slurry-loop process for HDPE homopolymer production. Figure 1 presents a simplified flow diagram.

Feed Preparation. This area comprises a catalyst activation system (fluidized-bed activator) and fixed-bed treaters for purification of ethylene monomer and isobutane, which are used as diluent in the polymerization.

Polymerization. In a loop reactor, the monomers and the catalyst suspension are mixed and circulated. As the polymer particles precipitate, they do not dissolve in the slurry. Cooling water in the reactor jacket removes reaction heat. The slurry is continuously discharged to a flash chamber, for removing residual monomers. The polymer product and residual dissolved hydrocarbons are fed to the purge column.

Separation. The flashed stream passes through a bag filter for polymer fines removal. While the fines are sent to the purge column, the vapor stream is sent to the diluent recovery unit. In diluent recovery, the vapors from the flash chamber are sent to a first partial condenser, where heavier hydrocarbons and part of the diluent are condensed and transferred to the heavies column. The uncondensed stream passes through a second condenser at lower temperatures for recovering the diluent, which is reused in the process. The remaining gaseous stream is sent to the heavies column.

In the purge column, the residual hydrocarbons are stripped from the polymer product with heated nitrogen gas. The resulting purge gas is sent to an isobutane-nitrogen recovery unit. Nitrogen is recovered and reused in the column, while gaseous isobutane is transferred to the heavies column.

In the heavies column, isobutane and unreacted monomers are separated in the overhead and sent to the lights column. Fresh isobutane make-up is also routed to the lights column for removing light impurities. The bottom product from this column, an olefin-free isobutane, is recycled to the feed-preparation stage.

The overhead material from the lights column is partially condensed by low-temperature refrigerant for recovering ethylene and light hydrocarbons, which are separated in an ethylene plant. Nitrogen gas and non-condensable material from the overhead are sent to a flare.

Finishing. The polymer powder from the purge column, additives and antiblocking agents are fed to a pelletizing system, where the mixture is melted, homogenized and pelletized. The pellets are homogenized in blending silos and finally packed in bags.

Production pathways

HDPE homopolymer production routes are based on ethylene manufacturing. Figure 2 presents different pathways for HDPE production.

Economic performance

The total operating cost (raw materials, utilities, fixed costs and depreciation costs) estimated to produce HDPE was about $1,350 per ton of HDPE in the fourth quarter of 2014. The analysis was based on a plant constructed in the U.S. with the capacity to produce 450,000 metric ton per year of HDPE.

This column is based on "HDPE Production via Slurry Loop Process – Cost Analysis," published by Intratec. The report can be found at the following URL: www.intratec.us/analysis/hdpe-production-cost. ■

Edited by Scott Jenkins

Editor's note: The content for this column is supplied by Intratec Solutions LLC (Houston; www.intratec.us) and edited by *Chemical Engineering*. The analyses and models presented are prepared on the basis of publicly available and non-confidential information. The content represents the opinions of Intratec only. More information about the methodology for preparing analysis can be found, along with terms of use, at www.intratec.us/che.

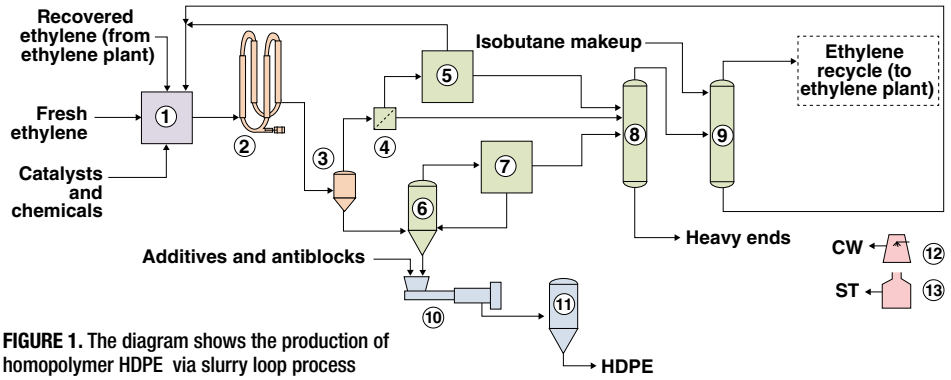

FIGURE 1. The diagram shows the production of homopolymer HDPE via slurry loop process

1. Feed preparation
2. Loop reactor
3. Flash chamber
4. Filter
5. Diluent recovery
6. Purge column
7. Isobutane-nitrogen recovery unit
8. Heavies column
9. Lights column
10. Pelletizing
11. Product silos
12. Cooling tower
13. Steam boiler

CW Cooling water
ST Steam

An Investigation of Premature Flooding in a Distillation Column

Surprising observations regarding flooding in the upper fractionation trays of an atmospheric crude-petroleum distillation column are investigated

Henry Z. Kister and Matthew Olsson
Fluor Corp.

In industial distillation processes, flooding is an abnormal, but relatively common, process condition in which liquid accumulates in the column. The accumulation may be caused by excessive upward vapor flow, which results in massive entrainment, or by a restriction in the downcomers, impeding liquid downflow in the column. Flooding usually results in dramatically reduced separation efficiency, excessive pressure drops and sometimes instability. In many cases, the situation leading to flooding is complicated. Here, the authors present findings from an investigation of flooding in a distillation column at a petroleum refinery that revealed some surprising observations involving the loss of valve floats from the column trays.

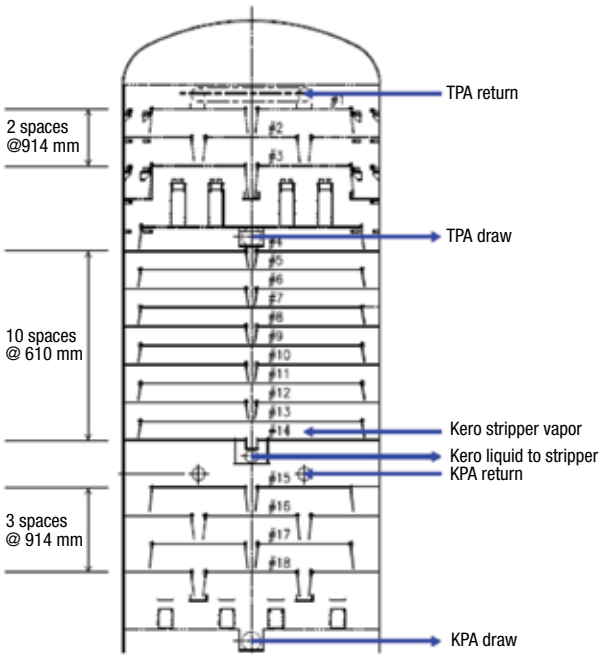

FIGURE 1. The diagram shows the internal geometry of the top section of the crude-petroleum distillation column

Crude tower flooding

The investigation centered on an atmospheric crude tower that experienced severe corrosion in the top pumparound (TPA) and upper fractionation trays. The likely cause of the corrosion was the entry of small quantities of water, which hydrolyzed chlorides, forming HCl that caused extensive corrosion and damage to the 410 stainless-steel trays.

Pressure-drop measurements on the column showed flooding taking place both in the four-pass TPA trays and also in the two-pass fractionation trays below. After some time, the pressure drop decreased. A gamma scan after the pressure drop went down confirmed flooding in the upper three trays in the fractionation section. Upon shutdown and inspection, corrosion and damage were observed in the TPA trays, as expected. The surprise was that the upper trays in the fractionation section were found clean, but missing most of the valve floats. The missing valve floats were not found, and were probably washed away or corroded away. The absent valve floats increased the open area on the trays, and should have moved the trays further away from flood, but flooding was indeed observed. The flooding only occurred near the end of that run, and did not occur in the earlier runs, when the valve floats of these trays were found in place.

This raised the question: could losing the valve floats have promoted flood in the frac-

IN BRIEF

CRUDE TOWER FLOODING
TOWER HISTORY
TRAY INSPECTION
VAPOR FLOWRATE BASICS
ANALYZING TOWER PRESSURE-DROP DATA
REVIEW OF GAMMA SCANS
MULTIPASS MALDISTRIBUTION MODEL
CASES MODELED
EXPLANATION OF THE TOWER FLOOD
RELATED EXPERIENCES
CONCLUDING REMARKS

FIGURE 2. On tray 6 of the column, most of the floats were missing

tionation trays? To gain a better understanding of the observation, we analyzed plant data and applied a method we developed, known as the Fluor multipass maldistribution model (MMM), to determine whether these observations can be modelled. In a previous article [*1*], we applied the same model to discover multiple steady-state vapor/liquid distributions in two-pass moving-valve trays at turndown.

Due to the symmetry of two-pass trays, a perfect split of both vapor and liquid between the passes is always one possibility and a well known steady-state distribution. Our analysis shows that uneven float removal on the trays can alter the vapor and liquid flows through each pass, leading to premature flood, but that an even removal of the valves from each of the passes, as observed in this tower, would not lead to premature conventional flood.

Application of criteria for vapor cross-flow channeling (VCFC) showed that the most likely cause of the flood was the reduction in dry tray pressure drop upon valve pop-out, which induced VCFC. The VCFC led to premature flooding and efficiency loss. Related experiences showed that leaving tray manways unbolted can cause flooding when the loads are high and the conditions favor channeling.

Under most circumstances, the loss of valve floats is unlikely to cause flood. This is by far the more common case. However, when the loads are high and, at the same time, conditions favor channeling, loss of valves can lead to flood. Likewise, unbolted manways usually only lead to efficiency loss or instability, but not to flood. In the cases described here, the flood occurred because the towers operated at high loads and under conditions conducive to channeling.

Tower history

The upper section in the tower (Figure 1) contains three TPA trays (Nos. 1 to 3), a chimney tray collector, and eleven naphtha-kerosene (N-K) fractionation trays (Nos. 4 to 14). The TPA is drawn from the chimney tray, cooled, and returned to tray 1. The remaining liquid from the chimney tray overflows through downcomers as reflux to the naphtha-kerosene fractionation section. Kerosene is drawn from a sump under tray 14 as a total drawoff and flows to the kerosene stripper. Vapor returning from the stripper enters the atmospheric tower above tray 14. Trays 15 to 18 are a kerosene pumparound (KPA).

Trays 1–14 are conventional round, uncaged moving-valve trays fabricated out of 410 stainless steel. The valve floats of each tray are 50% light valves and 50% heavy valves, in accordance with a common industry practice [*1*]. The valves on trays 15–18 (the KPA) are small-size fixed valves. The TPA and KPA trays are four-pass trays at 914 mm spacing, while trays 4 to 14 are two-pass trays at 610 mm spacing.

Historically, no fouling and only a limited amount of corrosion were observed near the top of the tower. In the 2015 turnaround, some corrosion was seen on the top tray. Most of the valve caps on tray 1 and many on trays 2 and 3 were blown off.

During the next run, conditions occurred beginning in April 2016 that are believed to have intensified the corrosion rate. Corrosion near the top of an atmospheric crude-petroleum tower is a common experience.

During early autumn 2016, the tower experienced high pressure drops in the TPA and N-K fractionation sections. By winter of the same year, the high pressure drops in both sections came down, but at the time the plant was experiencing difficulty achieving the desired naphtha product (according to ATSM Standard D86; 95% point). Gamma scans on trays 4 through 18 taken in January 2017 showed flooding in the upper fractionation trays 4–6.

This behavior would normally indicate some combination of corrosion, fouling and damage. An inspection of the tower in May 2017 showed surprising results: there appeared to be corrosion and corrosion damage, but little evidence of fouling. Along with the refinery owner/operator, we launched a joint study to closely understand the experience. This investigation led us to an unexpected phenomenon not previously reported. This article describes our troubleshooting and findings.

Tray inspection

During a maintenance shutdown in May 2017, the tower was opened. The following observations were made:

1. Many valves floats were missing on the top seven trays (for example, Figure 2). On trays 1 through 4, about 90% of the valve floats were missing. On trays 5 and 6, about 80% of the valve floats were missing, and on tray 7, 30% of the floats were missing. Some of the blown-off valve floats found had no legs, but most of the floats found had legs. The panels around the holes were corroded. The corrosion appeared to be uniform across the trays. It appears that the valve floats were blown off due to corrosion. One of the tray panels with missing valves is shown in Figure 2.
2. Most of the missing floats could not be found. The inspectors checked the trays below trays 4 to 7 as well as the chimney trays, but could not find most of the missing floats. It appears that most of the floats were washed away or dissolved.
3. Few valve floats were missing on trays 8 through 11. Hard rust was found on the tray floor between trays 8 and 11. However, these trays, as well as trays 12 through 16, were found in good shape without any irregularities.
4. There was limited corrosion damage to the center and side downcomers from tray 3.
5. On tray 4, a piece of tray panel (downcomer seal area) was detached.
6. There was some foulant and scale on the trays, but not a large amount. There is a possibility that foulant could have been removed during shutdown, chemical decon-

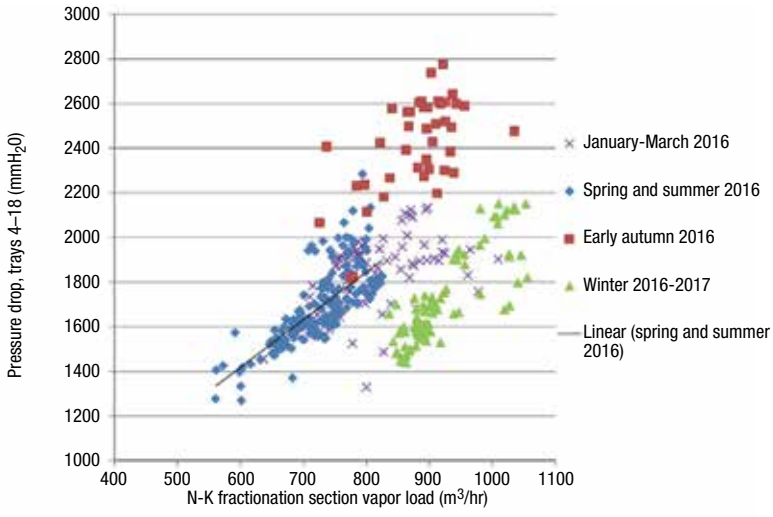

FIGURE 3. The plot shows the pressure drops in the N-K fractionation and the KPA sections of the column against vapor load in the N-K section

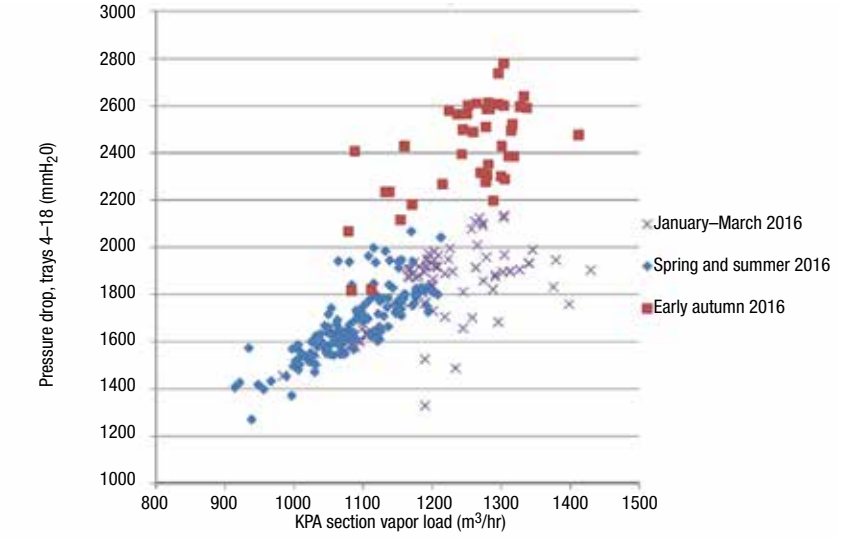

FIGURE 4. This plot shows the pressure drop in the N-K fractionation and KPA sections against vapor load in the KPA section

tamination and steam purge, but this is unlikely.

Vapor flowrate basis

In the following sections, as well as in Figures 3 and 4, the column internal vapor loads are expressed in m^3/h of standard liquid. The internal vapor loads were calculated from plant instrumentation by mass balance. For instance, the vapor load at the top of the fractionation section, as well as at the bottom of the TPA, equals the overhead products flowrates plus the vapor condensed by the TPA. However, for hydraulic and flood calculations, internal vapor and liquid loads and physical properties were obtained from the refinery's detailed simulation.

Analyzing pressure-drop data

The absence of apparent fouling led our investigation to closely examine the pressure drop data over the last 18 months of operation. Tower pressure drop was monitored between trays 2 and 3 in the TPA and between trays 4 and 18, which includes the naphtha-kero (N-K) fractionation section, as well as the KPA section.

Figure 3 shows that for trays 4 to 18 there were no signs of flood at loads as high as 1,000 m^3/h in this section prior to March 2016. Flooding appears to initiate at a vapor load of about 750 m^3/h in the autumn and even the summer data. Hydraulic calculations showed that with the trays intact, there should not be any flooding in the N-K fractionation section (trays 4 to 14). Using the Glitsch Equation [*2*] as recommended in Perry's Handbook [*3*], we calculated the highest-loaded tray in this section to operate at 76% of jet flood and 56% downcomer backup (clear liquid) for the abnormally high vapor load of 990 m^3/h, well above the vapor load at which the flood occurred. The FRI (Fractionation Research Inc.; Stillwater, Okla.; www.fri.org) jet flood correlation gave the higher value of 93% of jet flood for the same abnormally high vapor load, which also supports no flood. The pressure drop in the N-K fractionation section came right down by the start of the 2016–2017 winter, and at vapor flowrates below about 900 m^3/h became even lower than during the period from January to March 2016.

Since the differential pressure measurement of trays 4 to 18 also includes the KPA section, it is necessary to address the possibility of the flood initiating there. Using the Glitsch Equation [*2*] as recommended in Perry's Handbook [*3*], corrected for the small capacity enhancement of the small valves, we calculate the highest-loaded tray in the KPA section to operate at 92% of jet flood and 37% downcomer backup (clear liquid) for the abnormally high vapor load of 1,400 m^3/h through this section. Figure 4 plots the pressure drop in this section against the KPA vapor load. The graph shows that the KPA vapor load at which the flood initiates is well below this 1,400 m^3/h level; it is probably about 1,250 m^3/h. Also, it shows that from January to March 2016, this section operated at vapor loads of 1,400 m^3/h and even higher with no signs of flooding. With the KPA trays found completely clean at the turnaround, it can be concluded with confidence that the flood observed on trays 4 to 14 was a premature flood initiating in the upper fractionation section (trays 4 to 14) and not in the KPA.

Pressure drop for the TPA section followed similar trends. Steady operation with normal pressure drops occurred during January to March 2016, slightly rising over the spring and summer. In early autumn, the pressure drops shot up dramatically, at vapor loads less than the previously experienced maximum. By the start of the 2016–2017 winter, the pressure drop fell, becoming even lower than it was from January to March 2016. Hydraulic calculations confirmed that with the trays intact, there should be no flooding in this section.

Historically, the naphtha product D86 95% point has run at 140–145°C. There was no problem keeping the 95% point within this range throughout the spring, summer and even early autumn of 2016, although it appeared to move up slightly in the early autumn of 2016. In the winter of 2016–2017, however, the naphtha D86 95% point increased to more than 145–155°C, indicating deterioration in tray efficiency in the N-K fractionation section.

Analysis of the differential pressure measurements indicates that during the early autumn and possibly earlier, salting out and corrosion products probably caused plugging of the TPA trays and of the upper fractionation trays below. This accounts for the high pressure drops observed during the early autumn. As time progressed, the corrosion products and salts were dissolved or washed away, and the plugging disappeared, causing the pressure drop to come down. The increase in open area on the TPA valve trays after the floats popped out caused the pressure drop in the winter of 2016–2017 to be less than when the floats were there. In the fractionation section, the same behavior occurred at lower vapor loads (below about 900 m^3/h), but at higher vapor loads, the pressure drops were about the same as those observed when the floats were in place.

Review of the gamma scans

The gamma scans (Figure 5) were conducted on the west side of the tower on January 17, with vapor loads in the N-K fractionation and TPA section at 900 m^3/h, and on the east side of the tower on January 18, with the higher vapor loads of 990 m^3/h in these sections. In Figure 5, the black and pink chords were shot on the west side at vapor loads of 900 m^3/h. The blue and green chords were shot on the east side at vapor loads in the N-K fractionation and TPA of 990 m^3/h. Since the east side was shot at a higher vapor load, any flooding is likely to appear more intense on the east, and any weeping is likely to be more intense on the west.

Figure 6 is a "Kistergram" [*4*], a graphic depicting gamma scan results on trays 4 through 14. Tray dimensions and froth heights are sketched to scale. The darkness reflects the froth density, with darker shades signifying denser froth.

Tray 4 was flooded. On the east side at the higher vapor load of 990 m^3/h, the accumulated froth was particularly dense. The west side of this tray at the lower vapor load of 900 m^3/h was flooded too, but as expected at the lower vapor load, with lower-density froth. Tray 5 was also flooded, again with froth accumulating on the east at the higher vapor load more dense than on the west at the lower vapor load. However, on both sides, the froths were less dense than that of those of tray 4 above. Tray 6 was also flooded, but here, the froth densities on the east and west sides were much the same and lower than those of the trays above. Tray 7 was not flooded on either side, and on the west side (at the lower vapor load), appeared to be weeping onto tray 6. The froth density was less than that of tray 5, and much the same as most of the trays below.

Trays 8 to 14 were not flooded. Their froth heights appear to have been about half of the tray spacing, and the froth densities were not high. This is similar to tray 7 above. Many trays showed liquid in their vapor spaces, but mostly only on the west side (at the lower vapor loads). This liquid is most likely weeping from the tray above, but entrainment cannot be ruled out as the cause. Distinguishing entrainment from weeping in these vapor spaces is difficult, although the observation of more liquid on the west vapor spaces (at the lower vapor loads) supports weeping. At the high vapor loads on both scan days (above 900 m^3/h),

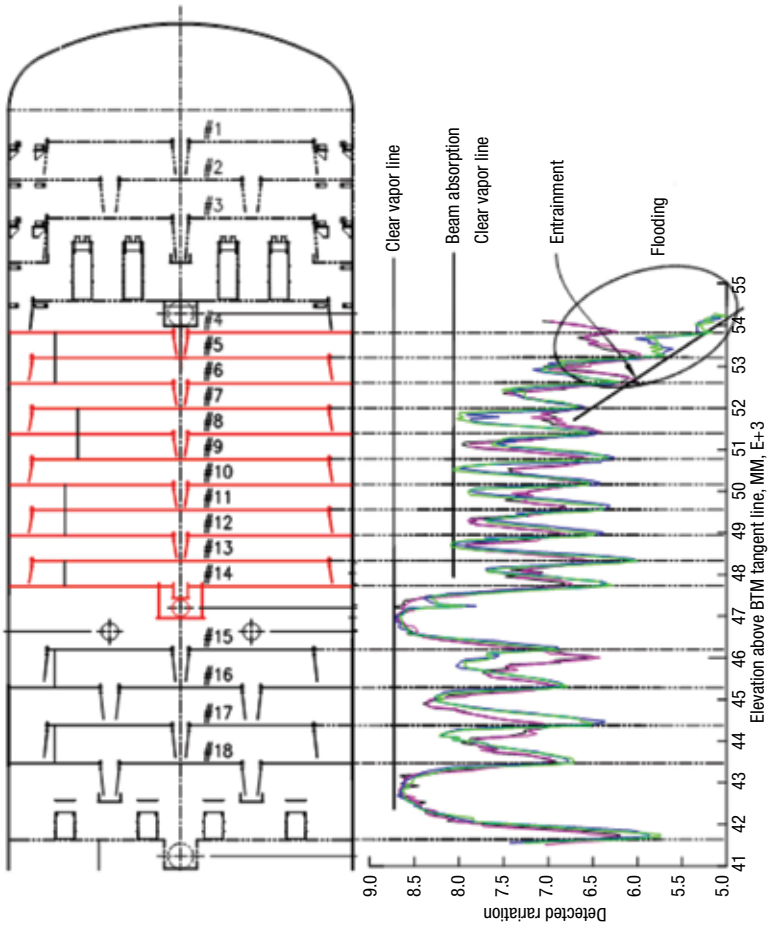

FIGURE 5. This diagram shows a gamma scan of the fractionation section of the crude distillation tower taken on January 17 and 18, 2017

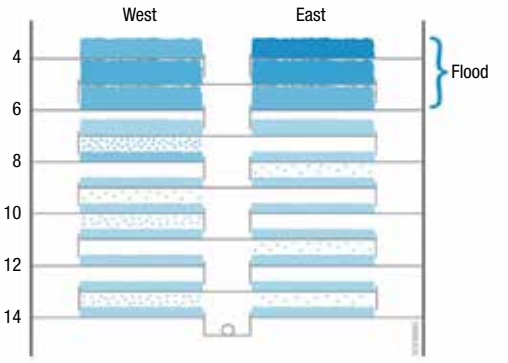

FIGURE 6. This "Kistergram" shows the tray froth heights and froth densities, as derived from the gamma scans

weeping should have been low. Interference from the lattice support beams on the trays may have also impacted some of these radiation absorptions.

What can be stated with confidence is that flooding took place on trays 4 to 6, which were the trays with more than 80% of the float valves missing. The flooding was more intense at the higher vapor loads, causing denser liquid to accumulate on the east side scans. Trays 7 through 14 (which did not lose their valve floats) appeared to be operating more or less normally.

An observation not shown on Figure 6, but that can be seen in Figure 5, is that there was no flooding in the KPA section. The trays appeared well loaded and possibly entraining, but no flood. The vapor loads in the KPA were 1,275 and 1,370 m^3/h on January 17 and 18, respectively.

One mystery raised by the gamma scan results is that trays 4–6 were flooded, but the pressure-drop data for trays 4 through 18 in Figure 3 did not support flooding on these dates. The pressure drop values measured for this section during the scans were 1,600 mm water (10 mbars per tray) on January 17 and 2,000 mm water (13 mbars per tray) on January 18.

Multipass maldistribution model

The tower modeled here is 8.23 meters in diameter, and contains two-pass sieve trays at 610 mm tray spacing. Tray dimensions, in mm, are shown in Figure 7. The open slot area with the valve floats in place is 10% of the active area, and the hole area of the valve holes with all the floats removed is 13.3% of the active area (not allowing for hole corrosion). Liquid to the top tray, and vapor to the bottom tray, were split equally between side A and B.

FIGURE 7. This diagram shows the key tray dimensions for the modeled column

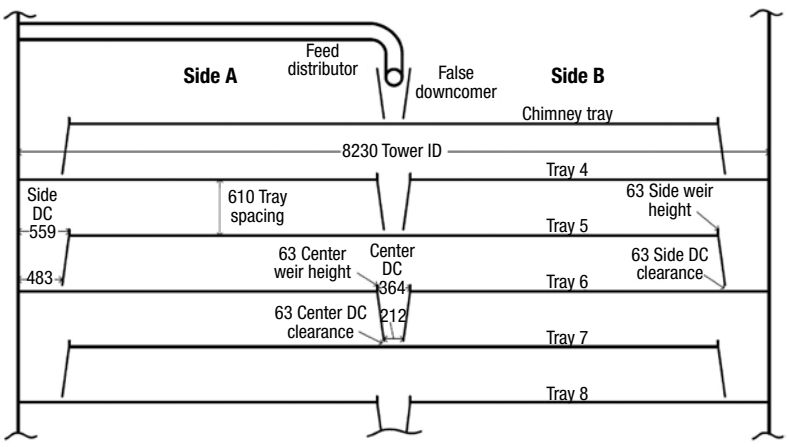

Two equalities are required for a hydraulically balanced distribution for two-pass trays (Figure 8):

1. *Pressure drop*. On trays with liquid flow from the center to the side, the center downcomer divides the vapor space, and the pressure on either side does not need to be equal. For trays with liquid flow from the side to the center, the vapor space is continuous, and the pressure equalizes in the shared space (that is, every two trays). For a balanced solution, the total pressure drop (through both trays) on either side of the shared downcomer must be equal.
2. *Downcomer backup*. As the center downcomer is shared, the calculated downcomer backup for either side must be equal.

All hydraulic equations are from the published literature and are the same as those in our earlier work [*1*]. For pressure-drop calculations, we used the Klein method [*5*] for valve trays, and the Summers and Cai sieve-tray pressure-drop correlation [*6*] for trays that had lost their valve floats. We used the Bolles and Fair method [*7*] for pressure losses through the tray aerated liquid. For downcomer backup, we used the classic downcomer backup equation in Perry's Handbook [*3*].

All cases modeled used the same vapor and liquid loadings, which were those for tray 4 on January 18, 2017. Because these loadings are high, all light and heavy valves were open on each tray, so multiple steady-state vapor and liquid distributions based on valves opening and closing, as previously reported for turndown [*1*], were not plausible. Thus, for each case, the MMM resulted in only one possible allocation of vapor and liquid in the tray section, dictated by the geometry that was used.

Cases modeled

When describing each case, the following acronyms are used:

- CDC: center downcomer
- DCB: downcomer backup, expressed in clear liquid height divided by (tray spacing plus weir height)
- JF: percent jet flood, calculated using the FRI correlation
- L: percent of the total internal liquid flowrate

• V: percent of the internal vapor flowrate

Case 1, all valve floats in place. This case gave the expected performance of the intact trays. As the geometry is symmetrical, there is equal distribution of vapor and liquid for all trays in the section. The percent jet flood was 93% and 84%, respectively, for the center-to-side and side-to-center flow trays. The clear liquid backups in the side and center downcomers were 56% and 55%, respectively.

Case 2, valve floats missing per inspection. In this case, 90% of valve floats were missing on tray 4, 80% missing on trays 5 and 6, and 30% missing on tray 7. This situation increases the open area of tray 4 from 10.1% to 13.1%. The open area of trays 5 and 6 are increased to 12.6% and 12.7%, and the open area of tray 7 is increased to 11.0%. In the model, the geometry is symmetrical, so there is still equal distribution of vapor and liquid for all trays in the section.

The change in geometry from Case 1 to Case 2 caused flooding in the actual tower, as shown in Figure 6, but the hydraulic calculations showed no flood. Percent jet flood marginally rose, from 81 to 84%, on trays 4 and 6 (side-to-center flow) and from 93% to 94% on tray 5 (center-to-side flow). On tray 7, the jet flood decreased from 93% to 92%. The percent flood stays relatively the same despite the large increase in open area because with the valve floats missing, the tray is more similar to a sieve tray than a valve tray, and the hydraulic diameters of the holes/slots are much larger. The downcomer backup decreased by 3–9% for trays 4–7. We conclude that, based on conventional hydraulic calculations, the loss of valves would not explain the flooding observed on trays 4–6.

Cases 3 and 4, asymmetric valve loss. We explored whether the maldistribution resulting from losing valve floats asymmetrically could result in the flood patterns observed on trays 4–6. These cases also show the extent to which maldistribution propagates through the tray section. Here, we report the results for two of these cases. More detailed analysis and another case can be found in Ref. 16. In all modeled cases, asymmetric valve losses generated flooding patterns vastly different from that observed in the actual tower. We therefore conclude that an asymmetric valve loss is not the root cause of the flood observed on trays 4–6.

Our analysis precluded downcomer

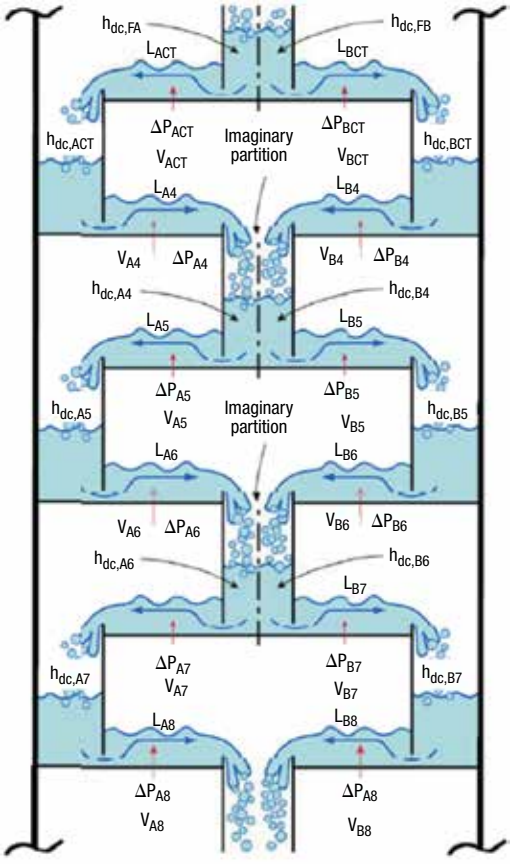

FIGURE 8. Here are key terms used in the multipass maldistribution model (MMM) equations

choke. The side downcomers are generously sized, and maldistribution could only increase downcomer inlet velocity to 0.31 ft/s, which is within the operable range for this service [*3*]. With a tighter downcomer design, maldistribution can lead to downcomer choke flood.

Case 3, 90% of the valve floats are missing on panel A of tray 4, but all other valve floats are present. The hydraulic performance for this case is shown on Figure 9. The missing valve floats on panel A of tray 4 lead to a slight vapor maldistribution toward side A for trays 4 and 5 and a large liquid maldistribution toward side A for trays 5 and 6.

The loss of valves on panel A of tray 4 largely reduces the tray pressure drop and the downcomer backup on the A side of the imaginary partition in the CDC from tray 4. To equalize the backup, the CDC sends more liquid to panel A of tray 5. Because the backup is far more sensitive to the pressure-drop reduction due to the valve loss than to changes in liquid rate, a large increase in liquid rate is required to counter. Solution is achieved with a 67–33% liquid split to panels A and B of tray 5, respectively. The higher liquid load to panel A of tray 5 increases the pressure drop of this tray, countering the pressure drop imbalance across trays 4 and 5 and reducing the vapor maldistribution. The maldistributed liquid continues to tray 6. This time, it increases the backup on side A of the CDC from tray 6. To counter, this downcomer sends more liquid to panel B of tray 7. This change is far smaller in magnitude, making the liquid split 45–55% to panels A and B, respectively. Again, there is a minimal change in vapor distribution. The liquid maldistribution continues to zigzag down the tower, each time at a reduced magnitude. By the time tray 10 is reached, it almost completely dissipates.

A key observation is that the pressure drop on these trays is far more sensitive to changes in vapor rate than to those in liquid rate, so there is a need to make large changes in liquid rate to make up for small changes in vapor rate. On the other hand, the downcomer backup is far more sensitive to the liquid flowrate.

The resulting rise of the percent jet flood from 93 to 103% and the downcomer backup from 56 to 66% (clear liquid) would likely flood tray 5, but on panel A only.

Case 4, 90% of the valve floats are missing on panel A of tray 4, and 80% are missing on panel A of tray 5. The hydraulic performance for this case is shown in Figure 10. For this case, the reduced dry pressure drop through panel A of trays 4 and 5 increases the fraction of total vapor flow to these panels. For Case 3, all valves were present on panel A of Tray 5, so the extent to which the vapor favored side A due to the lower pressure drop through panel A of tray 4 was limited by the greater pressure drop through panel A of tray 5. For Case 4, with 80% of the valves missing on panel A of Tray 5, the vapor favors side A to a much greater extent. With more vapor on side A, the dry pressure drop through either side of tray 4 is almost equal (a significant difference from Case 3). The result is a much smaller liquid imbalance, still favoring side A. Below tray 5, both the vapor and liquid imbalance completely dissipate. The rise of the percent jet flood from 93 to 109% would likely flood tray 5, but again, on panel A only.

Explanation of the tower flood

Our analysis shows that loss of valves can lead to flooding only if it occurs unevenly on the trays. However, the loss of valves observed in this tower has been even, similar to that modelled by Case 2. It can therefore be concluded that using the conventional flood equations, none of the cases modeled can explain the flooding observed on trays 4-6.

Our previous work showed that large open areas on trays can induce vapor channeling, such as vapor cross-flow channeling [*8,*

9], or other types [4, 10] of channeling. Such channeling generates high vapor velocity zones, accompanied by excessive entrainment and premature flooding, and high-liquid zones with excessive weeping.

For sieve and valve trays, the most common type of channeling, which is vapor cross flow channeling (VCFC), was shown to occur when the following four factors occur simultaneously:

1. A high fractional hole area on the tray (greater than 11% of the active area with sieve trays, and greater than 13–14% of the active area with sharp-orifice valve trays)
2. A ratio of liquid flowpath length to tray spacing above 2
3. A weir load exceeding 50–60 m^3/h m of outlet weir
4. Pressure below 7 barg

In the N-K fractionation section of this tower, the ratio of flow path length to tray spacing is extremely high, more than 5.5:1. The liquid flowrate is in the VCFC range, a high, 96 m^3/h m of outlet weir to the side downcomers and 50 m^3/h m of outlet weir to the center downcomers, and the pressure is low (about 1 barg). The combination of these factors, especially with the long flow path length, is highly conducive to the onset of VCFC.

For as long as the valve floats were in place, the open slot area of the valves was about 10% of the active area, making them resistant to VCFC. Hartman [11] observed that at the high ratio of flow path length to tray spacing of 3.6, even sharp-orifice valve trays with about 13–14% open slot area can experience VCFC. With the higher ratio in this tower (5.5:1), it appears that the relatively low open area of these trays (10%) kept them well below the threshold of VCFC, thus protecting them from VCFC. However, once the valve floats were lost, the trays became sieve trays with about 13% open area, the trays entered the VCFC range. The onset of VCFC upon major valve loss was therefore the root cause of the premature flood, along with poor efficiency experienced in this section. VCFC leads to tray inlet weep [8,9], which is highly detrimental to tray efficiency.

Initially, when the trays experienced plugging or salting out, the pressure drop rose, signifying flooding, but there was not a great deal of efficiency loss, so the naphtha endpoint did not largely rise. Once the valve floats popped out, VCFC set in. The VCFC flood proceeds without a large increase in pressure drop, so the pressure drop decreased as it did in the late fall of 2016. However, this channeling induced large inlet weep that caused the tray efficiency of trays 4–6, and possibly 7, to drop significantly, causing the observed rise in naphtha endpoint.

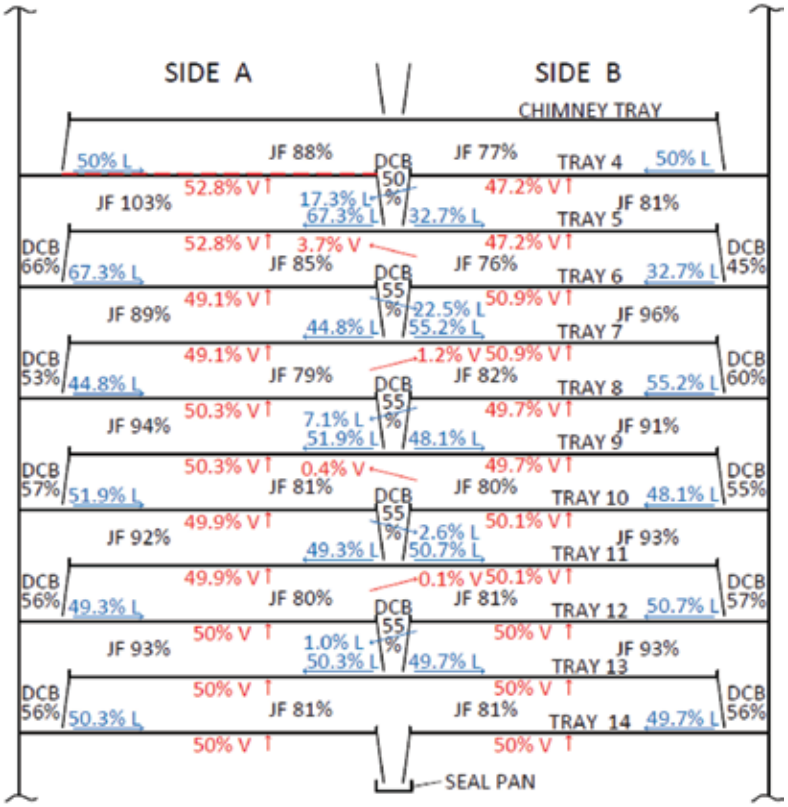

FIGURE 9. Case 3 of the modeling had 90% of the float valves missing on panel A of tray 4

Davis [12] explained the VCFC phenomenon as a force balance between the hydraulic gradient that tends to channel the vapor and the dry pressure drop that tends to evenly distribute the vapor. Davis proposed a rule of thumb that states that to prevent the onset of VCFC, the hydraulic gradient needs to be kept below 0.4 of the dry pressure drop. For the N-K fractionation trays, based on the January 18 loads, and the valve floats in place, we calculated a dry pressure drop of about 110 mm of liquid, and hydraulic gradients of about 50–60 mm. Once the valves popped out, the hydraulic gradients remained essentially the same, but the dry pressure drops were halved (to about 50 mm of liquid), which is about the same as the hydraulic gradients, and is in major violation of Davis' criterion. It is certain that under these conditions, VCFC set in.

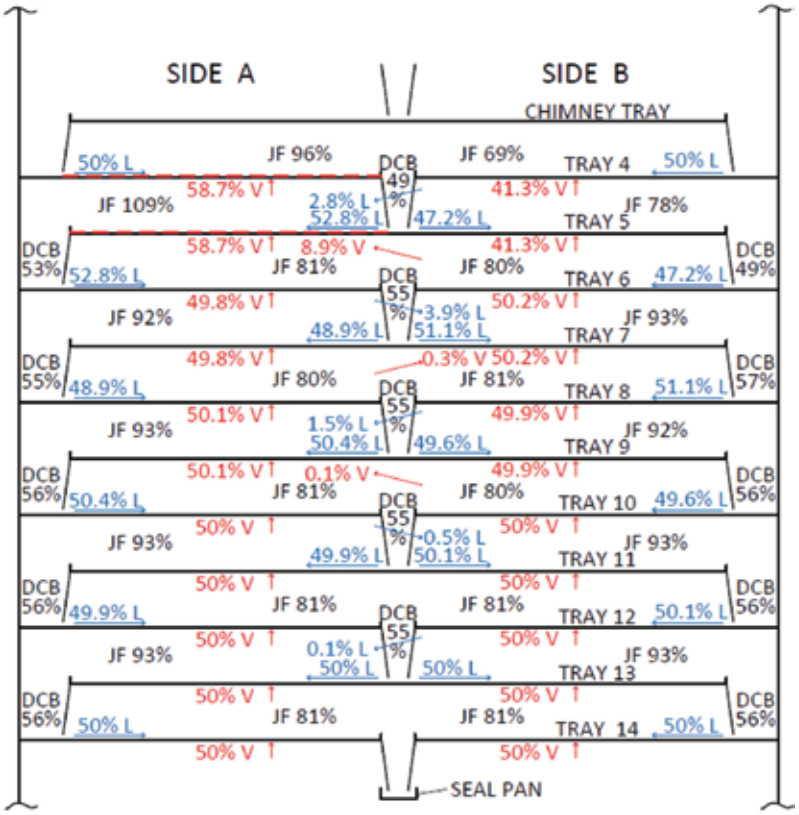

FIGURE 10. Case 4 of the modeling had 90% of the float valves missing on tray 4 and 80% missing on tray 5

Related experiences

A colleague [*14*] of the authors brought to our attention some related experiences. In several towers, there have been experiences in which leaving the tray manways uninstalled led to flooding. He described one experience in particular. A 3-m, inner dia. chemical distillation tower operating at about 1 barg with 80 single-pass sieve trays at 460 mm tray spacing and weir loads of 80–90 m^3/h m of weir length was returned to service after a routine turnaround in which no modifications to the trays were performed. The tray manways were dismantled for inspection but were not re-installed following the inspection. The tower flooded at 70% of the rated jet flood, which did not happen prior to the turnaround. The flood was recognized by excessive entrainment from the top of the tower, which doubled the measured reflux flowrate for the normal amount of reboiler steam. It was difficult to keep the level down in the reflux drum. Like in the crude tower, the pressure drop was normal. Not installing the manways can be expected to drop the tray efficiency, as it usually does, but increasing the open area can be expected to give the trays a larger margin from flooding.

As in the crude tower, the most likely explanation for the flood is channeling, in this case induced by the gap generated at the open manways rather than the hydraulic gradient. Again, all the conditions conducive to channeling (as described above) existed in the tower, except for the large open area. Once the manways were removed, the open area largely increased, causing channeling to set in and initiate premature flood.

Concluding remarks

The analysis reported in this article shows that loss of valves, or open manways, can lead to channeling, which in turn, can lead to premature flooding. Whether the channeling will result in flood depends on the operating rates and whether the tray geometry makes it prone to channeling. In the case described, it can be stated with confidence that the loss of valves led to VCFC, which in turn led to flood.

Under most circumstances, loss of valve floats is unlikely to cause flood. This is by far the more common experience. However, when the loads are high and at the same time, conditions favor channeling, loss of valves can lead to flood. Likewise, unbolted manways usually only lead to efficiency loss or instability but not to flood. In the cases described here, the flood occurred because the towers operated at high loads and under conditions conducive to channeling.

Our modeling work showed that for two-pass trays, an even loss of valves on both tray panels is unlikely to lead to flood in the absence of channeling. However, an uneven loss of valves on one of the panels is likely to move this panel closer to flood, and if the loads are high enough, initiate flood on the tray.

Finally, the study discussed here demonstrates that combining field data and gamma scans with hydraulic and maldistribution analysis using our recommended procedure [*1,15*] is a powerful tool for analyzing and diagnosing column problems. This approach has been successful for diagnosing and analyzing multipass tray maldistribution, unexpected efficiency loss at turndown, channeling, and uneven fouling. ■

Edited by Scott Jenkins

References

1. Olsson, M., and Kister, H.Z., "Can We Count on Good Turndown in Two-Pass Moving Valve Trays," *Chem. Eng. Progr.*, p. 43, November 2018.

2. Glitsch, Inc., Bulletin 4900, 6th Ed., Dallas, Texas, 1993.
3. Kister, H.Z., P. Mathias, D.E. Steinmeyer, W.R. Penney, V.S. Monical and J. R. Fair, "Equipment for Distillation, Gas Absorption, Phase Dispersion, and Phase Separation", Sec. 14, in Perry and Green's "Chemical Engineers' Handbook," 9th ed., 2018.
4. Kister, H.Z. , Apply quantitative Gamma Scanning to High-Capacity trays, *Chem. Eng. Progr.*, p. 45, April, 2013.
5. Klein, G.F., "Simplified Model Calculates Valve Tray Pressure Drop", *Chem. Eng.*, May 3, 1982, p. 81
6. Summers, D. R., and T. J. Cai, "Dry Tray Pressure Drop of Sieve Trays Revisited," *Chem. Eng.*, August 2017, p. 38.
7. Bolles, W., and J. R. Fair, in J. M. McKetta (Ed.) "Encyclopedia of Chemical Processing and Design", vol. 16, p. 86, 1982.
8. Kister, H. Z., K. F. Larson, and P. E. Madsen, Vapor Cross Flow Channeling on Sieve Trays: Fact or Myth?, *Chem. Eng. Progr.*, p.86, November 1992.
9. Kister, H. Z., Can Valve Trays Experience Vapor Cross Flow Channeling?, *The Chemical Engineer*, p.18, June 10, 1993.
10. Kister, H. Z., N. O'Shea, and D. Cronin, Loss into Gain in High-Capacity Trays Part 2: Reverse Vapor Cross flow Channeling, *PTQ*, p.27, Q3, 2016.
11. Hartman, E. L., New Millennium, Old Problems: Vapor Cross Flow Channeling on Valve Trays, in "Distillation 2001: Frontiers in a New Millennium," Proceedings of Topical Conference, p. 108, AIChE Spring National Meeting, Houston, Texas, April 22–26, 2001.
12. Davies, J. A., Bubble Trays – Design and Layout, *Pet. Ref.* 29(8), p.93, 1950, and 29(9), p.121, 1950.
13. Kister, H. Z., "Is the Hydraulic Gradient on Sieve and Valve Trays Negligible?" Paper presented at the Topical Conference on Distillation, AIChE Meeting, Houston, Texas, 2012.
14. Olsson, F.R., Private communication, March, 2018.
15. Kister, H. Z., R. W. Dionne, W. J. Stupin, and M. Olsson, "Preventing Maldistribution in Multi Pass Trays", *Chem. Eng. Prog.*, April 2010, p. 32.
16. Olsson, M., and H. Z. Kister, "Can Loss of Valve Floats Lead to Premature Flood? Paper Presented at the Distillation Symposium, AIChE Spring Meeting, Orlando, Florida, April 22–26, 2018. Full copy is available from the author.

Authors

Henry Z. Kister is a senior fellow and the director of fractionation technology at Fluor Corp. (3 Polaris Way, Aliso Viejo, Calif.; Phone: 949-349-4679; Email: henry.kister@fluor.com). He has over 30 years experience in design, troubleshooting, revamping, field consulting, control and startup of fractionation processes and equipment. Kister is the author of three books, the distillation equipment chapter in Perry's Handbook, and over 100 articles, and has taught the IChemE-sponsored "Practical Distillation Technology" course more than 500 times in 26 countries. A recipient of several awards, Kister obtained his B.E. and M.E. degrees from the University of New South Wales in Australia. He is a Fellow of IChemE and AIChE, Member of the NAE, and serves on the FRI Technical Advisory and Design Practices Committees.

Matthew Olsson was a part of the Distillation Expertise Team at Fluor Corp., in both Sugar Land, Tex., and Aliso Viejo, Calif. He has now moved to Eastman Chemical Co. in Longview, Tex., where he is a process design engineer. He has ten years of experience in design, troubleshooting and revamping fractionation processes and equipment. Olsson holds a B.S.Ch.E. from Texas A&M University in College Station, Tex.

Commercializing Process Technologies

New technologies can provide competitive advantages compared to established processes, but significant effort is required to transition a promising concept into a commercial reality

Vincent Welch and Joseph Peters
TechnipFMC

IN BRIEF

GETTING STARTED
COMMERCIALIZATION STEPS
CATALYST DEVELOPMENT
PILOT VERSUS DEMONSTRATION
REACTION SYSTEM DESIGN
PATENT AND LITERATURE SEARCH
KEY RELATIONSHIPS
DESIGNING AN EFFECTIVE PILOT PLANT
FEEDSTOCK CONSIDERATIONS
SIMULATION AND MODELING
CAPITAL COST ESTIMATES
SCALEUP AND DEMONSTRATION
REACTOR SCALEUP
SCALING MAJOR EQUIPMENT
PROCUREMENT AND CONSTRUCTION
DEMONSTRATION UNIT STARTUP

Many students study chemical engineering with the aspiration of someday inventing an innovative process that could be a true game changer. As we all know, creating a new process is quite complex. Compared to the rapid pace of advancements in other progressive industries, such as consumer electronics, telecommunications, software and automotive, in the world of high-volume, low-margin commodity chemicals, higher-value specialty chemicals and newer sustainable chemicals, process development and commercialization are more methodical and time-consuming.

This article is largely directed at illustrating the development lifecycle for petroleum refining and petrochemical processes, rather than those in the pharmaceutical, biochemical, mining or inorganic chemical industries. The intent is to describe how best to navigate the complex maze of process development, starting from basic research and development (R&D) to technical readiness and commercialization (Figure 1).

FIGURE 1. Demonstrating a promising new technology in a laboratory setting is just one of many complex steps in commercializing a new process technology

Getting started

One of the most difficult challenges facing the chemical process industries (CPI) today is the cost and timeline to commercialize new, innovative technologies. The conventional textbook approach of multiple incremental steps of tenfold scaleup (typically from bench scale to pilot plant to demonstration unit and finally to commercial plant) can take as long as a decade and be prohibitively expensive. Using a staged-gate approach — where process viability and economics are assessed at each step during the development program — is crucial not only for risk mitigation, but also for maintaining management and investor confidence. Because each subsequent step typically requires significantly larger capital and operating cost outlays, the staged-gate approach compels the development team to pause and take an objective view of test results, process design issues and economics.

It is clear that the revamp or building of any chemical plant involves significant investment and market risk. For producers in

mature markets, the risk of investing in a large-scale demonstration or full-scale commercial unit for an "unproven" process technology is nearly impossible to justify without a thorough evaluation, including testing at bench and pilot scales. As many readers can attest, few, if any, changes to a chemical plant or process are simple and turn out exactly as calculated at the start of the development program.

Even with justifiable economics and appropriate incentives from the technology developer or owner, most CPI companies are reluctant to be the first, or even the second, adopter of a new process or catalyst system. Most building-block petrochemicals and high-value specialty chemicals produced today are very mature technologies with well-known competitive economics. Being an early adopter can actually have a significant upside because projects can take years to realize. For companies to significantly improve their competitive position, they must move from the standard tried-and-true processes to more forward-looking innovative technologies. Those who choose to "wait and see" run the chance of operating with a sustained disadvantage once the new technology is commercialized. However, on the downside, the risk to the early adopters is failure of the new technology to meet expected performance, thus jeopardizing the entire investment. The chances for success improve with a deeply thought-out and rigorously executed development plan.

Process improvements can take many forms that can save operating cost or capital expenditures, as well as improve product purity and properties. These may include higher catalyst selectivity and conversion, improved reactor productivity, lower catalyst or feedstock costs, reduced environmental impact and more. True stepouts may embody completely new chemistry routes, alternative feedstocks and reactor designs, improved catalyst formulations or enhanced manufacturing techniques, such as improving energy recovery or plant reliability.

The decision to start a technology-development program depends on your perspective. Existing plant owners must protect their market share. They should be constantly evaluating competitive technologies to determine when and if they must purchase or develop new technologies to replace those already in place. Engineering and licensing companies look for advantaged technologies that can be competitive in the marketplace. Their interest is in licensing these technologies and deriving income from license fees, engineering services, proprietary equipment and catalyst sales.

Commercialization steps

Each process-development program requires several project phases, from the initial proof-of-concept through numerous levels of technical readiness, stage gates and eventually to the construction of the commercial plant. These reassessment requirements vary greatly from company to company. As one can imagine, the technical readiness requirements for a major petroleum or chemical company are likely different from those of a technology licensor or engineering company. Even within the same organization, depending on starting point and complexity, each technology-development program has its own path and strategy to get from the initial concept to full-blown commercialization. Additionally, risk mitigation and individual risk tolerances set and drive the scaleup progression and development lifecycle. The textbook rules of process scaleup include steps going from a very small-scale testing apparatus (bench scale) to a more representative pilot plant, then possibly to a demonstration unit and finally to the commercial plant (Figure 2). It should be highlighted that scaleup is not only limited to the key process-unit operations, but also to the catalysts, feedstocks, additives and equipment that form the complete basis for the new process.

Defining the required number of steps and their scale greatly influences program cost and timeline. From a capital expenditure standpoint, an automated pilot plant may cost $1–3 million, an integrated demonstration unit in the range of $10–50 million and a full commercial plant could easily be in the hundreds of millions of dollars. These costs must be taken into consideration before undertaking any process-development program.

Deciding on the need for the intermediate demonstration unit step can be one of the toughest decisions. With an outline of the known facts and assumptions, researchers and engineers will have lively debates on the need for this time-consuming and expensive step. Avoiding the demonstration-unit step could reduce the time to commercialization by two or three years, albeit with a potentially higher risk profile. In the end, the final decision may come down to risk tolerance, identifying ways to mitigate risk and adding design safety margins or perhaps even a "gut feel" based on experience. For example, the development team could determine the consequences of lower-than-expected performance. What if the selectivity improvement is only 95% of the expectation? What if the catalyst life is two months shorter or only partially regenerable? Once the most likely performance gaps have been identified, the team should develop a strategy and identify the steps needed to account for or remediate the shortfall.

Simplistically, the number of process-development steps is a function of reaction chemistry complexity, the non-ideality of the components involved and the scalability of the unit operations. While the sequence of process-development steps is outlined here, deciding which steps are mandatory should be determined by an experienced team of researchers and engineers in cooperation with business leaders and plant operations managers.

Catalyst development

For many programs, the earliest project phase involves the development of an alternate chemistry path or an improved catalyst. Nowadays, it is common practice that these improved pathways and catalysts are developed using high-throughput testing methods that study multiple catalyst

FIGURE 2. Bench-scale tests set the foundation for scaling a new technology up to a more representative pilot plant

samples in parallel, significantly shortening the time required to evaluate candidate catalysts or investigate reaction pathways. High-throughput testing is a powerful tool for identifying trends and variables that may lead to fully optimized catalyst formations. During a typical screening project, testing a few dozen or even several hundred materials and conditions is not unique.

As is typical in the early stages of process development, high-throughput testing protocols are performed on a very small scale under isothermal conditions with crushed catalyst. Moderately exothermic reactions or high-activity catalysts typically utilize a catalyst bed diluted with inert material. Not surprisingly, subsequent catalyst testing utilizing a particle size more representative of the commercial catalyst (for example, pellet, cylinder or sphere) operating under simulated commercial-scale conditions may produce considerably different results. While single stage or bed testing is acceptable at this point in the program, managing heat transfer requires careful consideration before moving forward. Options may include multibed reactors, pseudo-isothermal tubular reactors, fluidized-bed reactors, interstage quenching, interstage heat transfer or interstage feed injection.

The most promising results from these early tests are compared to the performance of the existing catalyst and process systems to determine if there is a potential significant advantage. This involves developing a new flowsheet, including the reactor design, and understanding the existing technology. Technical and economic analyses of the new and existing processes result in a decision to proceed to bench-scale testing (Figure 3).

Bench-scale experiments utilizing the most promising catalyst samples are usually performed on a very small or microscale and could involve glassware, small stirred-tank reactors, microreactors or other systems that use a minimum of amount catalyst and feedstock to obtain proof-of-concept data. The evaluation includes a determination of not only catalyst activity and selectivity, but also gathering preliminary information on catalyst life or regenerability. The experimental results are also compared to those obtained at the earliest phase.

If the results continue to look promising, the next step involves producing the catalyst at a large enough capacity such that it can be considered representative of commercial-scale production. This typically involves working with a catalyst supplier to develop the commercial production techniques required to economically produce a catalyst with performance parameters close to or better than those of the laboratory-scale material. It is common that the catalyst vendor will perform an abbreviated plant trial to produce a sufficient quantity of material. This activity can be the most challenging step because the commercial catalyst must not only have similar activity and selectivity to the sample, but also the physical properties, such as crush strength, required to operate at commercial scale.

Pilot versus demonstration

The terms "pilot plant" and "demonstration unit" are sometimes used interchangeably. For the sake of this article, pilot plants are configured to facilitate fundamental learning, determine rate-controlling steps and collect large amounts of data at a wide range of conditions to ultimately support the design basis for the commercial plant. Within practical limits, the pilot plant should attempt to simulate the envisioned commercial plant and be flexible enough to accommodate projected operating scenarios and numerous experimental runs. Pilot plants are highly instrumented to ensure a complete understanding of the operating conditions and the impact of the equipment on the process being studied. A pilot-plant reactor may have dozens of thermocouples and numerous sample ports to support the understanding of kinetics, reaction mechanisms and catalyst performance and lifetime. A rigorous pilot development program will carefully examine issues well beyond the basic process chemistry and kinetics. Several of these considerations are listed in Table 1.

Conversely, the demonstration unit should be at a scale such that equipment size has little or no impact on the results compared to the envisioned commercial unit. For reactor designs, the configuration should be virtually identical to that expected to be used commercially. Overall, the demonstration unit provides a validation of the commercial process but at a smaller, less risky scale. It should also have some limited built-in flexibility and be designed to operate continuously for long periods of time. Compared to pilot plants, demonstration units typically will have far fewer instruments and connections, which are mainly used for control and safety purposes. Demonstra-

tion units should also be a source of valuable information on operational issues (such as startup, shutdown and controllability) and maintenance issues (such as fouling, cleaning intervals and equipment reliability).

For reaction systems, kinetics, fluid dynamics, flow regimes and the reactor type play a central role in determining the appropriate number of scaleup steps. Fixed- and trickle-bed systems, for both liquid or vapor phase, can typically be scaled up from pilot-plant data. Fluidized-bed systems (Figure 4) require larger demonstration-scale testing where reactor size does not constrain the hydrodynamics of the catalyst system. Scaleup of continuous stirred-tank reactors (CSTRs) is done in successively larger vessel sizes because mixing, heat transfer, active reaction zone and gas-fluid contacting are very much dependent on equipment size and geometry.

Notwithstanding, the scalability of supporting unit operations also contributes to the thought process. If vapor-liquid equilibrium (VLE) behavior is well known, piloting of distillation columns is usually not required for determining separation parameters. However, separation of recycle streams and final product are key elements of an integrated pilot system and are critical to the ability to scale up directly to commercial size. The impact of recycle on catalyst performance and life, potential byproduct purge and product quality all factor into the evaluation of ultimate plant performance.

If vapor-pressure and enthalpy data are readily available, heat exchangers will likely not require piloting. Conversely, unit operations, such as extraction, drying and crystallization, typically require more scaleup steps and may involve working directly with equipment suppliers. Processes with significant solids-handling requirements, two-phase flow or non-Newtonian fluids, such as foams or sludge, will also require more steps prior to full-scale commercialization. Similarly, processes that deal with powders or non-free-flowing solids can be particularly challenging and difficult to scale up.

FIGURE 3. Early tests and bench-scale experiments can help to narrow a project's focus to the most promising catalyst candidates

As noted, not all development projects require all four scaleup steps. For something relatively simple, such as an incremental change to a polymer formulation, or if past laboratory results have been validated by previous experiments and practical commercial experience, it may be possible to go directly from bench to commercial scale.

Similarly, for some purely thermal-driven processes, such as ethylene production, where developments are typically aimed at larger capacities, increased yield, improved heat transfer, shorter residence time and longer cycle times, the textbook approach may not apply. In the steam-cracking process, where plant capacities can regularly exceed 1,000,000 metric tons per year, even very small incremental improvements can make a huge impact on a producer's net margin. Here, commercial implementation of advancements may not require a laboratory or pilot program. Sometimes, technology advancements can be accomplished by using commercially available kinetic-yield model software, along with performing engineering calculations with advanced tools, such as computational fluid dynamic (CFD) simulation.

For the most part, however, because piloting nearly always exposes the unpredictable or unknown, and given the enormous financial risks at the commercial scale, it is almost unthinkable not to pilot a new process. Surprises and revelations can include unexpected catalyst performance, feedstock poisoning, safety issues, equipment corrosion, fouling, foaming and plugging. Most chemical-reaction pathways are complex — their true mechanism may not be fully understood and is likely considerably different from the simplified overall stoichiometric equations. The combination of a properly constructed and instrumented pilot plant, along with a well thought-out experimental program, can efficiently and effectively sort out the myriad issues that need to be addressed for scaleup.

Reaction system design

By and large, the reactor is the core of most chemical plants, and its feeds, products, solvents, catalysts and diluents dictate the downstream processing requirements. Reaction-system fluid dynamics (for example, heterogeneous versus homogeneous or single-phase versus multiphase) and the reactor type play a central role in determining the appropriate number of scaleup steps.

For example, in some cases, the scaleup of a homogeneous CSTR system with simple chemistry can be straightforward, allowing the development to go directly from pilot to commercial scale. Assuming heat transfer is not a controlling issue and mixing characteristics do not signifi-

TABLE 1. SELECTED PILOT-PLANT CONSIDERATIONS	
Separations	Vapor–liquid equilibrium (VLE) Liquid–liquid equilibrium (LLE) Vapor–liquid–liquid equilibrium (VLLE)
Process safety	Runaways Flammability and toxicity
Corrosion	Type Mechanism Estimated rate
Temperature control	Heat input Heat removal Reaction quenching
Catalyst deactivation	Replacement Regeneration Installing pretreatment
Hydrodynamics	Mixing Pressure drop Phase separation Flow distribution

cantly affect the kinetic rate, scaleup could be accomplished by using the same operating conditions as the pilot plant, maintaining similar reactor geometry, liquid hold-up volume and residence time. Conversely, a CSTR with multiple phases, complex chemistry, a high heat-transfer load, solids or catalyst addition or solids removal would probably require additional validation beyond the normal pilot scale. Similarly, a bio-based CSTR with live organisms, enzymes or yeast certainly requires multiple steps.

To reduce the overall development timeline, a different tactic may be to incorporate the innovation into an existing operating plant possibly as part of a revamp, debottlenecking or modernization project. Or alternatively, a short, controlled "plant trial" could be attempted. For some researchers, a plant trial with a new catalyst is regarded as a simple "drop in." Conversely, for plant and operations managers, just the mere thought of this "experiment" can them give nightmares, as any unexpected loss in performance can have an enormous impact on plant economics and profitability. Nevertheless, using existing hardware and infrastructure assets may allow the development to go straight from the pilot-plant stage to commercialization without the expense of a full-blown demonstration unit.

One approach for commercializing new reaction systems is to incorporate an incremental slip-stream reactor in parallel with the existing reactor. While this approach avoids some of the costs associated with a large-scale demonstration, it may present less than ideal conditions for validating the new technology. Examples of limitations could be restrictions on equipment location or plot area, the inability to independently control pressure or flows, difficulties with equipment during startup and shutdown or the inability to maintain steady operations because of moving production-rate targets. Lastly, because the highest priority of plant operating personnel will always be the main production unit, the experimental program and the demonstration unit may not get the attention needed to guarantee success.

Unquestionably, irrespective of the number of development steps, before operating companies fully commit to commercializing improvements, they must be convinced that this new investment provides significantly enhanced economics, the technology has longterm viability and sustainability and the process development was rigorous, covering all aspects of the design and operation.

Patent and literature search

After an initial idea is formed, two critical tasks need to be completed: a project justification study and a patent or literature search of previous work in the field prior to embarking on any development program.

Even before proof-of-concept has been fully cemented, the R&D program needs to have economic justification to determine its viability. This usually begins by completing a survey of the current market conditions and evaluating existing commercially available technologies. Pertinent background information and data from trusted sources and dedicated industry reports are helpful in building the business case to move forward. Knowledge on several factors can help support the decision to fund or abandon the program, including the following:

- Market size
- Forecasted growth
- Competition and any emerging technologies
- Estimated production costs
- Worldwide production facilities and announced projects

This analysis can answer key questions: Does the new technology significantly reduce variable operating cost? Is the current market overbuilt with low plant-capacity utilization? What are the price trends and preferred feedstocks? Armed with recent and credible data, this detailed justification study provides the support and confidence to proceed with what will most likely be a multimillion-dollar investment.

Before embarking on any new program, a careful assessment of the patent landscape should be performed to ensure that the new idea is not infringing on the rights of others. If infringement is suspected, the program can be abandoned, or ways to circumvent the claim(s) need to be considered. This initial examination will ultimately serve as the foundation for a comprehensive "Freedom to Operate" (FTO), which is the legal opinion on whether the process, catalyst, equipment or their combination may be infringing on patents held by others. A careful review of past work can also sometimes point the current program to more productive areas of research. If an idea or concept is completely new to the field, it is important to decide early on whether to file for patent protection or keep it as a closely held trade secret. Keep in mind that patenting a novel idea or process that may take 10 years to commercialize is a double-edged sword — while it does grant you the right of unencumbered use, it also alerts competitors to your plans.

Key relationships

Once the initial small-scale catalyst testing and economic analysis have yielded promising results, the leading catalyst formulation is identified and there were no red flags raised by the patent search, it is now time to establish two key relationships — one with an engineering company and one with a catalyst vendor.

It is important to employ an experienced team of researchers and engineers that is capable of executing multiple stages of the development project. It is also essential to select an engineering firm that has pilot facilities of the appropriate scale, the necessary analytical capabilities and experience in process scaleup. A competent engineering contractor should also provide guidance on the scope and requirements of the development program by outlining the matrix of experiments and studies needed to create the design basis for the commercial plant.

The second important relationship to establish is with a catalyst supplier. Process development cannot continue unless the catalyst formulation can be reliably manufactured on a commercial scale. The goal is to select a supplier that has the capabilities to generate catalyst samples at a scale that closely resembles the ultimate commercial version. Typically, this requires engaging the expertise of an established catalyst manufacturer, preferably one with experience that is at least tangentially related to your invention. Catalyst vendors also provide valuable insight into critical matters, such as precious-metal loadings, supports, binder types and target physical properties.

Translating the optimal catalyst formulation, which was tested on a very small scale, directly into a commercial catalyst can often be problematic. In most cases, multiple trials are required before a commercially viable catalyst is produced. Samples from each trial must be evaluated at the pilot scale to determine activity, selectivity, regenerability and catalyst life. Of equal importance is data reproducibility. For the same catalyst batch, experimental results performed under similar conditions should be in close agreement. Eventually, more thorough evaluations are done on the final form of the commercial catalyst to fine-tune the performance envelope and ultimate catalyst life. Overall, developing a commercial version of a laboratory-prepared catalyst is no simple matter, and in some cases can control and significantly extend the entire development effort. This phase of the project is by far the most difficult to predict and can be very frustrating for a development team trying to meet schedule and budget projections.

Designing an effective pilot plant

Automated pilot plants (Figure 5) truly provide the foundation and are the workhorse of all chemical process development. The benefit of operating a small-scale pilot plant is that it allows numerous operating conditions and variables to be explored efficiently and economically on a relatively short time scale. The primary function of the pilot plant is to demonstrate the viability of the new process and generate the required data to support the plant design.

Determining the appropriate size of a pilot plant is not always a straightforward task. Beyond generating technical data for scaleup, one other function of the pilot plant may be to generate quantities of product samples for analysis and market testing. Another key decision is construction philosophy. Should the unit be skid-mounted, modular-design or stick-built? Should the unit be placed in a dedicated enclosure? Will it eventually be moved to the plant site? Selecting between these options depends on the complexity of the chemistry and process, as well as project schedule, budget, in-house expertise and the projected length of the program.

The design of the pilot plant is based on the conceptual design of the process, which includes a preliminary reactor design and required separations. The key factor in the design is how small the equipment can be to provide accurate and reproducible data for direct scaleup to a commercial plant. Obviously, a smaller unit using smaller flows will require less capital, use less feedstocks and generate less waste. But making the unit too small may introduce scaleup uncertainties for subsequent phases of the program. In small reactors and equipment, phenomena like wall effects, inlet thermal-void reactions, bed bypassing, plugging, heat transfer and heat losses, are not only more difficult to control, but may not be obvious at first and can be difficult to quantify.

FIGURE 4. A fluidized-bed reactor requires testing at larger scales than other reactor types, due to the unique hydrodynamics of the system

The translation of pilot-scale data for direct scaleup is done based on proven methodologies validated through the collection and comparison of data collected on both the pilot and commercial scale. These methodologies have been proven at progressively smaller scales for numerous reaction and separation systems.

Fixed- and trickle-bed vapor- and liquid-phase reactions can typically be done in single-tube reactors as small as ¾-inch diameter. However, this is very much dependent on catalyst particle size, reaction energetics and expected commercial thermal profile. Careful sizing and loading of the reactor are required to prevent bridging and uneven flow distribution. Inert materials are sometimes used to dilute the catalyst bed for improved flow distribution and thermal control.

Handling the waste and effluent streams is another factor to consider in determining the size or capacity of

FIGURE 5. An advanced, automated pilot plant, such as this multibed unit, provides opportunity to efficiently study the process at various operating conditions

the unit. Feedstock and disposal of toxic waste can add considerable cost to a pilot program. Reactor effluents that can be condensed are easier to handle, store and discard. Conversely, effluents containing a high percentage of light gases, such as hydrogen, ethylene, nitrogen and propane, may require onsite oxidation or incineration. Permitting and code issues can place restrictions on the total quantity of hazardous materials that can be stored and used in a facility.

Pilot-plant size and complexity also have a direct bearing on the ability to automate the pilot plant for unattended operation. Staffing a pilot plant 24/7 is usually prohibitively expensive. Most catalyst systems require extensive parametric and life testing, which can require months, if not years, of run time. Automation is essential to bring the cost of operation to a reasonable level, allowing for the most part staffing a day shift only. Experience has shown that the payback for automating a typical pilot plant is less than a year of operation. Automation also improves data quality because measurements are taken at regular, defined intervals so that trends previously difficult to see become evident. In the past, an operator with a clipboard taking hourly readings and then graphing the results was effective, but the tools available through automation are quite valuable, given the close operating margins of today's markets.

Another potential difference between the pilot and demonstration unit could be the materials of construction. For the pilot plant, it may be expeditious or only a small added cost to use a high-alloy material for the reactor and its associated tubing. In the end, however, researchers need to ensure that metallurgy will not influence the chemistry by catalyzing coking or other undesirable reactions. Materials selection for the demonstration and commercial plant should be based on known reaction and corrosion-rate data available from literature or data generated in the laboratory. Where possible, critical pilot-plant systems are made of the same materials of construction as those projected for commercial scale. For example, the pilot-scale reactor itself acts as the "corrosion coupon" since it was exposed to the fluids, temperatures and pressures of the actual reaction system. Metallographic analysis of the reactor after removal from service provides data crucial to the selection of materials of construction going forward.

Finding equipment capable of efficiently handling flows in the grams-per-hour range is certainly possible, but the number of options can be limited. While off-the-shelf equipment items are certainly available, much of the equipment used at the pilot scale is custom-fabricated and tailored to each unique application.

Frequently, the main emphasis of a pilot program is to validate the chemistry fundamentals and catalyst performance that are usually not available in literature or predictable via calculation. Understanding reaction kinetics and byproduct formation mechanisms help determine which reactor type is best suited for a given chemistry. Establishing the approach to theoretical thermodynamic equilibrium governs the maximum attainable conversion. While heats of reaction fix the energetics of the reaction system, they also greatly influence reactor type and design.

Beyond bench-scale testing, the pilot-plant design should attempt to mimic the commercial plant as much as possible. The key element to this approach is ensuring that the reaction system is designed such that the catalyst bed operates as close as possible to expected commercial conditions. This includes the expected linear and radial temperature profiles, operating pressures, space velocity and number of stages. Linear velocity can be difficult to match, given potential limits on reactor length. Thus, to support scaleup, parametric studies should be done at varying linear velocities to determine whether bulk mass transfer is an issue at the lower velocities of the pilot scale. Additionally, startup and shutdown procedures should be synchronized with those of the future commercial plant and recommended by the catalyst supplier.

Highly exothermic and endothermic reactions, which have large extremes between bed inlet and outlet conditions, can also produce noticeably different results compared to nearly isothermal operation. Per-pass conversion, yield and selectivity can be greatly impacted by all of the above. Consequently, while a prime catalyst candidate can certainly be identified using small-scale, high-throughput testing, alternatives should be available when unforeseen results are encountered.

The goals and schedule of the pilot plant program should be established by the researchers working collaboratively with the engineering team and catalyst supplier. The team should identify the critical data sets required to support the commercial design and the potential demonstration unit.

In addition to the research program schedule, the team must also develop timelines for pilot-plant construction and commissioning. Pilot-plant construction can take months. The unit must be designed and the process equipment, controls and analytical apparatus procured. During the period leading up to construction, the required permits should be obtained, control logic developed, a hazard and operability (HAZOP) study and layer-of-protection analysis (LOPA) performed and the feedstocks obtained or synthesized.

Feedstock considerations

It is always best to perform pilot testing with industrially produced feedstocks. However, care must be taken to pre-purify these materials before use in the pilot plant, as the very act of drumming or packaging these materials may introduce air, moisture and heavy materials left over from drum manufacture. Scrupulous precleaning of the containers and purging of the sampling lines is critical to minimize feedstock contamination.

Feedstocks should also include representative recycle streams. Generation of recycle streams normally requires that product-separation steps be included in the program. For pilot plants with relatively small flowrates, separations, such as distillation or filtration, can be accomplished in batch mode, but care must be taken to ensure that the level of separation would be feasible at the commercial scale. Better yet would be to perform the separations on a continuous basis according to the projections from process modeling software, so that the recycle streams and product compositions represent commercial operation. These separations can be done in a semi-continuous mode, such that the columns run continuously during the day shift at a high enough capacity to keep up with the 24-hour operation of the catalysis plant. Repeating this over many iterations results in recycle streams close to those that would be seen if the distillation system was directly connected to the reaction system.

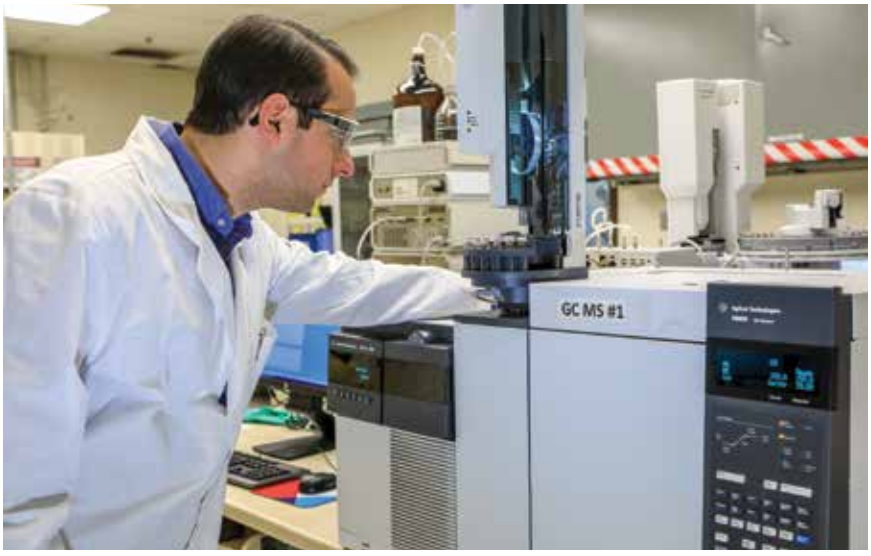

FIGURE 6. Access to advanced analytical capabilities is essential in determining feedstock integrity and monitoring plant performance

FIGURE 7. Process simulation, especially CFD, is an important step in estimating process behavior and identifying potential problematic anomalies

If this is not possible or practical, synthetic or reagent-grade feedstocks may be used with certain caveats. Reagent-grade feedstocks with extremely high purities, readily available from many sources, are convenient but may produce overly optimistic results. Typically, these materials will contain an entirely different slate of impurities or poisons that may or may not affect catalyst performance and aging. Chemical suppliers offer a wide range of materials and use the same handling equipment for a variety of substances. As much as they try to clean equipment between uses, trace amounts of different substances may carry over and can contaminate the feedstock. The chemical supplier is only required to meet their certificate of analysis and, for the most part, is not worried about trace impurities. Often, these impurities can be below the detection limits of a supplier's analytical equipment.

Having access to advanced analytical capacities, such as gas chromatography (GC) methods like thermal conductivity detectors (TCD), flame ionization detectors (FID) or nitrogen-phosphorous detectors (NCD), as well as GC mass spectrometry, are key to validating the catalyst performance data, identifying the effect of trace compounds and ultimately providing the team with confidence in the results (Figure 6). Online GCs and process analyzers can provide realtime data for close monitoring of plant performance. Offline analysis typically provides more detailed and accurate composition data, particularly at extremely low levels. Relationships with local universities and third-party analytical providers can also be helpful when specialized analyses are required, such as nuclear magnetic resonance (NMR). For most moderately sized companies, the use of third parties for specialized analytical work saves both on the initial investment and longterm upkeep needed for highly sophisticated equipment.

The importance of having accurate analytical methods cannot be overstressed. New processes typically produce a different mix of byproducts and minor impurities. Developing reproducible analytical methods to identify the minor trace components is crucial for not only determining stoichiometry and kinetics, but also for performing material and carbon balances and maintaining adiabaticity and temperature profiles.

Simulation and modeling

While the researchers are typically focused on reaction kinetics and catalyst life, so that the economics of the integrated plant can be determined and the commercial plant designed in the future, the flowsheet for the entire plant should be defined and a simulation model created. The simulation should include all relevant separations (distillation columns, strippers, dryers, absorbers, decanters, flashes and so on), and heat addition or removal, as well as all recycle, byproduct, vent and purge streams. At the most basic level, model development requires a detailed definition of the components or pseudo-components, including low-level impurities that could affect separations and final product purity. A key undertaking for model development is determining the best methods for estimating thermodynamic properties, equilibrium data and other physical properties. For many chemical compounds, the built-in data banks and estimation methods available in commercially available process-modeling software may be a good starting point. For other lesser-known components, data may have to be generated in the laboratory or determined via literature sources. Likewise, if not available from literature sources, parameters, such as the solubility of water or a solvent in the process streams, may also have to be determined empirically in the laboratory.

Reactor modeling can range from straightforward empirical equations to a full-blown kinetic model with rate constants and equilibrium-based interactions. Constructing a robust kinetic model with frequency factors and activation energies that accounts for temperature, pressure and concentration effects is a large effort and can take months to create. As a result, the process developer needs to decide what level of detail is needed for commercialization. A true kinetic model is the ideal tool for optimization but could be redundant or unnecessary for plant scaleup.

As more pilot data (kinetics and VLE) become available, the model should be used to optimize the flowsheet. However, one of the more important uses of the simulation model is to determine variable operating costs and perform an economic assessment. Raw material and utility consumption figures gleaned from the simulation, along with other variable operating costs, such as catalyst and chemical usage, should provide a representative benchmark when comparing the competitiveness of the new technology versus the incumbent process or other alternatives.

Capital cost estimates

With the information available at the pilot-plant stage, the capital cost of the anticipated commercial unit should be estimated. It goes without saying that the estimate is only as good as the pedigree of the input information. To achieve a robust estimate, one of the first activities should be creating an equipment list encompassing all the equipment on the flowsheet. The equipment list should summarize equipment size and type, dimensions (diameter and length), mechanical design conditions (temperature and pressure) and materials of construction. For pumps and other rotating equipment, volumetric capacity and differential pressure are required to determine driver requirements. Using current equipment pricing or pricing scaled from similar equipment or plants, an order-of-magnitude factored estimate can provide a relatively good idea of inside battery limits (ISBL) investment. Equipment costs can be obtained directly from vendors and past projects, or based on historical cost indices or scaling similar equipment. While having access to accurate equipment pricing is important, knowledge of installation factors and regional location factors, such as construction costs, are also key to determining an accurate investment picture. A more accurate estimate will include a breakdown of direct costs, such as piping, instruments, structural steel, electrical systems, concrete and insulation, as well as construction and field labor.

Armed with the capital estimate, typically ±30–40% at this stage, along with the operating cost and calculated return on investment, the economic feasibility of new process can once again be scrutinized. Nowadays commonly referred to as the techno-economic analysis, this evaluation can help business leaders understand the economic upsides, costs, benefits and potential risks. The goal of the analysis should provide the technology developer, business stakeholders and any potential first adopter the confidence that the future plant will be profitable. In parallel, the team should also outline the goals of the demonstration unit, list areas of concern and define future work or pilot studies.

Scaleup and demonstration

Following successful piloting and continued positive economics, the next step toward commercialization could be the construction of a demonstration unit. The time required to design, procure, construct and commission a demonstration unit could be two years or longer. In this interim period, to support the overall program, fine-tune the economics and further reduce risk, it is recommended that the pilot-plant program and other key development activities continue. Even a scaled-back R&D program can reinforce the underlying basic assumptions used in the go-forward decision.

As discussed previously, the need for an intermediate-scale demonstration unit depends on numerous technical factors, as well as commercial requirements. For example, a key step in the commercialization of novel bio-based fuels, polymers and chemicals might be the production of large quantities of materials for market testing and qualification by the end users. Typically, the required volumes for market testing of new products are difficult to produce at the pilot-plant scale.

In many cases, demonstration units can be located near or co-located within an existing operating facility. This should allow the demonstration unit to leverage existing utilities, feedstock handling, waste disposal and permits, as well as operate at higher rates for extended periods. As expected, the capital investment for a demonstration unit can be many times higher than a pilot plant. With sufficient data from the pilot plant, the conceptual design and optimization of the demonstration unit or commercial plant can begin.

Unlike pilot plants, the equipment and flow scheme in a demonstration unit should be nearly identical to the commercial plant. While it is important that equipment scaleup use the pilot data as a guide, direct extrapolation to the demonstration scale is not always possible. Pilot plants typically have higher holdup volumes, different surface-area-to-volume ratios, heat losses and lower fluid linear velocities.

Reactor scaleup

After deciding on the most efficient reactor system, the process and mechanical design of the reactor and ancillary equipment should be completed. For reactors using heterogeneous catalysts, to accurately calculate pressure drop, researchers should be prepared to provide catalyst physical properties, such as bulk density, void faction and a characterization of the pellet's nominal or wetted diameter. Scaleup of many reactor types can be accomplished using mathematical models and scaling rules.

One of the most important goals of reactor design is to replicate the mass- and heat-transfer characteristics, fluid linear velocities, flow regimes (turbulent versus laminar) or Reynolds numbers used during piloting. CFD modeling of reactor systems is a powerful tool to predict and optimize flow distribution, heat transfer and mixing (Figure 7). For irregular reactor geometries, CFD can provide a reasonable estimate of pressure drop and flow patterns. CFD can highlight problem areas, such as unwanted backmixing, stagnant areas and elements that may be prone to vibration. CFD is particularly helpful in developing reactor details, such as feed injections and mixing elements, which are very difficult to translate directly from the pilot scale.

In addition to selecting materials of construction, reactor design includes developing details of the reactor internals, including the following:

- Feed or quench spargers
- Bed supports
- Manway access
- Catalyst loading/unloading nozzles
- Internal instrumentation

Less obvious details, such as shipping braces, insulation details, clearances, tolerances and expansion joints, also need to be considered.

Scaling major equipment

In the scaleup of most towers, drums, vessels and heat exchangers, the basic rules of chemical engineering frequently apply. For some unit operations, often the simplest approach to scaleup is to maintain the same or similar geometry and fluid hydrodynamics as the pilot unit. But from a

practical standpoint, given the very nature of pilot-plant equipment, direct scalability and geometric similarity is never truly possible. For example, in the pilot plant, the nearly ideal separation of two immiscible liquids could be achieved using a decanter/coalescer based on a nominal holdup time of one hour. Simplistically, using the same basis for the demonstration plant could result in an extremely large horizontal vessel that may not be the most economic or elegant solution. However, knowing the relative liquid densities, average droplet size and the viscosity of the continuous phase, Stokes' law can be used to estimate the droplet settling rate that may lead to a more cost-effective design and practical solution.

While piloting of heat exchangers is usually not required, there are still numerous important decisions to be made. Considerations include the type of exchanger (for example, shell-and-tube, plate or spiral), fluid allocations (shellside versus tubeside), configuration (horizontal, vertical, thermosyphon, kettle or forced circulation), as well as arrangement details (tube diameter, TEMA head and shell type, number of passes, baffle spacing and so on), most of which can be determined by an experienced engineering contractor.

While many times overlooked, the engineering team will also be responsible for establishing more routine design elements, such as the following:

- Distillation tray efficiencies
- Physical properties
- Fouling factors
- Corrosion allowance
- Control schemes
- Materials of construction
- Overpressure protection
- Effluent or wastewater treatment
- Design codes

Before equipment design can begin in earnest, fluid physical properties must be determined. Properties, such as density, viscosity, thermal conductivity and surface tension, can be found in the literature, estimated by the process simulation software using a validated database such as Design Institute for Physical Properties (DIPPR), calculated using various contribution methods, as outlined in the API Technical Data book or measured in the laboratory.

Procurement and construction

After basic and detailed engineering are complete, the timeline of most large-scale demonstration units follows the norms of a typical chemical plant project. During procurement activities, special attention should be given to equipment items and specialized instrumentation that are critical or unique to the new process. After vendor selection is complete, the engineering team should establish a close relationship with the fabricator. The team should carefully review and comment on vendor prints, ensuring full compliance with the original intent of the design drawings. Then again, many times during equipment fabrication and assembly, vendors have valuable recommendations to improve the design and constructability.

As noted earlier, developing the commercial version of a laboratory catalyst can be challenging, costly and time consuming. During the engineering and construction phases of the demonstration project, the development team should collaborate with the catalyst supplier to ensure large volumes of high-quality, on-specification catalyst can be produced. Consistently producing tons and tons of a new catalyst formulation is quite different and much more challenging than running a short plant trial to produce a drum or two of catalyst for the pilot plant. To avoid unpleasant surprises prior to demonstration unit startup, it is beneficial to benchmark the full production batch of catalyst compared to the catalyst used during piloting.

Demonstration unit startup

Commissioning, startup and operation of the demonstration unit requires a dedicated workforce and laboratory support. After the typical plant-commissioning struggles, once unanticipated issues have been addressed and the unit's operations have lined out, the gathering, analyzing and reporting of data should become a regular routine. After process performance targets have been met (or exceeded), the larger risks mitigated and the stakeholders convinced that the process is competitive, the new process can be deemed ready for full commercialization. Whether it be for a captive company internal project or broad-based licensing to industry, the next hurdle is convincing customers, management and business partners to invest many millions of dollars for the full-scale commercial unit.

Given that years have probably transpired from that first "ah-ha" moment, with any luck, management will continue to support the project and customers will see the value of the new process. Furthermore, it is important that market demand is still strong, capital-cost estimates have remained reasonable, raw materials are readily accessible, the price of petroleum is stable and environmental permits are obtainable. While it is understandable to be buoyant over the successful demonstration, clearly the challenges and barriers for full process commercialization are far from over.

Each technology has a unique pathway from concept to commercialization. Developing a new chemical process can be one of the most rewarding experiences in one's chemical engineering career. It demands a committed team effort, hard work, innovative thinking, good timing and a bit of luck. ■

Edited by Mary Page Bailey

Authors

Vincent (Vinny) Welch is the managing director of TechnipFMC's Boston office (One Financial Center, Boston, MA, 02111; Email: vincent.welch@technipfmc.com). He is responsible for managing engineering, development, licensing and research efforts. With over 35 years of experience, he has spent most of his career licensing and developing process technology for the petrochemical industry. He holds a B.S.Ch.E. degree from Northeastern University.

Joseph Peters is a senior director at TechnipFMC's Weymouth research facility (56 Woodrock Road, E. Weymouth, MA 02189; Email: joseph.peters@technipfmc.com). He manages the research center and is responsible for the execution of complex development programs aimed at the commercialization of new chemical process technologies, as well as further improvements to TechnipFMC's existing portfolio of novel process technologies. With over 35 years of experience, he has spent most of his career developing new technologies from concept, through bench, pilot and demonstration scale and finally to commercialization. He holds an M.S.Ch.E. degree from Northeastern University and is a Registered Professional Engineer in Massachusetts.

Cost Engineering: Equipment Purchase Costs

A methodolody and examples for estimating equipment costs are presented

Thane R. Brown
Procter & Gamble (retired)

Engineers have the responsibility to create projects having attractive returns on investment and to create economically sound designs — designs that produce high-quality, competitively priced products. This requires the technical and economic[1] study of many different options. When doing studies, the design is usually not well defined, so one will often use factor methods for capital estimating. With these methods, one first determines the purchase cost of the equipment and multiplies that by a factor to determine the capital cost of a process or plant.[2]

The accuracy of factored estimates is usually good enough to produce high-quality decisions.

Purchase cost data. This article presents up-to-date equipment purchase cost data for nine different types of process equipment.

- Agitators
- Air compressors
- Boilers
- Cooling towers
- Fans
- Heat exchangers
- Pressure vessels
- Pumps, centrifugal
- Tanks, storage

The cost data are presented for each of these types of equipment in Figures 1–9 on p. 52. Each begins with a general specification. For example in Figure 2 (air compressors) the specification is: Centrifugal, rotary screw and reciprocating compressors that produce 100–150 psig oil-free air. The price also includes intercoolers and aftercoolers, a lubrication system and a totally enclosed, fan-cooled (TEFC) motor.

Each figure contains a log-log graph plotting purchase cost versus capacity, an equation for cost as a function of capacity, and a size exponent for capacity ratioing. Most also contain factors that permit adjusting costs for different materials of construction, operating pressure or equipment type (such as API versus ANSI pumps).

All costs are quoted at a *Chemical Engineering* Price Cost Index (CEPCI) of 570, which corresponds to August 2017. The graphs were developed from actual purchase cost or vendor quotation data. Of special note is that BSI Engineering (Cincinnati, Ohio; www. bsiengr.com) allowed me to use their cost database as one of the key information sources.

Ratioing for different capacities and size exponents. When the cost of equipment, processes, or plants having the same design features is plotted versus capacity on log-log paper, the plot usually is a straight line. Thus, one can write the following equation, where *n* is the size exponent.

$$\frac{Cost_{size2}}{Cost_{size1}} = \left(\frac{Capacity_{size2}}{Capacity_{size1}}\right)^{n} \quad (1)$$

For equipment, the average size exponent is 0.6, for plants 0.67.

To illustrate, if you know the price of a 500 ft^2 plate-and-frame exchanger is $10,500, you can estimate the price of an 800 ft^2 exchanger using Equation (1). Referring to Figure 6, note that the size exponent for plate-and-frame exchangers is 0.71. Rearranging Equation (1), the cost is:

$Cost_{800\ ft2} = \$10{,}500 \times (800\ ft^2 / 500\ ft^2)^{0.71} = \$14{,}700.$

Adjusting for inflation using the CEPCI. To keep track of the effects of inflation, several organizations publish cost indices. For chemical plant construction, I feel the CEPCI is the preferred index. *Chemical Engineering* publishes the index each month. One can use it to escalate costs. The relationship between costs and indices is given by Equation (2):

$$\frac{Cost_{at\ time\ 2}}{Cost_{at\ time\ 1}} = \frac{Index_{at\ time\ 2}}{Index_{at\ time\ 1}} \quad (2)$$

For example, if you know the price of a 10,000-gal. storage tank in August 2017 (CEPCI = 570) was $33,000, you can estimate the price in mid-2019 (CEPCI ~ 590) using Equation (2). Rearranging (2):

$\$_{CEPCI,\ 590} = \$33{,}000\ (590/570) = \$34{,}200.$

Using the graph factors. Six of the graphs include factors that permit adjusting costs for different materials of construction, different operating pressures or different equipment variations. Their use is simple. To adjust a price, simply multiply the price by the appropriate factor.

To illustrate, the small boiler prices in Figure 3 are for units generating 150 psig steam. If you wish to price a 100-hp unit that produces 15 psig steam, you would multiply the cost from the graph, $82,000, by the 15 psig

1. For an economic comparison, one usually has to estimate the capital and production cost for each option and use that information to calculate the net present value (NPV) or annualized cost (AC) of each. The NPV or AC is then used to find the economic option.
2. Brown's book [1] explains economic comparison methodology, Lang and Hand factors, plus production cost estimating in depth.

Figures 1–9 depict up-to-date equipment purchase cost data for nine different types of process equipment: agitators (**Figure 1**); air compressors (**Figure 2**); boilers (**Figure 3**); cooling towers (**Figure 4**); fans (**Figure 5**); heat exchangers (**Figure 6**); pressure vessels (**Figure 7**); centrifugal pumps (**Figure 8**); and storage tanks (**Figure 9**)

Figure 1
Agitators
Side-entering: Single 316SS propeller, Stuffing box, and Motor
Top-entering: Single 316SS turbine, Stuffing box, Gear reducer, and Motor

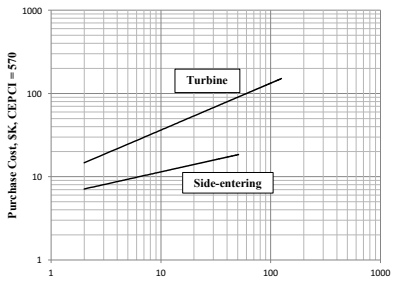

Size Exponents
Propeller: 0.29
Turbine: 0.56
Equations
Propeller: $K=5.8*HP$^{0.29}$
Turbine: $K=9.9*HP$^{0.56}$

Material Factors

CS	0.8
304 SS	0.9
316 SS	1.0
Hastelloy	1.9
Monel	1.2
Other	
Mechanical seal	1.3
Two turbine blades	1.1

Figure 2
Air Compressors
Centrifugal, Rotary Screw, Reciprocating
100-150 psig discharge pressure, Oil free air,
Includes: Intercoolers/aftercoolers,
Lubrication system, TEFC motor

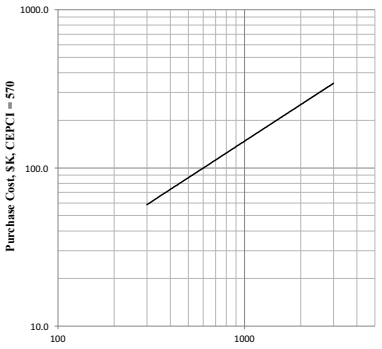

Size Exponent: 0.77
Equation: $K = .74*SCFM$^{0.77}$

Figure 3
Boilers, Package & Field-erected
Oil & Gas fired, No superheat
Small:150 psig steam
Large: 250 psig steam

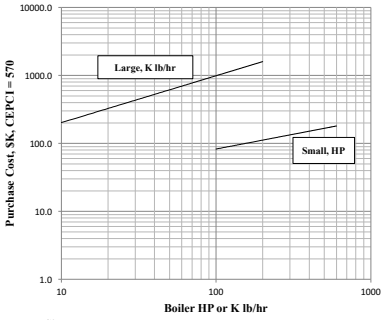

Size Exponents
Small: 0.44
Large: 0.69
Equations
Small: $k = 11.1 *HP$^{0.44}$
Large: $K = 41.6*[(lb/hr)/1000]$^{0.69}$

Pressure Factors
Small

15 psig	0.85
150 psig	1.00
200 psig	1.05
250 psig	1.11

Large

150 psig	0.83
250 psig	1.00
500 psig	1.15
600 psig	1.25

Figure 4
Cooling Towers
10-20°F Range

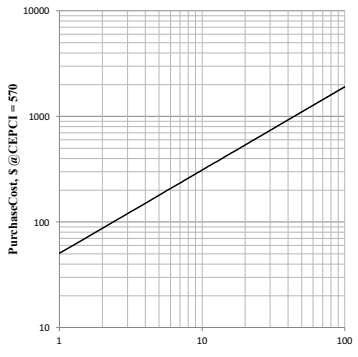

Size Exponent: 0.79
Equation: $K = 50.5*(gpm/1000)$^{0.79}$

Figure 5
Fans
Carbon Steel, Static pressure = 10 in of water

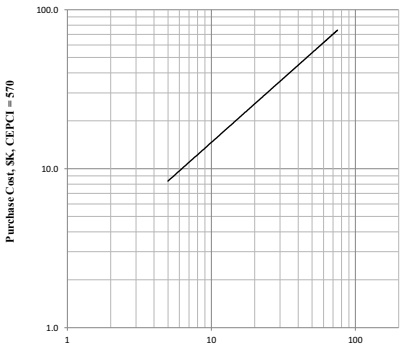

Size Exponent: 0.81
Equation: $K = 2.29*(cfm/1000)$^{0.81}$

Figure 6
Heat Exchangers
Shell & Tube: U-tube & Fixed tube sheet, Carbon steel shell and tubes, 150 psig
Plate and Frame: Stainless steel plates, Nitrile (NBR) gaskets, 150 psig

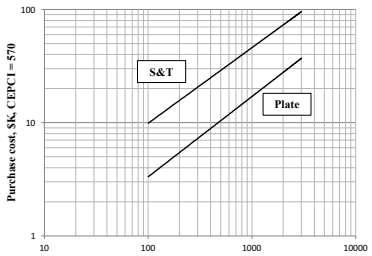

Size Exponents
Shell & Tube: 0.67
Plate & Frame: 0.71
Equations
S&T: $K = 0.458*A$^{0.67}$
Plate: $K = 0.128*A$^{0.71}$
Floating Head Factor: 1.3
Pressure Factors:

S&T		Plate	
200 psig	1.06	235 psig	1.23
600 psig	1.26	370 psig	1.35
1000 psig	1.44		

Material Factors
S&T

CS shell/CS tubes	1.0
CS/SS	1.25
SS/SS	1.4
CS/Titanium (Ti)	2.2

Plate & Frame

SS	1.0
Ti	1.6
Hastelloy C	3.5

Gaskets

NBR	1.0
EPDM	1.6
Viton	2.1

Figure 7,
Pressure Vessels
Carbon steel, 150 psig design pressure

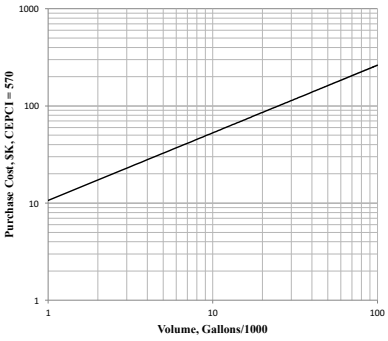

Size Exponent: 0.70
Equation: $K = 10.6*(gallons/1000)$^{0.7}$

Pressure Factors
For pressures other than 150 psig
F= 0.0023P + 0.66
Full vacuum 1.1

Material Factors

CS	1.0
SS	1.4
Monel 400	3.5
Inconel 600	3.4
Titanium	2.0

Figure 8
Pumps, Centrifugal
ANSI, Carbon steel, including TEFC motor

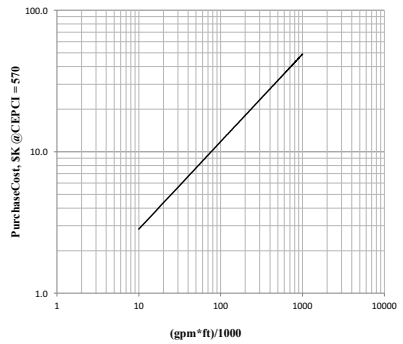

Size Exponent: 0.62
Equation:
$K = 0.683*((gpm*ft)/1000)$^{0.62}$
API/ANSI Factor:
$F = 6.18*((gpm*ft)/1000)$^{-0.25}$

Material Factors

CS	1.0
SS	1.8
Monel	4.0
Titanium	6.0

Figure 9
Tanks
Carbon steel, Atmospheric,
Shop & Field fabricated

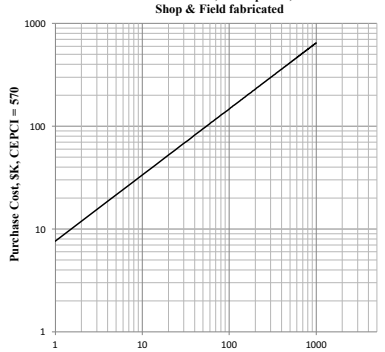

Size Exponent: 0.64
Equation: $K = 7.64*(gallons/1000)$^{0.64}$
Material Factors

CS	1.0
SS	1.7
Rubber-lined	1.5
Epoxy-lined	1.25

factor, which is 0.85. Hence,
$\$_{15\ psig}$ = \$82,000 (0.85) = \$69,700.

A few examples will illustrate the use of the figures.

Example 1. Determine the purchase price, at a CEPCI of 570, of a top-entering turbine agitator. The agitator will have a mechanical seal, carbon steel shaft with two turbine blades, a gear reducer, and a 25-hp motor.

Using the graph in Figure 1, enter it at 25 hp and go up to the top-entering curve. You then find the base price of the unit is \$60,000. This price will have to be adjusted for the mechanical seal (F_{seal} = 1.3), for carbon steel metallurgy (F_{CS} = 0.8), and two turbine blades ($F_{2\text{-blades}}$ = 1.1). Thus the purchase price for the specified unit is:
$\$ = \$60,000 (F_{seal}) (F_{CS}) (F_{2\text{-blades}}) = \$60,000 \times 1.3 \times 0.8 \times 1.1 = \$68,600$.

Example 2. Estimate the purchase price, at a CEPCI of 570, of a stainless-steel API centrifugal pump rated at 260 gallons per minute (gpm) with a total developed head of 310 ft.

Use Figure 8. First calculate (gpm*ft)/1,000 to find the value of the *x*-axis: gpm*ft/1,000 = (260 × 310)/1,000 = 80.6.

From Figure 8, you find the cost of a carbon-steel ANSI pump to be \$10,500. Next, you adjust this price for materials and for an API pump as opposed to an ANSI pump.
$\$_{SS,API} = \$10,500 \times (F_{SS}) \times (F_{API}) = \$10,500 \times 1.9 \times [6.18 \times (80.6)^{-0.25}] = \$41.100$

Example 3. Estimate the price of a 10,000-gal, specially designed reactor at a CEPCI of 600. Your reactor is to be made of carbon steel and will have a pressure rating of 350 psig. In 2013 (CEPCI = 567), your company bought a similar reactor for \$33,900. That reactor has a capacity of 7,500 gal, is made of stainless steel, and has a pressure rating of 150 psig.

Since the reactors are both pressure vessels, you decide to use the factors in Figure 7 to adjust the 2013 price. You adjust for reactor size using Equation (1), for inflation using Equation (2), and for titanium construction and the higher pressure rating using the factors in Figure 7.
$\$_{new} = \$_{old}(Capacity_{new}/Capacity_{old})^{0.70} \times$ (CS factor/SS factor) $\times$ $(Pressure\ factor_{new}/Pressure\ factor_{old}) \times (CEPCI_{600}/CEPCI_{2013})$
= \$33,900 (10,000/7,500).70 (1/1.4) {[0.0023(350) + 0.66]/1.0} (600/567) = \$46,000.

Summary. One can use the information in this article for the following:
- Preliminary estimating of equipment purchase costs
- Adjusting price data for equipment size, materials of construction, design pressure, and equipment type
- Creating mathematical models used in economic option analyses

In turn, the purchase cost data can be used to create order-of-magnitude and study grade estimates. While vendor quotations can be more accurate than the data in the graphs, the data here are generally accurate enough for use developing costs early in a project and when doing economic option analysis. ■

Edited by Gerald Ondrey

References

1.Brown, T.R., "Engineering Economics and Economic Design for Process Engineers," CRC Press, Boca Raton, Fla., 2006.

Author

Thane Brown (Email: trbnjb@earthlink.net) worked for more than 36 years for Procter & Gamble in a variety of engineering and manufacturing roles, primarily in the food-and-beverage business and in health, safety and environmental engineering. In his last position there, Brown was director of North American engineering. After retiring, he taught engineering economics at the University of Cincinnati, and plant design at the University of Dayton. Brown is presently a member of the Chemical Engineering Advisory Committees at the University of Dayton, at Miami University (Oxford, Ohio), at the University of Louisville and at the University of Cincinnati. He also works as a SCORE counselor, providing free assistance to small businesses in the Cincinnati area. Brown authored the book "Engineering Economics and Economic Design for Process Engineers" [*1*], as well as a number of articles on engineering economics, batch pressure filtration and heat transfer. He is a registered professional engineer in Ohio (inactive), and holds a B.S.Ch.E. from Oregon State University.

Accelerating Six Sigma Research with the Definitive Screening Design (DSD) Technique

DSD is a new design-of-experiments (DOE) technique that is expected to bring huge benefits when using a Six Sigma optimization strategy

Bart Peeters, Marc Roels and Sam Van Aeken
Bayer Crop Science
Guido Desmarets
Stanwick Consultants

Statistical tools are deeply ingrained in the Six Sigma methodology to optimize processes and products during chemical process industries (CPI) operations. In fact, Six Sigma has been an important contributing factor for the widespread use of statistics in many different industrial sectors over the past several decades [*1*]. In Six Sigma's DMAIC (define-measure-analyze-improve-control) roadmap, many statistical methods are pivotal for the proper collection of data and the ability to translate gathered data into useful information and actionable knowledge. In particular, the design of experiments (DOE) methodology appeals to many chemical engineers (see, for example, *Chem. Eng.*, Nov. 2014 and Sept. 2016 issues [*2,3*]) as a methodology for systematically quantifying cause-and-effect relationships between input and output variables during both manufacturing processes and laboratory research and development (R&D) efforts. DOE is also widely used during the Improve phase of Six Sigma projects.

This article discusses the importance of DOE in R&D, and the new definitive screening design (DSD) technique. It also presents a case study to illustrate the power of the DSD technique by comparing its results with those obtained from a classic DOE process, the latter with a much larger number of experimental runs. Overall, with this practical tutorial, we aim to bring the DSD tool to the attention of individuals throughout the CPI.

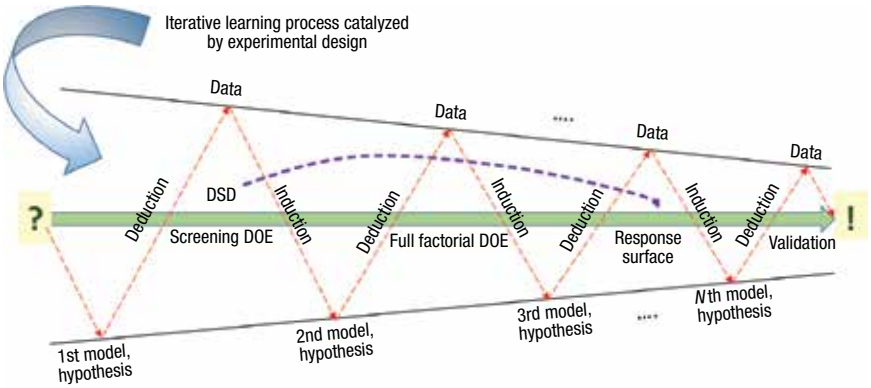

FIGURE 1. DOE is a useful scientific method to gain knowledge about a particular problem in a manufacturing process. A classic research strategy follows the sequence of a screening DOE, a full factorial DOE, and a response surface method to find optimal process settings. A DSD may find these settings with a significantly reduced number of experimental runs (adapted from [*4*])

DOE for scientific investigation

When a chemical engineer is confronted with a manufacturing or product-related problem, he or she will initially propose a first tentative model or hypothesis (which is usually based on speculation) to explain or solve the issue, as shown at the left side of Figure 1 [*4*]. From this first model, the engineer will then deduce certain inherent consequences, which, in a next logical step, should be compared with data to support or refute the first model. Here DOE comes into play most of the time, as a technique to acquire new data using a scientific approach.

In many cases, the newly gathered data will not agree (or will only partially match) with the consequences of the initial model. As a result, engineers will usually call for a second, data-driven DOE model, which, likewise, will often lead again to some necessary consequences. Some variables from the DOE will turn out to have or not have an effect on the studied problem; some unexpected insights may appear and the engineer's way of thinking about the studied problem will change accordingly. Hence, a second cycle in the iteration of the deduction-induction process is initiated, and so on [*4*]. Throughout this process, the discrepancy between model consequences and data diminishes (this is visualized by the converging lines, from left to right, in Figure 1), and new knowledge is generated — the key to process and product improvement.

Through the different stages of experimentation, different types of DOE are typically used, as shown in Figure 1. In the early stages of research, a screening DOE (called fractional factorial) is used to identify the important input variables (called the vital few) and to eliminate the irrelevant ones (called the trivial many) that affect the process performance or product quality. Starting with a large number of potentially important input variables (also called factors), screening DOEs aim to identify the vital few variables that demand further investigation; that is, the active factors that have the largest effect on the response of interest [*5*].

In the next stage of research, a full factorial DOE consists of all possible combinations of levels for the

active factors. The purpose here is to quantify the effects of the latter on the response in a more precise and reliable way using linear models (main effects and interactions). Because the input variables are changed simultaneously in a DOE, possible synergistic and antagonistic interactions between the input variables can be detected; this is in contrast to a so-called OVAT approach, which involves changing only "one variable at a time." Equally important to the detection of possible interactions is the recognition of eventual departure from linear relationships between response and input variables by including a center point in the design. This is shown on the left side of Figure 2.

The first-order design can detect global curvature, but it cannot separately estimate the quadratic effects of each factor. At this stage of experimentation, interpretation of the results combined with process and product expertise may allow the identification of the direction of steepest improvement toward an optimum in the response, possibly leading to another series of designed experiments — this time closer to the optimum — which can yield another first-order model before proceeding to the final stage. Finally, when it comes to optimization of the manufacturing process or product, a more elaborate model will be needed to describe the region around the optimal response and to locate the latter. A linear model will no longer be sufficient. Instead, a quadratic model will be used in a so-called response surface method (RSM) to fit the optimum.

Central composite design

Since we initially made use of a central composite design (CCD) in our case study discussed below, we will shortly discuss this type of RSM first. At the left side of Figure 2, a CCD is depicted for three factors. The CCD is very flexible as it can be set up in a modular way: initially, one starts with the execution of a two-level factorial DOE, where each factor is set at its low (–1) and high (+1) level to verify the effects on the response of interest. A center point, depicted as (0,0,0) in the center of the 3–D representation in Figure 2, may help

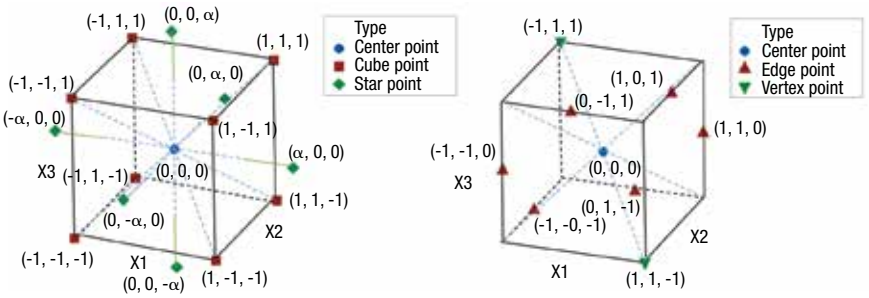

FIGURE 2. Shown here is a central composite design (CCD; left side) and a definitive screening design (DSD; right side) for three factors. For the CCD, α is the axial distance of the start points, which are included in the experimental design to quantify quadratic (curvature) effects between the response and the input factors

TABLE 1. DSD DESIGNS FOR 4 TO 6 FACTORS (ADAPTED FROM REF. 7)

	N = 4			
run	X1	X2	X3	X4
1	0	1	-1	-1
2	0	-1	1	1
3	-1	0	-1	1
4	1	0	1	-1
5	-1	-1	0	-1
6	1	1	0	1
7	-1	1	1	0
8	1	-1	-1	0
9	0	0	0	0

	N = 5				
run	X1	X2	X3	X4	X5
1	0	1	1	-1	-1
2	0	-1	-1	1	1
3	1	0	-1	-1	1
4	-1	0	1	1	-1
5	1	-1	0	1	-1
6	-1	1	0	-1	1
7	1	-1	1	0	1
8	-1	1	-1	0	-1
9	1	1	1	1	0
10	-1	-1	-1	-1	0
11	0	0	0	0	0

	N = 6					
run	X1	X2	X3	X4	X5	X6
1	0	1	-1	-1	-1	-1
2	0	-1	1	1	1	1
3	1	0	-1	1	1	-1
4	-1	0	1	-1	-1	1
5	-1	-1	0	1	-1	-1
6	1	1	0	-1	1	1
7	-1	1	1	0	1	-1
8	1	-1	-1	0	-1	1
9	1	-1	1	-1	0	-1
10	-1	1	-1	1	0	1
11	1	1	1	1	-1	0
12	-1	-1	-1	-1	1	0
13	0	0	0	0	0	0

the engineer to detect curvature in the relation between response and the factors. At that moment, star points (at levels –α -and +α) can be added to the design afterward to allow the engineer to properly quantify quadratic effects. This flexibility makes a CCD very popular in industrial process development [*6*]. From the CCD representation shown in Figure 2, it is clear that the design points are uniformly distributed in the experimental space.

Definitive screening design

In contrast to the most familiar screening designs where input variables are set at only two levels (–1 and +1, or low and high level), the definitive screening design (DSD) introduced in 2011 by Jones and Nachtsheim, employs three levels for the variables: –1, 0 and +1; or low, center and high level [*7*]. For *N* variables the DSD requires only 2*N*+1 experimental runs. In Table 1, the designs for the case of 4 to 6 factors are shown, as presented in the paper from the DSD-inventors Jones and Nachtsheim. The DSDs are comprised of *N* fold-over pairs plus one overall center run consisting of the center values of all variables (This is indicated in red color on the last rows of Table 1).

The following design pattern further characterizes a DSD [*7*]:

1. *Regarding the location of the zeros (highlighted in grey color in Table 1)* — The first two runs have zeros in the column of the first variable *X1*; the next two runs have zeros in the column of the second variable *X2* and so on
2. *Regarding the pair of runs* — These are mirrored (folded over), which means that the second run of a pair is found by multiplying the first run of this pair by –1. Hence, the first 2*N* runs have exactly one variable at its center value (0), while all other variables are at their extremes (–1 or +1) and are referred to as "edge runs," because the 3-D projections involving these variables, they are on the edges of the cube [*8*]. In case the number of factors *N* is uneven, it is recommended to choose the DSD design for *N*+1 factors and then to drop the extraneous column, which results then again in an *N*-factor design with 2*N*+3 runs [*8*]. The two extra runs are, inherently,

TABLE 2. DESIGN OF THE RESPONSE SURFACE (90 RUNS)

Run	Type	*A*	*B*	*C*	*D*	*E*	*F*	pH
63	Cube point	-1	-1	-1	-1	-1	-1	7.29
76		1	-1	-1	-1	-1	-1	6.87
6		-1	1	-1	-1	-1	-1	8.37
68		1	1	-1	-1	-1	-1	7.83
32		-1	-1	1	-1	-1	-1	6.77
59		1	-1	1	-1	-1	-1	6.55
18		-1	1	1	-1	-1	-1	7.45
46		1	1	1	-1	-1	-1	7.08
10		-1	-1	-1	1	-1	-1	7.21
22		1	-1	-1	1	-1	-1	6.81
1		-1	1	-1	1	-1	-1	8.35
67		1	1	-1	1	-1	-1	7.80
87		-1	-1	1	1	-1	-1	6.84
56		1	-1	1	1	-1	-1	6.58
12		-1	1	1	1	-1	-1	7.47
13		1	1	1	1	-1	-1	7.09
88		-1	-1	-1	-1	1	-1	7.30
74		1	-1	-1	-1	1	-1	6.90
45		-1	1	-1	-1	1	-1	8.23
83		1	1	-1	-1	1	-1	7.80
80		-1	-1	1	-1	1	-1	6.81
57		1	-1	1	-1	1	-1	6.55
38		-1	1	1	-1	1	-1	7.48
43		1	1	1	-1	1	-1	7.12
82		-1	-1	-1	1	1	-1	7.25
30		1	-1	-1	1	1	-1	6.85
70		-1	1	-1	1	1	-1	8.32
58		1	1	-1	1	1	-1	7.79
34		-1	-1	1	1	1	-1	6.85
66		1	-1	1	1	1	-1	6.61
24		-1	1	1	1	1	-1	7.47
77		1	1	1	1	1	-1	7.13
61		-1	-1	-1	-1	-1	1	7.39
85		1	-1	-1	-1	-1	1	6.86
72		-1	1	-1	-1	-1	1	8.39
84		1	1	-1	-1	-1	1	7.85
37		-1	-1	1	-1	-1	1	6.86
49		1	-1	1	-1	-1	1	6.56
29		-1	1	1	-1	-1	1	7.49
50		1	1	1	-1	-1	1	7.14
9		-1	-1	-1	1	-1	1	7.28
21		1	-1	-1	1	-1	1	6.85
51		-1	1	-1	1	-1	1	8.38
19		1	1	-1	1	-1	1	7.85
65		-1	-1	1	1	-1	1	6.84
52		1	-1	1	1	-1	1	6.58
71		-1	1	1	1	-1	1	7.49
8		1	1	1	1	-1	1	7.15
3		-1	-1	-1	-1	1	1	7.33
47		1	-1	-1	-1	1	1	6.93
69		-1	1	-1	-1	1	1	8.33
73		1	1	-1	-1	1	1	7.83
20		-1	-1	1	-1	1	1	6.87
54		1	-1	1	-1	1	1	6.61
16		-1	1	1	-1	1	1	7.51
23		1	1	1	-1	1	1	7.16
89		-1	-1	-1	1	1	1	7.31
53		1	-1	-1	1	1	1	6.87
55		-1	1	-1	1	1	1	8.34
14		1	1	-1	1	1	1	7.78
81		-1	-1	1	1	1	1	6.87
90		1	-1	1	1	1	1	6.60
33		-1	1	1	1	1	1	7.54
7		1	1	1	1	1	1	7.16
31	Star point	-2.83	0	0	0	0	0	7.92
78		2.83	0	0	0	0	0	6.72
39		0	-2.83	0	0	0	0	6.40
42		0	2.83	0	0	0	0	8.43
25		0	0	-2.83	0	0	0	8.42
26		0	0	2.83	0	0	0	6.78
17		0	0	0	-2.83	0	0	7.19
64		0	0	0	2.83	0	0	7.21
44		0	0	0	0	-2.83	0	7.13
2		0	0	0	0	2.83	0	7.21
4		0	0	0	0	0	-2.83	7.11
35		0	0	0	0	0	2.83	7.29
48	Center point	0	0	0	0	0	0	7.26
40		0	0	0	0	0	0	7.18
41		0	0	0	0	0	0	7.19
86		0	0	0	0	0	0	7.16
60		0	0	0	0	0	0	7.20
5		0	0	0	0	0	0	7.20
11		0	0	0	0	0	0	7.21
27		0	0	0	0	0	0	7.22
28		0	0	0	0	0	0	7.17
79		0	0	0	0	0	0	7.20
15		0	0	0	0	0	0	7.17
36		0	0	0	0	0	0	7.19
62		0	0	0	0	0	0	7.17
75		0	0	0	0	0	0	7.23

TABLE 3. CONCENTRATION (WT.%) OF VARIABLES *A–F* CORRESPONDING WITH THE CODED VALUES USED IN TABLE 2 AND TABLE 4

	Coded values				
	–2.83	**–1**	**0**	**1**	**2.83**
A	0.449	0.618	0.710	0.802	0.971
B	0.846	1.062	1.180	1.298	1.514
C	0.702	0.966	1.110	1.254	1.518
D	0.430	0.540	0.600	0.660	0.770
E	3.585	4.500	5.000	5.500	6.415
F	0.108	0.135	0.150	0.165	0.192

TABLE 4. DESIGN OF THE DSD (13 RUNS)

Run	Type	*A*	*B*	*C*	*D*	*E*	*F*	pH
13	Edge point	0	1	1	1	1	1	7.40
7		0	-1	-1	-1	-1	-1	7.06
5		1	0	1	1	-1	-1	6.88
2		-1	0	-1	-1	1	1	7.93
6		1	1	0	-1	-1	1	7.50
4		-1	-1	0	1	1	-1	7.03
10		1	1	-1	0	1	-1	7.86
8		-1	-1	1	0	-1	1	6.87
9		1	-1	-1	1	0	1	6.92
11		-1	1	1	-1	0	-1	7.55
1		1	-1	1	-1	1	0	6.60
3		-1	1	-1	1	-1	0	8.42
12	Center	0	0	0	0	0	0	7.25

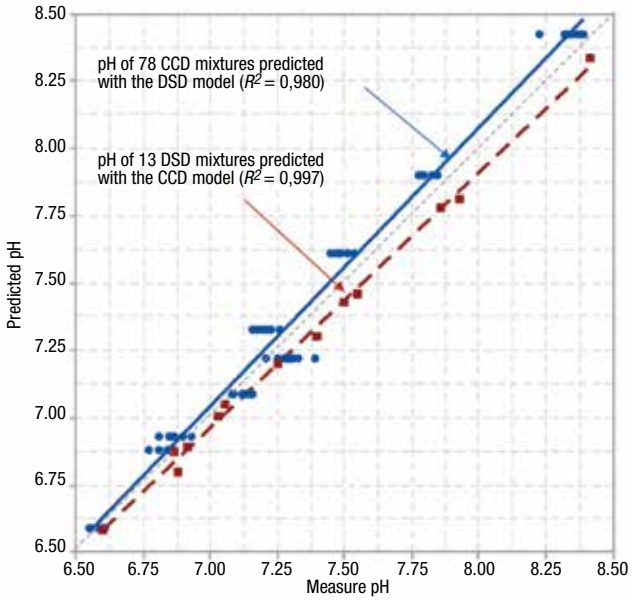

FIGURE 3. Predicted pH values of 78 mixtures (from the CCD experiments) using the DSD model, and the predicted pH values of 13 mixtures (from the DSD experiments) using the CCD model, to validate both models.

TABLE 5. COMPARISON OF MODELS OBTAINED WITH THE CCD (BASED ON 90 RUNS) AND THE DSD (BASED ON 13 RUNS)

CCD		**DSD**	
(90 runs)		(13 runs)	
MODEL			
pH=		pH =	
7,198		7,328	
-0.199	× *A*	-0.204	× *A*
+0,391	× *B*	+0.425	× *B*
-0.286	× *C*	-0.289	× *C*
+0.021	× *F*		
-0,024	× *AB*	-0,058	× *AB*
+0.042	× *AC*		
-0.099	× *BC*	-0.117	× *BC*
+0.016	× A^2		
+0.028	× B^2		
+0.051	× C^2		
MODEL SUMMARY			
R^2	0.996	R^2	0.991
R^2_{adj}	0.995	R^2_{adj}	0.985
R^2_{pred}	0.992	R^2_{pred}	0.977

without center values for any factor and are referred to as "vertex runs" by the DSD-inventors [*8*]. Likewise, to increase the power of any DSD, one may choose initially a design with a larger number of factors than necessary (for example, in total *N*+k factors), and then drop the extra *k* columns [*7–9*].

For the sake of visualization, a 3-D representation for a DSD with three factors is shown at the right side of Figure 2, although a DSD with only three factors is not recommended [*9*]. For this visualization, we took the DSD design for *N* = 4 from Table 1 and then dropped the last column. One can clearly see the so-called DSD edge runs and vertex runs (which comes down to cube points), together with the single DSD center run at the right side of Figure 2.

The advantages of a DSD are as follows (For more, see [*7–9*]):

1. Each factor is analyzed at three levels, which makes it possible to analyze quadratic effects, and, thus, to model curvature with a very limited amount of runs, rendering DSDs a relatively inexpensive technique for users in the field
2. Advantages are specifically found with regard to confounding variables (note: The term confounding, used in statistics, indicates that the effects of model terms cannot be calculated separately):

- The main effects are completely independent of each other, completely independent of two-factor interactions, and completely independent of quadratic effects (thus, there is no confounding at all)
- The two-factor interactions are not completely confounded with other

two-factor interactions, although they may be correlated a little

- The quadratic effects are estimable and are independent of the main effects (no confounding) and not completely confounded, though correlated, with the two-factor interaction effects
- Last but not least, for DSDs with at least six factors, the DSD can fit — with very high level of statistical efficiency — the full quadratic models in case only three or fewer factors turn out to be active. As such, the DSDs become efficient response surface designs with three or fewer factors, rendering follow-up experiments (for the purpose of model optimizing) not necessary in many circumstances [*7*]. "The capability to project these designs to efficient response surface designs makes possible the screening and optimization of a system in a single step," according to the co-inventors Jones and Nachtsheim [*8*]. This potentially huge benefit (making a shortcut from screening straight to optimization) is shown in Figure 1 with the dashed purple arrow. For comparison, a response surface design with three factors would require 20 runs.

In the original DSDs, the factors had to be quantitative to allow for 3 levels. New DSDs have very recently been developed that allow for combinations of continuous and categorical input variables [*10*].

Case study

Part of a particular Six Sigma project consisted of making a model using a CCD for the pH of formulations made of six ingredients (*A*–*F*), whereby the ingredients were varied independently of each other. The number of laboratory test formulations prepared and evaluated was 90. In a laboratory-scale environment, this is doable. However, in a manufacturing plant, this would be difficult, perhaps impossible. The different test runs are shown in Table 2, where the cube points, star points and center points are clustered together for the sake of overview. The run order as executed in the laboratory is shown in the first column. The variables are shown with their coded levels, with the value of α (star points) being 2.83. The corresponding concentrations (wt.%) of the variables *A*–*F* are summarized in Table 3. The measured pH of the formulations can be found in the last column.

After these CCD experiments were executed, Six Sigma training was given at the Bayer Antwerp site (where the work was carried out), including the new statistical technique of DSD. In the context of the training, the Six Sigma project leader sought to verify which model would be found using a DSD with only 13 runs for the six factors, compared to the CCD model obtained earlier. For this, 13 extra formulations were prepared, as shown in Table 4.

The data sets were analyzed using Design-Expert (from Stat-Ease Inc.), including only model terms at a significance level of 0.05. A summary of both models is depicted in Table 5. The CCD model includes the main effects *A, B, C* and *F*, the interaction effects *AB*, *AC* and *BC*, and the quadratic effects A^2, B^2 and C^2. The DSD model includes fewer terms, namely the main effects *A, B* and *C*, and the interaction effects *AB* and *BC.* It is remarkable that the coefficients in the DSD model are very similar to the one of the CCD model.

Regarding the CCD model, the R^2_{adj} (that is, the raw coefficient of determination, R^2, being adjusted for the number of model predictors) indicates that 99.5% of the variation in the pH is explained by the variation in the input variables; based on the complete CCD statistical analysis (not shown) the terms *F, AC*, A^2, B^2 and C^2 — which are not included in the DSD model — account only for 2% of the explained pH variation in the data set of the CCD, which is, after all, a rather minor contribution of these extra CCD model terms. Based on their high R^2_{adj} (99.5% for the CCD, and 98.5% for the DSD) we can state that they each fit well with their respective existing data set.

But how do both models compare when it would come down to predict the pH of new mixtures? We will first have a look to their predicted R^2 (R^2_{pred}). This model summary is calculated by setting aside a single observation from the whole model data set, and then re-estimating the model based on all observations minus the one that is excluded (for example, in the case of the CCD, this would be 90 – 1 = 89 observations). Then the pH is calculated for the mixture that was intentionally ignored to build the model. Next, the predicted residual error is estimated for this single observation; that is the difference between the calculated pH (pH_{calc}) and the experimentally determined pH (pH_{obs}) for the observation. This procedure is repeated for all observations. Finally, the so-called predicted residual error sum of squares (*PRESS*) is calculated according to Equation (1):

$$PRESS = \sum \left(pH_{calc} - pH_{obs} \right)^2 \quad (1)$$

This *PRESS* value is compared to the Sum of Squares (*SS*) around the mean value of the whole data set (SS_{tot}); in other words, in the latter case, a "mean model" is used that simply takes the mean response as a prediction for every mixture in the data set. The R^2_{pred} is finally found via Equation (2):

$$R^2_{pred} = 1 - \frac{PRESS}{ss_{tot}} \quad (2)$$

The somewhat larger R^2_{pred} of 99.2% for the CCD compared to 97.7% for the DSD model suggests that the CCD has some greater predictive ability. However, the DSD model as such can certainly be classified as a model having a great predictive power.

Another way (and by far a better way) to validate a model is to use a completely new data set that was not used during the development of the model. This new data set — used in the stage of model validation — is frequently called a test set, in contrast to a training set that is used to calibrate (build) the model [*11*]. The test set should ideally span the same "space" of the input variables as was the case for the training set. We then let the calibrated model predict the responses of the test set and compare them to the known, real responses.

In this case study, we will use the data set of the CCD as a test set for the DSD model; likewise, we will use the DSD data as a test set to validate the CCD model. Because the 12

axial points in the CCD data set are beyond the design space, wherein the DSD model was built (remember, the DSD model factor settings were between –1 and +1, whereas the CCD star points were going from –2.83 to +2.83), we will exclude the CCD mixtures with the star points to validate the DSD model; hence, the pH of the remaining 78 CCD mixtures were predicted with the DSD model and compared with the measured pH values. Figure 3 presents the predicted versus measured pH values for the validation of both models. Visually, one can see that both models adequately predict the pH, with some more variation in the case of the DSD model. In the context of model validation, the root mean square error of prediction (*RMSEP*) can be calculated as an estimate of the prediction error [*11*], using Equation (3):

$$RMSEP = \sqrt{\frac{\sum (pH_{calc} - pH_{obs})^2}{N}} \quad (3)$$

The *RMSEP* can be interpreted as the average error to be associated with future predictions. In practice, $t_{0.025;\ n\text{-}1}$ times the RMSEP (with t obtained from a Student's *t* table [*12*], and *n* the number of data points of the test set; for example, based on the test set to validate the CCD model, $t_{0.025;\ 13\text{-}1}$ is 2.16. With larger test sets, the *t* value will approach 1.96. This may be used as estimated precision for predicted pH values. For the CCD model the RMSEP is 0.07 pH units, and for the DSD model, it amounts to a somewhat higher value of 0.09 pH units. For example, the pH of the mixture of DSD run 13 with an observed pH of 7.40 (first row in Table 4) is predicted by the CCD model to be 7.30 +/– 0.15 (the latter being 2.16 times 0.07).

Final thoughts

Chemical engineers and scientists in the CPI embrace the DOE methodology developed by statisticians to efficiently investigate and optimize products and manufacturing processes. We therefore gratefully acknowledge the work done by statisticians to constantly search for even more efficient design-of-experiments approaches.

The DSD methodology lately developed by Jones and Nachtsheim is highly efficient with the number of runs required far below the number needed in classical screening designs. As a low number of experimental runs is in most cases a desirable requirement for many experimenters in the CPI, and certainly in cases where experiments need to be done in manufacturing plants, the DSD can be called a revolution in performing designed experiments. In case the statistical analysis of the experiments, *a fortiori* indicates that the number of active factors is limited, so for these cases, the use of definitive screening allows the engineer to make a shortcut from screening straight to optimization. It can be expected that the CPI will benefit from this latest statistical research, and that definitive screening designs will be applied with growing frequency over time, especially in CPI Six Sigma projects where a lot of factors need to be tested. ■

Edited by Suzanne Shelley

Authors

Bart Peeters is a manufacturing technologist at Bayer Crop Science (Haven 627, Scheldelaan 460, 2040 Antwerp, Belgium; Phone: +32 3 568 5762; Email: bart.peeters@bayer.com), where he has been working since 1998. He first served as a process improvement engineer at Eastman's PVB polymer manufacturing plant onsite (until 2004). Since then, he has been working at the environmental department of the company. Peeters is a certified Six Sigma Black Belt and coordinates the Six Sigma program at the Bayer Antwerp site. While working at Bayer's WWTP, he obtained his Ph.D. in engineering from the KU Leuven (Belgium) on the research topic "Effect of activated sludge composition on its dewaterability and sticky phase."Prior to that, he earned an M.S.Ch.E. degree from the KU Leuven, and an M.Bio. Ch.E. degree in 1996 from the university college De Nayer. Peeters is the author of 20 articles in scientific journals, technical magazines and international conferences.

Guido Desmarets is a senior management consultant at Stanwick NV (Axess Business parkbuilding B-Guldensporenpark 20, 9820 Merelbeke, Belgium; Phone +32 9 210 59 50; Email: guido.desmarets@stanwick.be), where he has been working since 1988. As a Master Black Belt he coaches worldwide companies in the field of Continuous Improvement, Lean Six Sigma, Operational Excellence, with major results in efficiency and quality improvements, cost reductions and delivery performance. Prior to joining Stanwick NV he held positions as R&D manager, process engineer, quality assurance and production management at international companies, where his interest to use DOE as a major process improvement tool was triggered and developed. He holds a master degree in chemistry (University of Ghent 1976). Subsequent research work resulted in several publications and patents on slow-release formulations for pesticides.

Marc Roels is a crop protection products laboratory specialist at Bayer Crop Science Europe N.V. (Phone +32 3 568 5185; Email: marc.roels@bayer.com), where he has been working since 1984. Roels provides analytical support for research, development, registration and manufacturing of herbicides at the Bayer Antwerp site and at different toller operations. For more than 15 years he is an enthusiastic user of DOE to study formulation robustness and formulation optimization. He received his B.S. in pharmaceutical and biological techniques in 1983. He is a certified Six Sigma Green Belt.

Sam Van Aeken was the team lead of the analytical services laboratory at Bayer Crop Science (Haven 627, Scheldelaan 460, 2040 Antwerp, Belgium), where he has been working since 2014. Prior to joining the firm, he worked from 2010 until 2012, as a process chemist in Eastman Ghent, managing new product trials. He was later employed at W.R. Grace / DeNeef as a R&D engineer, where he researched new urethane based grouting systems. Van Aeken graduated as a bio-engineer in 2004 at the Vrije Universiteit Brussel and obtained a Ph.D. in organic chemistry in 2010 with a dissertation on new synthetic routes towards aza-heterocyclic quinone compounds.

References

1. Steinberg, D.M., Industrial statistics: the challenges and the research, *Quality Engineering*, 28 (1), pp. 45–59, 2016.
2. Kleppmann, W., Design of Experiments (DOE): Optimizing products and processes efficiently, *Chem. Eng.*, November, pp. 50–57, 2014.
3. Anderson, M.J., Design of Experiments (DOE): How to handle hard-to-change factors using a split plot, *Chem. Eng,* September, pp. 83–86, 2016.
4. Box, G.E.P., Hunter, J.S. and Hunter, W.G. "Statistics for experimenters: design, innovation, and discovery", 2nd ed., John Wiley & Sons, Inc., 2005.
5. Jones, B., 21st century screening experiments: what, why and how. *Quality Engineering* 28 (1), pp. 98–106, 2016.
6. Anderson, M.J. "RSM simplified: optimizing processes using surface methods for design of experiments", 2nd Ed., Productivity Press, 2016.
7. Jones, B. and Nachtsheim, C.J. A class of three-level desings for definitive screening in the presence of second-order effects, *Journal of Quality Technology* 43, pp. 1-15, 2011.
8. Jones, B. and Nachtsheim, C.J. Blocking schemes for definitive screening designs. *Technometrics* 58 (1), pp. 74-83, 2016.
9. Jones, B., JMP Blog on proper and improper use of Definitive Screening Designs (DSDs) (https://community.jmp.com/t5/JMP-Blog/Proper-and-improper-use-of-Definitive-Screening-Designs-DSDs/ba-p/30703), 2016.
10. Jones, B. and Nachtsheim, C.J., Definitive screening designs with added two-level categorical factors. *Journal of Quality Technology* 45, pp. 121–129, 2013
11. Esbensen, K.H. "Multivariate Data Analysis – In Practice. An Introduction to Multivariate Data Analysis and Experimental Design", 5th Ed., CAMO software, 2010.
12. Bass, I. "Six Sigma Statistics with Excel and Minitab", 1st Ed., Mc. Graw Hill, 2007.

Economic Indicators

2016 2017 2018

Download the CEPCI two weeks sooner at www.chemengonline.com/pci

CHEMICAL ENGINEERING PLANT COST INDEX (CEPCI)

(1957–59 = 100)	Oct. '18 Prelim.	Sept. '18 Final	Oct. '17 Final
CE Index	616.4	617.7	574.7
Equipment	751.5	753.3	694.4
Heat exchangers & tanks	666.9	671.1	610.0
Process machinery	728.2	731.4	690.6
Pipe, valves & fittings	982.8	980.8	900.3
Process instruments	419.8	422.0	409.0
Pumps & compressors	1038.0	1030.7	985.3
Electrical equipment	552.6	551.0	521.7
Structural supports & misc.	830.6	834.7	740.8
Construction labor	340.5	340.1	331.2
Buildings	601.2	603.7	565.6
Engineering & supervision	316.6	317.2	309.2

Annual Index:
2010 = 550.8
2011 = 585.7
2012 = 584.6
2013 = 567.3
2014 = 576.1
2015 = 556.8
2016 = 541.7
2017 = 567.5

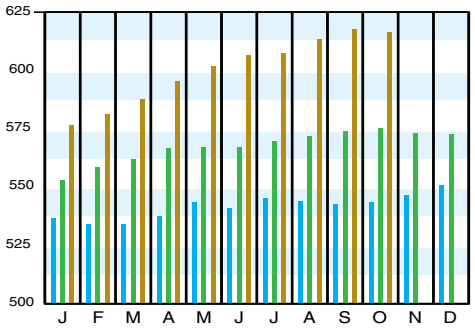

Starting in April 2007, several data series for labor and compressors were converted to accommodate series IDs discontinued by the U.S. Bureau of Labor Statistics (BLS). Starting in March 2018, the data series for chemical industry special machinery was replaced because the series was discontinued by BLS (see *Chem. Eng.*, April 2018, p. 76–77.)

CURRENT BUSINESS INDICATORS

	LATEST	PREVIOUS		YEAR AGO
CPI output index (2012 = 100)	Nov. '18 = 103.1	Oct. '18 = 102.7	Sept. '18 = 102.4	Nov. '17 = 102.0
CPI value of output, $ billions	Oct. '18 = 2,035.8	Sept. '18 = 2,029.1	Aug. '18 = 2,008.6	Oct. '17 = 1,841.4
CPI operating rate, %	Nov. '18 = 76.6	Oct. '18 = 76.3	Sept. '18 = 76.2	Nov. '17 = 76.5
Producer prices, industrial chemicals (1982 = 100)	Nov. '18 = 279.2	Oct. '18 = 287.7	Sept. '18 = 278.8	Nov. '17 = 265.8
Industrial Production in Manufacturing (2012 =100)*	Nov. '18 = 104.9	Oct. '18 = 104.9	Sept. '18 = 105.0	Nov. '17 = 102.9
Hourly earnings index, chemical & allied products (1992 = 100)	Nov. '18 = 186.4	Oct. '18 = 184.0	Sept. '18 = 185.2	Nov. '17 = 182.2
Productivity index, chemicals & allied products (1992 = 100)	Nov. '18 = 96.4	Oct. '18 = 96.4	Sept. '18 = 96.8	Nov. '17 = 99.1

CPI OUTPUT INDEX (2000 = 100)†

CPI OUTPUT VALUE ($ BILLIONS)

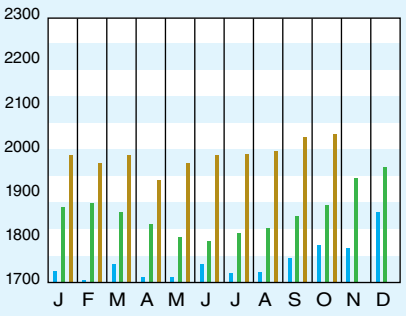

CPI OPERATING RATE (%)

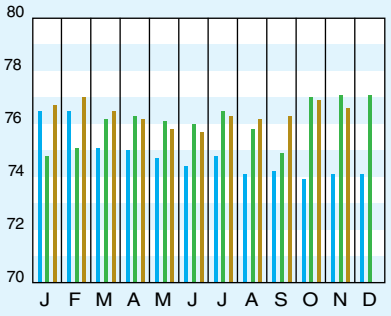

*Due to discontinuance, the Index of Industrial Activity has been replaced by the Industrial Production in Manufacturing index from the U.S. Federal Reserve Board.
†For the current month's CPI output index values, the base year was changed from 2000 to 2012
Current business indicators provided by Global Insight, Inc., Lexington, Mass.

CURRENT TRENDS

The preliminary value for the October 2018 *CE* Plant Cost Index (CEPCI; top; most recent available) fell slightly compared to the previous month's value. The decrease reversed an upward trend that had been ongoing throughout 2018. The Equipment, Buildings and Engineering & Supervision subindexes all decreased in October, offsetting a small rise in the Construction Labor subindex. The overall CEPCI value for October stands at 7.3% higher than the corresponding value from October 2017. Meanwhile, the CBI data (middle) for November 2018 show a small increase in the CPI output index from the previous month. In addition, the data show an increase in the October 2018 number for CPI value of output.